



1 **Abstract**

2  
3  
4  
5 3 We present detrital zircon U–Pb SHRIMP age patterns for the central segment  
6  
7 4 (34–42°S) of an extensive accretionary complex along coastal Chile together  
8  
9 5 with ages for some relevant igneous rocks. The complex consists of a basally  
10  
11 6 accreted high pressure/low temperature Western Series outboard of a frontally  
12  
13 7 accreted Eastern Series that was overprinted by high temperature/low pressure  
14  
15 8 metamorphism. Eleven new SHRIMP detrital zircon age patterns have been  
16  
17 9 obtained for metaturbidites from the central (34–42°S) segment of the  
18  
19 10 accretionary complex, four from previously undated metamorphic complexes  
20  
21 11 and associated intrusive rocks from the main Andean cordillera, and three from  
22  
23 12 igneous rocks in Argentina that were considered as possible sediment source  
24  
25 13 areas. There are no Mesozoic detrital zircons in the accretionary rocks. Early  
26  
27 14 Paleozoic zircons are an essential component of the provenance, and Grenville-  
28  
29 15 age zircons and isolated grains as old as 3 Ga occur in most rocks, although  
30  
31 16 much less commonly in the Western Series of the southern sector. In the  
32  
33 17 northernmost sector (34–38°30'S) Proterozoic zircon grains constitute more  
34  
35 18 than 50% of the detrital spectra, in contrast with less than 10% in the southern  
36  
37 19 sector (39–42°S). The youngest igneous detrital zircons in both the northern  
38  
39 20 Western (307 Ma) and Eastern Series (345 Ma) are considered to closely date  
40  
41 21 sedimentation of the protoliths. Both oxygen and Lu-Hf isotopic analyses of a  
42  
43 22 selection of Permian to Neoproterozoic detrital zircon grains indicate that the  
44  
45 23 respective igneous source rocks had significant crustal contributions. The  
46  
47 24 results suggest that Early Paleozoic orogenic belts (Pampean and Famatinian)  
48  
49 25 containing material recycled from cratonic areas of South America supplied  
50  
51  
52  
53  
54  
55  
56  
57  
58  
59  
60  
61  
62  
63  
64  
65

1  
2  
3  
4  
5  
6  
7  
8  
9  
10  
11  
12  
13  
14  
15  
16  
17  
18  
19  
20  
21  
22  
23  
24  
25  
26  
27  
28  
29  
30  
31  
32  
33  
34  
35  
36  
37  
38  
39  
40  
41  
42  
43  
44  
45  
46  
47  
48  
49  
50  
51  
52  
53  
54  
55  
56  
57  
58  
59  
60  
61  
62  
63  
64  
65

1 detritus to this part of the paleo-Pacific coast. In contrast, in the southern  
2 exposures of the Western Series studied here, Permian detrital zircons (253–  
3 295 Ma) dominate, indicating much younger deposition. The northern sector  
4 has scarce Early to Middle Devonian detrital zircons, prominent south of 39°S.  
5 The sedimentary protolith of the northern sector was probably deposited in a  
6 passive margin setting starved of Devonian (Achalian) detritus by a topographic  
7 barrier formed by the Precordillera, and possibly Chilenia, terranes. Devonian  
8 subduction-related metamorphic and plutonic rocks developed south of 39°S,  
9 beyond the possible southern limit of Chilenia, where sedimentation of  
10 accretionary rocks continued until Permian times.

11  
12  
13 **Keywords:** SHRIMP detrital zircon ages, Devonian, Carboniferous, Permian,  
14 accretionary complex, Central Chile

# 1. Introduction

A fossil Late Paleozoic subduction complex is exposed continuously along the Chilean margin south of 34°S. Willner (2005) quantified the metamorphic P-T conditions which affected the rocks near the northern end of the 34°–42°S sector considered here, and Glodny et al. (2005, 2008) suggested accretionary modes for different portions of the complex, mainly south of 36°S (see below). Dating of metamorphic processes has also been dealt with in a number of papers since Munizaga et al. (1974) with K-Ar, Hervé et al. (1982) with Rb-Sr whole rock methods and more recently by Willner et al. (2005) with Ar-Ar and Glodny et al. (2008) with Rb-Sr mineral whole rock isochrons. Detrital zircon age data, however, have remained very scarce or nonexistent for large tracts of the accretionary complex between 34 and 42°S. Willner et al (2008) presented the results of two samples analysed by ICP-MS and Duhart et al (2001) presented data for individual detrital zircons for several samples of the southern (39°–42°S) sector, analysed by TIMMS. In this contribution, 13 new metasedimentary samples were analysed for their U-Pb detrital zircon age spectra with SHRIMP and age determinations are presented for three samples from possible source igneous rocks in Argentina and two foliated granitoids from Liquiñe, east of the accretionary complex. The main purpose of this study is to examine the detrital zircon population present in the accretionary complex, detect their variations in space if any, try to relate them to source areas and interpret the tectonic setting of deposition. Additionally, isotopic studies of the detrital zircons were made to improve the possibilities of identifying the source areas, and to characterize some aspects of their geologic evolution. The results

1 obtained indicate that previously unknown large variations in the areal  
2 distribution of the detrital populations of zircon are detectable in the accretionary  
3 prism. N-S variations in these populations are described and interpreted in  
4 terms of their geological significance for the Late Paleozoic development of the  
5 continental margin of Pangea in this portion of Terra Australis orogen (Cawood,  
6 2005) which represent the vestiges of tectonic activity within the paleo-Pacific  
7 Ocean (Murphy et al., 2009).

## 9 **2. Geological setting**

11 Two units with differing lithology and structure are recognized within the  
12 complex - the Western and Eastern series (Godoy, 1970; Aguirre et al., 1972).  
13 These have been recognised as paired metamorphic belts (*sensu* Miyashiro,  
14 1961), now interpreted as representing the products of basal and frontal  
15 accretion respectively in an active continental margin (Willner et al., 2005;  
16 Richter et al., 2007; Glodny et al., 2008). The Eastern Series is intruded by the  
17 N-S elongated Coastal Batholith of Late Paleozoic age (see below).

19 In the study area (Fig. 1) the southern section is dominated by the Western  
20 Series (WS) whereas in the northern section it is confined to relatively small  
21 coastal outcrops. Although the limit between these sectors is not precisely  
22 determined, it must be close to the north-west trending Lanalhue lineament (Fig.  
23 1), which has been interpreted as a suture zone (Ernst, 1973), a sharp transition  
24 between the two series (Hervé, 1977) and more recently as the Lanalhue Fault  
25 Zone (Glodny et al., 2008). The last authors state that “the Lanalhue Fault Zone

1 juxtaposes Permo-Carboniferous magmatic arc granitoids and associated,  
2 frontally accreted metasediments (Eastern Series) in the northeast with a late  
3 Carboniferous to Triassic basal-accretionary forearc wedge complex (Western  
4 Series) in the southwest". They further considered that an Early Permian period  
5 of subduction erosion to the north contrasted with ongoing accretion to the  
6 south, so that the coastal batholith appears to be displaced 100 km to the west  
7 north of the fault zone, with contrasting lithologies and metamorphic signatures  
8 across it.

9  
10 The Eastern Series (ES) consists of alternating metasandstones and  
11 metapelites, with preserved bedding except in the easternmost, higher-grade  
12 areas; volumetrically small but ubiquitous calc-silicate pods are found  
13 throughout. The WS is composed of micaschists, greenschists, quartzites and  
14 scarce serpentinite bodies; rare primary sedimentary structures are observed,  
15 as well as occasional pillow structures in the greenschists.

16  
17 The rocks of the two series differ in fabric and small-scale deformational  
18 features. The ES is mainly deformed into upright folds with subvertical  $S_1$   
19 foliation or cleavage in the metapelites, in which a less steep  $S_2$  foliation is  
20 occasionally observed. In contrast, the main foliation in the WS rocks is  
21 generally  $S_2$ , accompanied by the main recrystallization and with transposition  
22 of earlier primary and tectonic fabrics. Peak metamorphic conditions also differ  
23 in the two series. Following Hervé (1977) it is clear that the ES represents low  
24 P/T (pressure/temperature) metamorphic gradients and the WS higher ones,

1 the thermal gradient for the latter estimated by Willner et al. (2005) as about 10  
2 to 12°C/km.

3  
4 Paleotectonic models of the evolution of the south-western Gondwana margin  
5 include the hypothesis (Ramos et al., 1986) that between 28–39° S an exotic  
6 continental block called Chilenia collided with Gondwana during the Devonian,  
7 with the suture lying east of the present Andean Cordillera in Argentina. South  
8 of this latitude the Paleozoic development has also been interpreted as  
9 indicating collision of Patagonia with Gondwana (Ramos, 1984, 2008;  
10 Pankhurst et al., 2006). The coastal accretionary complex studied here should  
11 contain a record that might help to confirm the occurrence of such collisional  
12 events.

### 14 **3. Methods**

15  
16 Samples were collected from localities that displayed the typical outcrop  
17 characteristics of either the WS or the ES. Zircons were recovered from heavy  
18 mineral concentrates obtained by the standard method of crushing, grinding,  
19 Wilfley table, magnetic and heavy liquid separation at Universidad de Chile. Not  
20 all the samples yielded zircons, and from several only a few grains were  
21 obtained; the proportion of failed separates probably reflects a characteristic of  
22 the rocks, as this problem was unusual in previous work by the authors in the  
23 metasedimentary complexes in southern Chile. It is possible that the protolith of  
24 many of the WS schists was originally made up of distal fine-grained turbidites  
25 or mafic igneous rocks, relatively devoid of zircon crystals.

1

2 Zircon analyses were undertaken at RSES (Research School of Earth  
3 Sciences, The Australian National University, Canberra). The grains were  
4 mounted in epoxy, polished to about half-way through the grains, and CL  
5 (cathodo-luminescence) images were obtained for every zircon. U-Th-Pb  
6 analyses were then conducted using two sensitive high-resolution ion  
7 microprobes (SHRIMP II and SHRIMP RG) following the procedures described  
8 by Williams (1998). In some cases fewer than 70 individual zircon crystals were  
9 analysed (see Electronic Supplement), which may lead to enhanced  
10 uncertainties in the identification of detrital zircon age populations, although the  
11 general consistency of the resulting age distributions suggests that that this is  
12 not a significant problem.

13  
14 Oxygen ( $^{18}\text{O}/^{16}\text{O}$ ) and Lu-Hf ( $^{176}\text{Lu}/^{177}\text{Hf}$  and  $^{176}\text{Hf}/^{177}\text{Hf}$ ) isotope ratios were  
15 measured in a selection of detrital zircons from various samples with the aim of  
16 better defining possible source rocks. Following the U-Pb analyses, the  
17 SHRIMP 1-2 $\mu\text{m}$  deep U-Pb pits were lightly polished away and oxygen isotope  
18 analyses made in exactly the same location using SHRIMP II fitted with a Cs ion  
19 source and electron gun for charge compensation as described by Ickert et al.  
20 (2008). Oxygen isotope ratios were determined in multiple collector mode using  
21 an axial continuous electron multiplier (CEM) triplet collector, and two floating  
22 heads with interchangeable CEM - Faraday Cups. The Temora 2, Temora 3  
23 and FC1 reference zircons were analysed to monitor and correct for isotope  
24 fractionation. The measured  $^{18}\text{O}/^{16}\text{O}$  ratios and calculated  $\delta^{18}\text{O}_{\text{VSMOW}}$  values  
25 have been normalised relative to an FC1 weighted mean  $\delta^{18}\text{O}$  value of +5.4 ‰



1 (Ickert et al., 2008). Reproducibility in the Duluth Gabbro FC1 reference zircon  
2  $\delta^{18}\text{O}$  value ranged from  $\pm 0.23$  ‰ to  $0.47$  ‰ ( $2\sigma$  uncertainty) for the analytical  
3 sessions, with most of the reference zircon analytical uncertainties in the range  
4  $0.21$ - $0.42$  ‰ ( $\pm 2\sigma$ ). As a secondary reference, zircons from the Temora 2 or  
5 Temora 3 zircons analysed in the same analytical sessions gave  $\delta^{18}\text{O}$  values of  
6  $+8.2$  ‰ and  $+7.59$  ‰ respectively, in agreement with data reported by Ickert et  
7 al. (2008) and unpublished data for the Temora 3 reference zircon.

8  
9 Lu-Hf isotopic measurements were conducted by laser ablation multi-collector  
10 inductively coupled plasma mass spectroscopy (LA-MC-ICPMS) using a  
11 Neptune MC-ICPMS coupled with a 193 nm ArF Excimer laser; similar to  
12 procedures described in Munizaga et al. (2008). Laser ablation analyses were  
13 centred on the same locations within single zircon grains used for both the U-Pb  
14 and oxygen isotope analyses described above. For all analyses of unknowns or  
15 secondary standards, the laser spot size was c.  $47$   $\mu\text{m}$  in diameter. The mass  
16 spectrometer was first tuned to optimal sensitivity using a large grain of zircon  
17 from the Mud Tank carbonatite (see Woodhead and Hergt, 2005). Isotopic  
18 masses were measured simultaneously in static-collection mode. A gas blank  
19 was acquired at regular intervals throughout the analytical session (every 12  
20 analyses). The laser was fired with typically 5–8 Hz repetition rate and 50–60  
21 mJ energy. Data were acquired for 100 seconds, but in many cases we  
22 selected an interval over which the  $^{176}\text{Hf}/^{177}\text{Hf}$  ratios were consistent.

23 Throughout the analytical session several widely used reference zircons  
24 (91500, FC-1, Mud Tank and Temora-2 or -3) were analysed to monitor data  
25 quality and reproducibility. Signal intensity was typically ca. 5–6 V for total Hf at

1 the beginning of ablation, and decreased over the acquisition time to 2 V or  
2 less. Isobaric interferences of  $^{176}\text{Lu}$  and  $^{176}\text{Yb}$  on the  $^{176}\text{Hf}$  signal were corrected  
3 by monitoring signal intensities of  $^{175}\text{Lu}$  and  $^{173}\text{Yb}$ ,  $^{172}\text{Yb}$  and  $^{171}\text{Yb}$ . The  
4 calculation of signal intensity for  $^{176}\text{Hf}$  also involved independent mass bias  
5 corrections for Lu and Yb.

#### 7 **4. Analysed samples**

8  
9 The age spectra of detrital zircons from six samples of micaschist from the WS  
10 and four metasandstones from the ES were determined. Analyses were also  
11 made on samples whose relationships with the coastal accretionary complex  
12 are not well established. These are a white mica-biotite paragneiss, a biotite-  
13 hornblende tonalite and a mylonite from a hitherto undated igneous and  
14 metamorphic complex at Liquiñe and a biotite-muscovite paragneiss from the  
15 Parque Alerce Andino area, whose relationships with the coastal accretionary  
16 complex are not well established, were also analysed. A felsic volcanic rock  
17 (FO0603), a biotite-perthite granodiorite (belonging to the Huingancó complex  
18 at Huaraco) and a biotite-hornblende tonalitic gneiss (SMA) from neighbouring  
19 parts of Argentina were dated, as they were considered potential source rocks  
20 for the detrital zircons of the coastal accretionary complex. The geographical  
21 location of all samples is listed in Table 1 and shown in Fig. 1, together with U-  
22 Pb ages for the mid-Carboniferous Coastal Batholith samples. Brief  
23 petrographic descriptions of analysed samples are given in Table 1. The most  
24 important place names referred to in the text are partly shown in Fig. 1; for  
25 others please refer to the corresponding references.

1  
2  
3  
4  
5  
6  
7  
8  
9  
10  
11  
12  
13  
14  
15  
16  
17  
18  
19  
20  
21  
22  
23  
24  
25  
26  
27  
28  
29  
30  
31  
32  
33  
34  
35  
36  
37  
38  
39  
40  
41  
42  
43  
44  
45  
46  
47  
48  
49  
50  
51  
52  
53  
54  
55  
56  
57  
58  
59  
60  
61  
62  
63  
64  
65

## 5. Previous geochronological data

Existing detrital zircon age data from this great expanse of the Chilean metamorphic basement is very scarce. Two U-Pb LA-ICP-MS detrital zircon patterns reported by Willner et al. (2008) - one each from WS and ES rocks, near the northern end of the study area - are shown in Fig. 2. The ES sample is in reasonable agreement with the data obtained here, but the WS sample shows significant differences, lacking any prominent Carboniferous zircon grains as reported herein (see below).

Duhart et al. (2001) report sparse detrital zircon TIMS U-Pb data for WS samples from the southern area. They obtained an upper intercept age of  $266 \pm 14$  Ma based on analysis of 6 discordant zircon crystals from Hueyusca and suggested maximum depositional ages based on single concordant grains of 275 Ma and 305 Ma (Pucatrihue), 278 Ma (Isla Mancera) and 285 Ma (Punta Huezhui), as well as older limits of 369 Ma (El Mirador) and 388 Ma (Guabún). In addition, they reported a U-Pb zircon crystallization age of  $396 \pm 1$  Ma for a trachyte at Zarao emplaced in mafic schists. Söllner et al. (2000) report a discordia line with a lower intercept of  $293 \pm 23$  Ma interpreted as the crystallization age of a meta-ignimbrite, a rare constituent of the WS.

Metamorphic ages can also be used to place a limit on the time of deposition, but give no information with respect to provenance. Hervé et al. (1984) reported a Rb-Sr whole-rock isochron age of  $310 \pm 11$  Ma ( $2\sigma$ ) for

1 blueschists/greenschists at Pichilemu (WS, northern area). Willner et al. (2005)  
2 used the Ar-Ar method on white mica to date the high P/T metamorphism of the  
3 WS to between 320 and 288 Ma and the high-temperature metamorphism of  
4 the ES to between 302 and 294 Ma, near the northern part of the study area. In  
5 the southern portion of the WS, Duhart et al. (2001) concluded, based on  
6 numerous Rb-Sr, K-Ar and Ar-Ar ages that the main metamorphism occurred at  
7 260-220 Ma, and the high P/T blueschist metamorphism at 320–300 Ma. More  
8 recently, Glodny et al. (2008) obtained Rb-Sr mineral isochron ages (essentially  
9 white mica ages) between 307 and 272 Ma for the ES outcrops north of the  
10 Lanalhue Fault Zone and 295 to 255 Ma for the WS to the south. Kato and  
11 Godoy (1995) dated white micas ( $304 \pm 9$  Ma, K-Ar) in rare eclogite boulders in  
12 the WS at Los Pabilos; these rocks subsequently yielded Ar-Ar ages of  $325 \pm 1$   
13 Ma for white mica (Kato et al., 1997) and  $361 \pm 2$  Ma for amphibole relict from the  
14 eclogite facies metamorphism (Kato et al., 2008). The overprinting event was  
15 dated at  $305 \pm 3$  Ma from a Rb-Sr mineral isochron by Willner et al. (2004), who  
16 dispute the older age of Kato et al. (1997).

17  
18 The Liquiñe gneisses have been poorly dated at  $242 \pm 42$  Ma by the Rb-Sr  
19 isochron whole-rock method (Hervé and Munizaga, 1979).

20 Rocks dated as possible components of the source areas for the accretionary  
21 prism sediments as the deformed tonalitic intrusive body at San Martín de los  
22 Andes has been dated as Devonian by U-Pb methods on zircon by Varela et al.  
23 (2005) and Pankhurst et al. (2006), the latter authors reporting a result of  $401 \pm$   
24  $3$  Ma, with a further age of  $395 \pm 3$  Ma for a granite outcrop 10 km to the north.

25 Also the Huingancó granite and a rhyolite from the Arroyo del Torreón

1 Formation of Cordillera del Viento had previous SHRIMP U-Pb zircon ages of  
2  $327.9 \pm 2$  Ma (Suarez et al., 2008) and  $281.8 \pm 2.1$  Ma respectively (in Ramos  
3 et al., 2011), in close coincidence with our results (see below)

## 5 **6. Results**

### 7 **6.1. U-Pb Zircon Data**

9 Analytical data for the studied samples are presented in Supplementary Tables  
10 S1 to S18, available from journal website. Age versus probability density  
11 diagrams for all the samples are presented in Figs 3-7. The most striking  
12 difference in the age distributions recorded is between the southern segment of  
13 the WS and the other samples.

15 All samples of the ES (Fig. 3) and the northern area WS samples (Fig. 4) show  
16 major input from Ordovician (c. 470 Ma = Famatinian) sources. In addition  
17 peaks at 530–510 Ma (Pampean), and 950–1250 Ma ('Grenvillian') are present  
18 in many, albeit in variable proportions, and sparse 'Brasiliano' (640–590 Ma)  
19 and Paleoproterozoic to Archaean ages are sometimes observed. These  
20 constitute the main features of a typical western 'Gondwana' margin  
21 provenance signature (Ireland et al.1998; Cawood et al.1999; Hervé et al. 2003;  
22 Goodge et al. 2004). In the northern segment, ES and WS samples have similar  
23 detrital zircon age spectra but the maximum possible sedimentation ages  
24 determined by the youngest reliable detrital zircons are significantly younger in  
25 the latter (mostly c. 330 Ma as opposed to mostly c. 345 Ma). This difference is

1 also apparent in the two samples analysed by Willner et al. (2008), albeit with  
2 older limits of 335 Ma (WS) and 365 Ma (ES). All zircons are older than the mid-  
3 Carboniferous Coastal Batholith, with the exception of some as young as 305  
4 Ma in the sample from Putu (FO1015). There is a high proportion of Proterozoic  
5 zircon grains (Table 2), although this is significantly lower in the younger Putu  
6 sample. With the exception of FO0966 and the two samples analysed by Willner  
7 et al. (2008), there are few zircons in the age range 350–450 Ma, a robust peak  
8 at 465–470 Ma and a significant proportion in the range 500–530 Ma.

9  
10 FO1018D (Fig. 5) is an exception, as it was previously mapped as part of the  
11 ES, but the well cleaved metasandstone-metapelite alternation gives a Jurassic  
12 sedimentation age and thus belong to the units deposited in the Hualañé-  
13 Gualleco extensional basin (Belmar and Morata, 2005), lying unconformably  
14 over the accretionary rocks. Its zircon age pattern indicates derivation from the  
15 erosion of the accretionary prism together with zircons from the Coastal  
16 Batholith (see below) and Jurassic igneous rocks.

17  
18 In the southern segment, the ES provenance patterns (Fig. 3) are similar to  
19 those in the north, but the WS samples (Fig. 4) have very different detrital zircon  
20 age spectra. All of the latter have a predominant population of zircons in the  
21 range 250–300 Ma (with a peak at c. 290 Ma). As in all the ES samples, the  
22 youngest Carboniferous zircons are around 345 Ma, but there is a significant  
23 Devonian input with ages between 350 and 420 Ma (peaking at around 380  
24 Ma). The Ordovician peak at 470 Ma is essentially absent from the southern

1 WS spectra and the proportion of Neoproterozoic ages is much smaller (<  
2 20%); zircons older than 'Grenvillian' are completely absent.

3  
4  
5  
6  
7 4 The Coastal Batholith yielded very consistent mid-Carboniferous U-Pb zircon  
8  
9  
10 5 ages of 300 to 320 Ma (late Mississippian to early Pennsylvanian) along its 700  
11  
12 6 km extent (see Fig. 1). The significance of the results from the Coastal  
13  
14 7 Batholith, including O and Lu-Hf isotope determinations on zircons, will be  
15  
16  
17 8 presented in a separate paper (Deckart et al., in prep).

18  
19  
20  
21  
22 10 The Liquiñe gneisses are considered to form part of the Colohuincul complex,  
23  
24 11 whose main outcrops are on the eastern slope of the Andes in Argentina (Hervé  
25  
26 12 et al. 1974). Sample FO0605 (Fig. 6) has a relatively low yield of complex zircon  
27  
28 13 grains and only 30 grains have been analysed. A number of the grains have a  
29  
30  
31 14 zoned core and homogeneous rim structure as seen under CL imaging (Fig. 6),  
32  
33  
34 15 or show a mottled texture consistent with alteration of mostly primary igneous  
35  
36 16 zircon. The resultant age spectra is quite varied, suggesting a polygenetic  
37  
38  
39 17 provenance. Three metamorphic rims, with low Th/U ratios ( $\leq 0.01$ ) record  
40  
41 18 Triassic ages; one of these grains has a Devonian core (grain 25 at c. 400 Ma).  
42  
43  
44 19 Four other grains record ages  $\leq 380$  Ma and three of these have low Th/U ratios  
45  
46 20  $\leq 0.01$ ; namely, analyses of mottled areas in grains 4 and 9, and an interpreted  
47  
48 21 metamorphic rim to grain 14. Note that grain 14 also has a Devonian core (c.  
49  
50  
51 22 380 Ma). The zoned igneous core to grain 21 is c. 330 Ma and has a normal  
52  
53 23 Th/U ratio for igneous zircon (c. 0.36). Whilst a single analysis does not  
54  
55  
56 24 constrain the maximum time of deposition for the protolith to this Liquiñe gneiss

1 it is either at c. 330 Ma, or the grouping at c. 380 Ma indicating a possible  
2 Devonian depositional age (Fig. 6).

3  
4 In the Parque Alerce Andino sample (FO0935; Fig. 6), many of the zircon grains  
5 have thin, ragged homogeneous CL overgrowths that are less than 10  $\mu\text{m}$  in  
6 width. The main components of these grains range in CL structure from  
7 oscillatory (grain 55) and sector zoning (grain 67) to more homogeneous,  
8 interpreted metamorphic CL features (grain 61). Core and rim areas were  
9 analysed on 4 grains, mostly recording Devonian or older ages. Grain 8  
10 however has a Triassic rim with a Grenville-age core. Four other grains record  
11 relatively young ages  $\leq 230$  Ma (grains 1, 55, 61 and 67) demonstrating that this  
12 rock has a protolith as young as Late Triassic or Early Jurassic. The prominent,  
13 but thin metamorphic rims probably formed in response to the Jurassic 182 and  
14 162 Ma intrusive event indicated by the mylonite (FO0606) and mylonitic  
15 granodiorite (FO0609) of the Liquiñe area, which has not up to now been  
16 detected in the poorly studied Alerce Andino area.

17  
18 The orthogneiss from San Martin de los Andes in Argentina records a well  
19 defined magmatic zircon crystallization age of  $393 \pm 3$  Ma in good agreement  
20 with the  $401 \pm 3$  Ma result of Pankhurst et al. (2006). Crystallization ages of  $283$   
21  $\pm 2$  Ma (Huingancó granite) and  $326 \pm 3$  Ma for a rhyolite of the Arroyo del  
22 Torreón Formation (Llambías et al (2007) were obtained from Cordillera del  
23 Viento in Argentina. These results, mentioned by Godoy et al. (2008), are  
24 shown in Figure 7.

25



## 6.2. Oxygen and Lu-Hf isotope data in zircons

In order to characterise, and trace potential source(s) of the detrital zircon grains oxygen and Lu-Hf isotope ratios were determined on a selection of the zoned igneous zircon components discussed above, mostly in the age range 250-580 Ma, with some random older grains (Supplementary Table S19). Whilst some Hf data are available from both detrital zircons and source rocks of geological units related to the ones studied here, there are few or no published oxygen isotope data. Hf studies have thus far concentrated on detrital zircon and in general the aim in such studies has been to cover the full gambit of the age spectra recorded; see for example Willner et al. (2008), Bahlburg et al. (2009), Rapela et al. (2010). More focused studies on specific age ranges are less common, but likely to be of greater value in unravelling specific detrital zircon sources (see Fanning et al., 2011). Further, by combining Lu-Hf with oxygen isotope analyses an extra dimension in characterisation and source identification is likely.

The Lu-Hf data on detrital zircons are presented in Figure 8a. Most of the analysed grains are typical magmatic zircons, with well developed oscillatory or sector zoning. In the samples from the WS, all the Permian zircons have negative initial  $\epsilon_{\text{Hf}}$  values (-1 to -8) similar to those shown by detrital zircons of similar age on the basement units of southern Chile and Antarctic Peninsula (Fanning et al., 2011). This indicates that the magmatic sources are evolved and have resided in the continental lithosphere for some time; i.e., there is a strong crustal contribution. The Early Paleozoic zircons include some with

1 slightly positive  $\epsilon_{\text{Hf}}$  values (up to +2), suggesting that the source of these  
2 zircons has been influenced by the addition of mantle-derived components  
3 within predominantly crustal magmas. The main exception, however, is for  
4 zircons that crystallized during the period c. 330 to 305 Ma, which have  
5 uniformly positive initial  $\epsilon_{\text{Hf}}$  values (+4 to +5) indicating a pulse of relatively  
6 juvenile magma overlapping emplacement of the Coastal Batholith. The  
7 Permian Huingancó granite in the Cordillera del Viento of Argentina is more  
8 juvenile than the rest of the predominant coeval detrital grains, with  $\epsilon_{\text{Hf}}$  values  
9 mostly in the range zero to -2.

10  
11 O isotope data on the same detrital zircons are presented in Figure 8b. The  
12  $\delta^{18}\text{O}$  values are mostly more positive than +6.5‰, well above the range  
13 recorded by zircons with a mantle oxygen isotope signature. This data confirms  
14 the strong crustal influence, especially in the pre-Carboniferous zircons, with a  
15 general trend to more primitive compositions, lower  $\delta^{18}\text{O}$ , from the older to the  
16 younger grains. Again, the only typical mantle values are shown by some of the  
17 grains in the age range of the Coastal Batholith and slightly older, i.e., 305–330  
18 Ma.

## 19 20 **7. Discussion**

### 21 22 **7.1. Provenance indications**

23  
24 The older components in the provenance patterns of all samples show a range  
25 of Early Paleozoic, Neoproterozoic and scarce older detrital zircons typical of

1  
2  
3  
4  
5  
6  
7  
8  
9  
10  
11  
12  
13  
14  
15  
16  
17  
18  
19  
20  
21  
22  
23  
24  
25  
26  
27  
28  
29  
30  
31  
32  
33  
34  
35  
36  
37  
38  
39  
40  
41  
42  
43  
44  
45  
46  
47  
48  
49  
50  
51  
52  
53  
54  
55  
56  
57  
58  
59  
60  
61  
62  
63  
64  
65

1 the Early Paleozoic tectonomagmatic belts of southern South America, notably  
2 the Pampean (Cambrian) and Famatinian (Ordovician) belts of western  
3 Argentina (e.g., Rapela et al., 2007; Verdecchio et al., 2011). These belts  
4 formed on the paleo-Pacific margin of the continent and are the most obvious  
5 sources for the older zircons in the basement complexes west of the Andes.  
6 The scarce Paleoproterozoic and Archaean content is similarly attributable,  
7 having been reworked from cratonic sources that are not specifically  
8 identifiable. The samples analysed in this study are more remarkable for the  
9 variations in their Late Paleozoic provenance, which are more diagnostic of  
10 tectonic influences in the sedimentary environment.  
11  
12 The prominent Early Permian provenance in the southern sector WS, which is  
13 absent from the remaining basement areas studied here, is traceable to the  
14 voluminous Permian igneous rocks of the Choyoi province and/or the  
15 presumably related subvolcanic granites of the North Patagonian Massif, the  
16 latter occurring directly to the present east of the coastal basement outcrops at  
17 40°–41°S. Although the major Choyoi rhyolite volcanism occurred rather later  
18 (250-260 Ma), recently published U-Pb zircon ages confirm an early phase at c.  
19 280 Ma (Rocha-Campos et al., 2011) and many of the Patagonian granites  
20 were emplaced at this time (Pankhurst et al., 2006), as was the Huingancó  
21 granite. Such a correlation would be compatible with the broadly crustal Hf  
22 isotope signature noted above for the Permian zircons (Fanning et al., 2011).  
23 The Choyoi province exhibits its major development north of about 34°S, but the  
24 absence of similar detritus from the ES and the northern sector of the WS is

1 explained by the fact that these rocks were deposited earlier, in Carboniferous  
2 times.

3  
4  
5  
6  
7 4 The Carboniferous provenance of the basement samples studied here indicated  
8  
9  
10 5 by the major peaks in their detrital zircon patterns are c. 345 Ma in the ES and  
11  
12 6 c. 330 Ma in the northern sector WS. These are maximum ages for deposition,  
13  
14 7 which as discussed above was pre-Permian. The fact that the ES is intruded by  
15  
16 8 the 300–320 Ma Coastal Batholith and the absence of zircons derived therefrom  
17  
18 9 means that these peak ages are probably very close estimates of sedimentation  
19  
20 10 age, which is thus constrained to the Mississippian (Early Carboniferous). Early  
21  
22 11 Carboniferous subduction-related granitoids of predominantly A-type  
23  
24 12 geochemistry, many with U-Pb zircon ages of c. 340–350 Ma, occur in the  
25  
26 13 Eastern Sierras Pampeanas of Argentina at 27–30°S (see Alasino et al., in  
27  
28 14 press, and references therein). It seems quite possible that similar magmatism  
29  
30 15 extended farther south than the Sierras Pampeanas, which are only exposed as  
31  
32 16 a result of uplift and exhumation above the 'flat-slab' portion of the Andean  
33  
34 17 subduction system, and that this is the source of the detrital zircons in the ES.  
35  
36 18 Carboniferous subduction-related magmatism migrated or jumped towards the  
37  
38 19 Pacific during the mid-Carboniferous and arc-derived I-type granitoids of 310–  
39  
40 20 330 Ma are known in the Frontal Cordillera itself (albeit so far without U-Pb  
41  
42 21 zircon ages). This event is also registered in the western border of the North  
43  
44 22 Patagonian Massif (Pankhurst et al., 2006) and there is no doubt that  
45  
46 23 subduction was active at this time along the whole of the Chilean proto-Pacific  
47  
48 24 margin. This is the obvious source of the younger Carboniferous detrital zircon  
49  
50 25 peaks seen in the northern sector WS. The virtual absence of zircons of  
51  
52  
53  
54  
55  
56  
57  
58  
59  
60  
61  
62  
63  
64  
65

1 Carboniferous age from the post-Early Permian southern WS probably indicates  
2 that the Coastal Batholith was not exhumed in this area during the Permian.  
3 The remaining difference between the northern and southern sectors is the  
4 significant proportion of Devonian detrital zircon in the latter which is largely  
5 absent from the former (although a few grains are seen in the northern WS  
6 samples). Bahlburg et al. (2009) also noted the scarcity or absence of Devonian  
7 detrital zircons in late Paleozoic metasedimentary rocks in northern Chile (31°–  
8 22°S). This is discussed further below.

## 10 **7.2. Provenance of Devonian detrital zircons**

11  
12 There is abundant evidence for Devonian magmatism and deformation in the  
13 eastern flank of the main Andean cordillera between 39° and 42°S that can be  
14 considered the most likely source of Devonian detrital zircons in the southern  
15 part of the Western Series. This is represented around San Martín de los Andes  
16 (c. 40°S, 71°W; see Fig. 1) by small outcrops of variably deformed igneous,  
17 orthogneissic and migmatitic rocks, consistently dated at c. 385–405 Ma by  
18 Varela et al. (2005), Pankhurst et al. (2006), Godoy et al. (2008) and the  
19 present paper (sample SMA,  $393.5 \pm 2.6$  Ma). Such a belt could even extend  
20 southeastwards to Colan Conhué at 43°S, 70°W (see figure 3 of Pankhurst et  
21 al., 2006). Lucassen et al. (2004) published a Rb-Sr mineral isochron age of  
22  $368 \pm 9$  Ma for a migmatite from San Martín de Los Andes, and a  $^{206}\text{Pb}$ - $^{238}\text{U}$   
23 age of  $380 \pm 2$  Ma for titanite from a gneiss–migmatite association 100 km  
24 further southeast near Piedra del Aguila, interpreted as approximating the time  
25 of the metamorphic peak. In the Alumine area at c. 39°S, approximately 150 km

1 north of San Martín, the oldest K-Ar age on fine fractions of metamorphic  
2 schists (c. 370 Ma; Franzese, 1995) indicates Late Devonian deformation or  
3 cooling of these rocks, and the overall range (c. 300–370 Ma) is consistent with  
4 partial resetting of the K-Ar system by contact metamorphism in the late  
5 Paleozoic. Devonian Rb-Sr whole-rock isochron ages have been obtained from  
6 metasedimentary rocks of the Cushamen Formation in the North Patagonian  
7 Massif close to Colán Conhué (Ostera et al., 2001). Recently, Martínez et al.  
8 (2011) have published single electron microprobe Th-U-total Pb monazite ages  
9 of  $392 \pm 4$  Ma and  $350 \pm 6$  Ma (interpreted as indicating collision metamorphism  
10 and a later retrograde event, respectively) in schists belonging to the  
11 Colohuincul complex on the eastern slope of the Andes near San Carlos de  
12 Bariloche (41°S). Ramos et al. (2010) have shown that Colohuincul complex  
13 rocks include Devonian detrital zircon grains. Even farther south at 42°–43°S in  
14 the western flank of the Andes, albeit on the coast, Duhart (2008) reports the  
15 existence of foliated granitoids of similar Devonian ages: the Chaitén  
16 metatonalite (c. 400 Ma) and the Pichicolo microdiorite (c. 386 Ma).  
17  
18 In one respect, the absence of Devonian detrital zircon in the northern region of  
19 the Central Chile basement is notable. Devonian granite magmatism and  
20 shearing in the sierras of Córdoba and San Luis of northwest Argentina have  
21 been dated by U-Pb and Ar-Ar methods and interpreted as constituting the  
22 Achalian orogeny (see Sims et al., 1998; Stuart-Smith et al., 1999). Dorais et al.  
23 (1997) and Rapela et al. (2008) have dated the major intrusive representative,  
24 the Achala granite batholith, with U-Pb zircon ages of  $368 \pm 2$  to  $379 \pm 4$  Ma.  
25 From c. 200 km to the southwest, in the Frontal Cordillera, Willner et al. (2010)

1 published Lu-Hf mineral isochrons for garnetiferous pelitic schists and  
2 amphibolites of the Guarguaraz complex, obtaining consistent ages of  $390 \pm 2$   
3 Ma. Additionally, Heredia et al. (2012) report the presence of clasts of plutonic  
4 rocks of western provenance in the Devonian Vallecito Formation on the  
5 eastern slope of the Andes at  $34^{\circ}\text{S}$ , which they relate to magmatism in Chilenia  
6 during pre-collisional west-directed subduction of the intervening ocean  
7 between Chilenia and Gondwana. Thus, although genetically different from the  
8 Devonian belt 600 km away in the southern region, there is clear expression of  
9 a contemporaneous mid-Devonian igneous and metamorphic belt to the east of  
10 the northern part of our study area, at latitudes  $31\text{--}34^{\circ}\text{S}$ .

### 12 **7.3. Tectonic considerations**

14 Thus contemporaneous Mid-to-Late Devonian granitoids and metasedimentary  
15 rocks, variously affected by tectonism, and metamorphic/thermal events,  
16 developed within the western margin of this segment of Gondwana from c.  $28^{\circ}$   
17 to  $42^{\circ}$  or even  $43^{\circ}\text{S}$  (Fig. 9). Regardless of their varied petrogeneses, these  
18 Devonian rocks constituted an eroding area while sediments of the southern  
19 portion of the WS were being deposited during the Permian, as Devonian  
20 zircons are found therein. The fact that few detrital zircons of this age reached  
21 the Early Carboniferous proto-Pacific margin deposits in the north may mean  
22 that they were still unexhumed at that time, but more probably indicate the  
23 presence of a topographical barrier. The Precordillera terrane could have  
24 formed such a barrier, having been accreted to the margin during the  
25 Ordovician Famatinian orogeny. Additionally, Stuart-Smith et al. (1999) ascribed

1 the Achaian magmatic and tectonic cycle to the Devonian collision of a further  
2 terrane to the west, i.e., Chilenia (Ramos et al., 1986). Massonne and Calderón  
3 (2008) and Willner et al. (2010) also argued that the P-T path determined for the  
4 metasedimentary rocks indicated crustal thickening, consistent with a Devonian  
5 terrane collision. A similar explanation for the metamorphism of the Colohuincul  
6 complex at 41°S was given by Martinez et al. (2011). A problem with the latter  
7 interpretation is that, according to current models, the southern limit of the  
8 Chilenia terrane is the E–W Huincul lineament, located near the latitude of the  
9 Lanahue Fault Zone (37°–38°30'S). Extension of Chilenia to 41°S to explain the  
10 Devonian metamorphism is problematic since at that latitude the coastal  
11 accretionary complex extends eastwards as far as the western flank of the  
12 present-day Andes, leaving little space for an intervening continental sliver. As  
13 suggested by Kato et al. (2008), subduction was already active here in the  
14 Devonian, a view that is supported by data presented here and by McDonough  
15 et al. (as cited by Duhart et al., 2001). Thus the proposed Devonian  
16 metamorphism of the Colohuincul complex could be related to the subduction  
17 episode that gave rise to the Devonian arc plutons, probably in a back-arc  
18 position. Another possible alternative is that the rocks studied by Martinez et al  
19 (2011) were tectonically “extruded” to the south of the Chilenia terrane limit  
20 during and or after the Chilenia–Gondwana collision. Also, as already pointed  
21 out by Duhart et al. (2001), sedimentation of the southern portion of the WS  
22 took place during the Permian, well after the peak metamorphism of the  
23 eclogites and blueschists.

24



1 Further difficulties for the Chilenia hypothesis are that no Devonian I-type  
2 plutons are known from the northern area and Rapela et al. (2008) showed the  
3 Achala granites to be geochemically peraluminous A-type rather than collision-  
4 related S-type. Alasino et al. (in press) have argued that the Devonian and Early  
5 Carboniferous A-type granites were generated above a zone of flat-slab  
6 subduction followed by rapid roll-back and renewed subduction with  
7 increasingly I-type magmatism at the Late Carboniferous margin outboard of an  
8 extensive retro-arc.

9  
10 Thus the mid-Carboniferous metasedimentary basement of the northern sector  
11 should have involved a wide Late Paleozoic depositional basin prior to the  
12 establishment of the Coastal Batholith. This basin developed either on the  
13 trailing edge of an exotic terrane accreted in the Devonian (Chilenia) or a long-  
14 lived accretionary platform west of the Precordillera terrane accreted in the  
15 Ordovician. Sedimentary detritus could have been received from  
16 contemporaneous Early Carboniferous I-type and A-type igneous activity far to  
17 the east but apparently did not include material from the Devonian complexes,  
18 which may have been buried at the time. It is also notable that there is a  
19 scarcity of zircons of *c.* 570 Ma, which Alvarez et al. (2011) suggested as  
20 possibly indicating the basement of Chilenia.

21  
22 In northern Patagonia, Carboniferous I-type magmatism represents east-to-  
23 northeastward subduction at 330 Ma (Pankhurst et al., 2006). The northernmost  
24 proven outcrop of these rocks near Bariloche is less than 100 km south of the  
25 Devonian magmatic and metamorphic rocks around San Martin de los Andes

1 (ibid., their figure 2) and thus appear to be slightly inboard of the Devonian  
2 margin. It is often considered that northern Patagonia collided with the rest of  
3 South America in the Carboniferous as in the model of Ramos (2008 for the  
4 latest version), and the paleomagnetic data would allow a separation of up to  
5 about 1500 km across the intervening 'Colorado Ocean' (Rapalini et al., 2010).  
6 If this were so we should expect a major discontinuity in the Devonian and Early  
7 Carboniferous record at the latitude of the Huincul Ridge at 39°S, which is not  
8 apparent. The collision suture suggested by Pankhurst et al. (2006) was south  
9 of the North Patagonian Massif and the Carboniferous outcrops, and so might  
10 still be viable, but if the Devonian granite at Colan Conhue is considered to be a  
11 continuation of the Devonian belt at San Martin de los Andes, this model also  
12 would be doubtful.

## 14 **8. Conclusions**

16 The metasedimentary basement rocks of Central Chile north of the Lanalhue  
17 lineament (c. 37°–38°30'S) form a penecontemporaneous paired metamorphic  
18 belt. Our data show that the Eastern Series was deposited in Early  
19 Carboniferous times, shortly before the Western Series but both prior to  
20 emplacement of the 305–320 Ma subduction-related Coastal Batholith, which  
21 intrudes the former. The provenance for both series was older Gondwana  
22 margin basement of the Pampean and Famatinian belts, including reworked  
23 cratonic material, and Carboniferous magmatism east of the present-day  
24 Andes. Metamorphism of the accretionary wedge seems to have overlapped

1 with the late plutonic phase, but may have continued later in the high P/T  
2 Western Series.  
3  
4  
5  
6  
7 4 The Eastern Series is of limited extent south of about 39°S, but is similar to the  
8  
9  
10 5 low P/T metasedimentary series in the north. However the predominant  
11  
12 6 Western Series in the southern sector is much younger, with abundant Permian  
13  
14 7 detritus derived from the Choiyoi province or subvolcanic plutonic rocks in the  
15  
16  
17 8 North Patagonian Massif. There is also a secondary provenance of Devonian  
18  
19 9 age which is absent from its northern counterpart and the entire Eastern Series.  
20  
21  
22 10 O and Lu-Hf data indicate a mature crustal source for all zircons except those  
23  
24 11 that crystallized during Carboniferous subduction.  
25  
26  
27 12  
28  
29 13 Analysis of igneous and metamorphic rocks from farther east show that inboard  
30  
31 14 of the southern sector there is a Devonian igneous and metamorphic block or  
32  
33  
34 15 belt of more significant extent than has been previously noted, which is the  
35  
36 16 presumed source of the detritus of this age in the southern Western Series. The  
37  
38  
39 17 relative paucity of Devonian provenance in the north is explained by a wide  
40  
41 18 crustal zone separating the Devonian igneous rocks of the Sierras Pampeanas  
42  
43  
44 19 in Argentina from the site of the Carboniferous accretionary deposits, including  
45  
46 20 the Precordillera terrane and possibly Chilenia, when subduction jumped to the  
47  
48  
49 21 west in the Early Carboniferous.  
50  
51  
52  
53 22  
54 23 The apparent continuity of the Devonian–Early Carboniferous magmatic and  
55  
56 24 metamorphic rocks as far as 43°S or more does not support the idea that the

1 North Patagonian Massif was separated from the rest of southern South  
2 America by a significant ocean at this time.

#### 4 **Acknowledgements**

6 This research is a main part of the FONDECYT project 1095099 and the  
7 International Collaboration project 7095099 of Comisión Nacional de  
8 Investigación Científica y Tecnológica (CONICYT). Thorough reviews that  
9 helped to improve the original version were provided by Dave Barbeau, Victor  
10 Ramos and an anonymous referee. Dr. Vreni Hausserman of Fundación Huinay  
11 provided logistic support to work on the extreme end of the studied area. M.  
12 Solari, C. Maureira, P. Hervé and B. Keller accompanied some of the field trips.

15 Supplementary item: Tables S1 to S19 available from the online version of the  
16 journal at: [yyyyyyyyy](#)

#### 18 **References**

20 Aguirre, L, Hervé, F, Godoy, E., 1972. Distribution of metamorphic facies in  
21 Chile, an outline. Kristalinikum, Prague 9, 7-19.  
22 Alasino, P.H., Dahlquist, J.A., Pankhurst, R.J., Galindo, C., Casquet, C.,  
23 Rapela, C.W., Larrovere, M., Fanning, C.M., in press. Early Carboniferous  
24 sub- to mid-alkaline magmatism in the Eastern Sierras Pampeanas, NW

1 Argentina: a record of crustal growth by the incorporation of mantle-derived  
2 material in an extensional setting. *Gondwana Research*.  
3 Álvarez, J., Mpodozis, C., Arriagada, C., Astini., R., Morata, D., Salazar, E.,  
4 Valencia, V.A., Vervoort, J.D., 2011. Detrital zircons from late Paleozoic  
5 accretionary complexes in northcentral Chile (28°-32° S): Possible  
6 fingerprints of the Chilenia Terrane. *Journal of South American Earth  
7 Sciences*, doi: 10.1016/j.jsames.2011.06.002  
8 Augustsson, C., Munker, M., Bahlburg, H., Fanning, M., 2006. Provenance of  
9 Late Palaeozoic metasediments of the SW South American Gondwana  
10 margin from combined U-Pb ages and Hf isotope compositions of single  
11 detrital zircons. *Journal of the Geological Society, London* 163, 983-995.  
12 Bahlburg, H., Vervoort, J.D., DuFrane, S.A., Bock, B., Augustsson, C., 2009.  
13 Timing of accretion and crustal recycling at accretionary orogens: insights  
14 learned from the western margin of South America. *Earth-Science Reviews*  
15 97, 227-253.  
16 Belmar, M., Morata, D., 2005. Nature and P-T-t constraints of very low-grade  
17 metamorphism in the Triassic-Jurassic basins, Coastal Range, central Chile.  
18 *Revista Geológica de Chile* 32 (2), 189-205.  
19 Campos, A., Moreno, H., Muñoz, J., Antinao, J., Clayton, J., Martin, M., 1998.  
20 Area de Futrono - Lago Ranco, Region de los Lagos. *Mapas Geológicos*,  
21 1:100.000, No. 8, SERNAGEOMIN, Santiago.  
22 Cawood, P.A., Nemchin, A.A., Leverenz, A., Saeed, A., Ballance, P.F., 1999.  
23 U/Pb dating of detrital zircons: implications for the provenance record of  
24 Gondwana margin terranes. *Geological Society of America Bulletin* 111,  
25 1107-1119.

1  
2  
3  
4  
5  
6  
7  
8  
9  
10  
11  
12  
13  
14  
15  
16  
17  
18  
19  
20  
21  
22  
23  
24  
25  
26  
27  
28  
29  
30  
31  
32  
33  
34  
35  
36  
37  
38  
39  
40  
41  
42  
43  
44  
45  
46  
47  
48  
49  
50  
51  
52  
53  
54  
55  
56  
57  
58  
59  
60  
61  
62  
63  
64  
65

1 Cawood, P.A., 2005. Terra Australis orogen: Rodinia breakup and development  
2 of the Pacific and Iapetus margins of Gondwana during the Neoproterozoic  
3 and Paleozoic. *Earth-Science Reviews* 69, 249-279.

4 Deckart et al. (in prep). The central Chile coastal batholith : zircon SHRIMP  
5 ages and Lu-Hf and O isotopic evidence of a short emplacement on a  
6 recycling continental margin.

7 Dorais, M., Lira, R., Chen, Y., Tingey, D., 1997. Origin of biotite-apatite-rich  
8 enclaves, Achala Batholith, Argentina. *Contributions to Mineralogy and  
9 Petrology* 130, 31-46.

10 Duhart, P., Mc Donough, M., Muñoz, J., Martin, M., Villeneuve, M., 2001. El  
11 Complejo Metamórfico Bahía Mansa en la Cordillera de la Costa del centro-  
12 sur de Chile (39°30'-42°S): geocronología K-Ar,  $^{40}\text{Ar}/^{39}\text{Ar}$  y U-Pb,  
13 implicancias en la evolución del margen sur-occidental de Gondwana.  
14 *Revista Geológica de Chile* 28, 179-208.

15 Duhart, P.L., 2008. Processos metalogenéticos em ambientes de arco  
16 magmático tipo andino, caso de estudo: mineralizações da região dos  
17 Andes Patagônicos setentrionais do Chile. Ph. D Dissertation, Sao Paulo  
18 University, 215 p., Sao Paulo.

19 Ernst, G., 1973. Blueschist metamorphism and P-T regimes in active  
20 subduction zones. *Tectonophysics* 17, 255-272.

21 Fanning, C. M., Hervé, F., Pankhurst, R.J., Rapela, C.W., Kleiman, L.E.,  
22 Yaxley, G.M., Castillo, P., 2011. Lu-Hf isotope evidence for the provenance  
23 of Permian detritus in accretionary complexes of western Patagonia and the  
24 northern Antarctic Peninsula region. *Journal of South American Earth  
25 Sciences* 32, 485 - 496.

1  
2  
3  
4  
5  
6  
7  
8  
9  
10  
11  
12  
13  
14  
15  
16  
17  
18  
19  
20  
21  
22  
23  
24  
25  
26  
27  
28  
29  
30  
31  
32  
33  
34  
35  
36  
37  
38  
39  
40  
41  
42  
43  
44  
45  
46  
47  
48  
49  
50  
51  
52  
53  
54  
55  
56  
57  
58  
59  
60  
61  
62  
63  
64  
65

1 Flowerdew, M.J., Millar, I.L., Curtis, M.L., Vaughan, A.P.M., Horstwood, M.S.A.,  
2 Whitehouse, M.J., Fanning, C.M., 2007. Combined U-Pb geochronology and Hf  
3 isotope geochemistry of detrital zircons Early Paleozoic Ellsworth Mountains  
4 Antarctica. Geological Society of America Bulletin 199, 275-288.

5 Fortey ,R., Pankhurst, R.J., Hervé, F., 1992. Devonian Trilobites at Buill, Chile  
6 (42°S). Revista Geológica de Chile 19, 133-144.

7 Franzese, J.R., 1995. El Complejo Piedra Santa (Neuquén, Argentina): parte de  
8 un cinturón metamórfico neopaleozoico del Gondwana suroccidental.  
9 Revista Geológica de Chile 22, 193-202.

10 Gana, P., Hervé, F., 1983. Geología del basamento cristalino de la Cordillera  
11 de la Costa entre los ríos Mataquito y Maule, VII Región. Revista Geológica  
12 de Chile 19, 37-56.

13 Glodny, J., Lohrmann, J., Echtler, H., Gräfe, K., Seifert, W., Collao, S.,  
14 Figueroa, O., 2005. Internal dynamics of a paleoaccretionary wedge:  
15 insights from combined isotope tectonochronology and sandbox modelling of  
16 the south-central Chilean fore-arc. Earth and Planetary Science Letters 231,  
17 23-39.

18 Glodny, J., Echtler, H., Figueroa, O., Franz, G., Gräfe, K., Kemnitz, H., Kramer,  
19 W., Krawczyk, C., Lohrmann, J., Lucassen, F., Melnick, D., Rosenau, M.,  
20 Seifert, W., 2006. Long-term geological evolution and mass flow balance of  
21 the South-Central Andes. In: Oncken, O., Chong, G., Franz, G., Giese, P.,  
22 Götze, H.-J., Ramos,V., Strecker, M., Wigger, P. (Eds.), The Andes - Active  
23 Subduction Orogeny. Frontiers in Earth Sciences, vol. 1. Springer Verlag,  
24 Berlin, pp. 401-442.

1  
2  
3  
4  
5  
6  
7  
8  
9  
10  
11  
12  
13  
14  
15  
16  
17  
18  
19  
20  
21  
22  
23  
24  
25  
26  
27  
28  
29  
30  
31  
32  
33  
34  
35  
36  
37  
38  
39  
40  
41  
42  
43  
44  
45  
46  
47  
48  
49  
50  
51  
52  
53  
54  
55  
56  
57  
58  
59  
60  
61  
62  
63  
64  
65

1 Glodny, J., Echtler, H., Collao, S., Ardiles, M., Burón, P., Figueroa, O., 2008.  
2 Differential Late Paleozoic active margin evolution in South-Central Chile  
3 (37°S - 40°S) - the Lanalhue Fault Zone. Journal of South American Earth  
4 Sciences 26, 397-411.

5 Godoy, E., 1970. El granito de Constitución y su aureola de metamorfismo de  
6 contacto. Graduation Thesis, Geology Department, Universidad de Chile,  
7 Santiago, 140 p.

8 Godoy, E., Hervé, F., Fanning, M., 2008. Edades U-Pb SHRIMP en granitoides  
9 del macizo norpatagónico: implicancias geotectónicas. XVII Congreso  
10 Geológico Argentino Vol. 3, 1288-1289.

11 Goodge, J.W., Williams, I.S., Myrow, P., 2004. Provenance of Neoproterozoic  
12 and lower Paleozoic siliciclastic rocks of the central Ross orogen, Antarctica:  
13 Detrital record of rift-, passive-, and active-margin sedimentation. Geological  
14 Society of America Bulletin 116, 1253-1279.

15 Heredia, N., Farias, P., García-Sanseguno, J and , Giambiagi, L., 2012. The  
16 Basement of the Andean Frontal Cordillera in the Cordón del Plata  
17 (Mendoza, Argentina): Geodynamic Evolution. Andean Geology 39 (2), 242-  
18 257.

19 Hervé, F., 1977. Petrology of the Crystalline Basement of the Nahuelbuta  
20 Mountains, Southcentral Chile. In Ishikawa, T. and Aguirre L. (Eds.),  
21 Comparative Studies on the Geology of the Circum Pacific Orogenic Belt in  
22 Japan and Chile. Japan Society for the Promotion of Science, 1-51, Tokyo.

23 Hervé, M., Munizaga, F., 1979. Antecedentes geocronológicos del área al este  
24 de Liquiñe, Cordillera de los Andes, latitud 39°45' S, Chile. Resúmenes, II  
25 Congreso Geológico Chileno, Arica, 45-46.



1  
2  
3  
4  
5  
6  
7  
8  
9  
10  
11  
12  
13  
14  
15  
16  
17  
18  
19  
20  
21  
22  
23  
24  
25  
26  
27  
28  
29  
30  
31  
32  
33  
34  
35  
36  
37  
38  
39  
40  
41  
42  
43  
44  
45  
46  
47  
48  
49  
50  
51  
52  
53  
54  
55  
56  
57  
58  
59  
60  
61  
62  
63  
64  
65

1 Hervé, F., Moreno, H., Parada, M.A., 1974. Granitoids of the Andean Range,  
2 Valdivia Province, Chile. *Pacific Geology* 8, 39-45.

3 Hervé, F., Kawashita, K., Munizaga, F., Basei, M., 1984. Rb-Sr isotopic ages  
4 from late Paleozoic metamorphic rocks of Central Chile. *Journal of the*  
5 *Geological Society, London* 141, 877-884.

6 Hervé, F., Fanning, C.M., Pankhurst, R.J., 2003. Detrital zircon age patterns  
7 and provenance in the metamorphic complexes of Southern Chile. *Journal*  
8 *of South American Earth Sciences* 16, 107-123.

9 Ickert, R.B., Hiess, J., Williams, I.S., Holden, P., Ireland, T.R., Lanc, P.,  
10 Schram, N., Foster, J.J., Clement, S.W., 2008. Determining high precision,  
11 in situ, oxygen isotope ratios with a SHRIMP II: Analyses of MPI-DING  
12 silicate-glass reference materials and zircon from contrasting granites.  
13 *Chemical Geology* 257, 114-128.

14 Ireland, T.R., Flötmann, T., Fanning, C.M., Gibson, G.M., Preiss, W.V., 1998.  
15 Development of the early Paleozoic Pacific margin of Gondwana from  
16 detrital-zircon ages across the Delamerian orogen. *Geology* 26, 243-246.

17 Kato, T.T., Godoy, E., 1995. Petrogenesis and tectonic significance of Late  
18 Paleozoic coarse-crystalline blueschist and amphibolite boulders in the  
19 coastal range of Chile. *International Geology Review* 37, 992- 1006.

20 Kato, T.T., Godoy, E., McDonough, M., Duhart, P., Martin, M., Sharp, W., 1997.  
21 Un modelo preliminar de deformación transpresional mesozoica y gran  
22 desplazamiento hacia el norte de parte de la serie occidental, complejo  
23 acrecionario (38°S a 43°S), Cordillera de la Costa. *Actas 8. Congreso*  
24 *Geológico Chileno, Antofagasta*, 1, 98-102.

1  
2  
3  
4  
5  
6  
7  
8  
9  
10  
11  
12  
13  
14  
15  
16  
17  
18  
19  
20  
21  
22  
23  
24  
25  
26  
27  
28  
29  
30  
31  
32  
33  
34  
35  
36  
37  
38  
39  
40  
41  
42  
43  
44  
45  
46  
47  
48  
49  
50  
51  
52  
53  
54  
55  
56  
57  
58  
59  
60  
61  
62  
63  
64  
65

1 Kato, T.T., Sharp, W., Godoy, E., 2008. Inception of a Devonian subduction  
2 zone along the southwestern Gondwana margin:  $^{40}\text{Ar}/^{39}\text{Ar}$  dating of  
3 eclogite - amphibolite assemblage in blueschist boulders from the Coastal  
4 Range of Chile ( $41^\circ\text{S}$ ). Canadian Journal of Earth Sciences 45, 337-351.

5 Llambías, E., Leanza, H., Carbone, O., 2007. Evolución tectono-magmática  
6 durante el Pérmico al Jurásico temprano en la Cordillera del Viento  
7 ( $37^\circ 05'/37^\circ 15'\text{S}$ ): nuevas evidencias geológicas y geoquímicas del inicio de  
8 la cuenca neuquina. Revista de la Asociación Geológica Argentina 62, 217-  
9 235.

10 Lucassen, F., Trumbull, R., Franz, G., Creixell, C., Vásquez, P., Romer, R.L.,  
11 Figueroa, O., 2004. Distinguishing crustal recycling and juvenile additions at  
12 active continental margins: the Paleozoic to recent compositional evolution  
13 of the Chilean Pacific margin ( $36^\circ$ - $41^\circ\text{S}$ ). Journal of South American Earth  
14 Sciences 17, 103-119.

15 Martinez, J.C., Dristas, J., Massonne, H.-J., 2011. Paleozoic accretion of the  
16 microcontinent Chilenia, North Patagonian Andes: high pressure  
17 metamorphism and subsequent thermal relaxation. International Geology  
18 Review 54 (4), 472-490.

19 Massonne, H.-J., Calderón, M. 2008., P-T evolution of metapelites from the  
20 Guarguaraz Complex, Argentina: evidence for Devonian) crustal thickening  
21 close to the western Gondwana margin. Revista Geológica de Chile 35, 215-  
22 231.

23 Miyashiro, A., 1961. Evolution of metamorphic belts. Journal of Petrology 2,  
24 277-311.

1  
2  
3  
4  
5  
6  
7  
8  
9  
10  
11  
12  
13  
14  
15  
16  
17  
18  
19  
20  
21  
22  
23  
24  
25  
26  
27  
28  
29  
30  
31  
32  
33  
34  
35  
36  
37  
38  
39  
40  
41  
42  
43  
44  
45  
46  
47  
48  
49  
50  
51  
52  
53  
54  
55  
56  
57  
58  
59  
60  
61  
62  
63  
64  
65

1 Munizaga, F., Maksaev, V., Fanning, C.M., Giglio, S., Yaxley, G., Tassinari,  
2 C.C.G., 2008. Late Paleozoic-Early Triassic magmatism on the western  
3 margin of Gondwana: Collahuasi area, Northern Chile. *Gondwana Research*  
4 13, 407-427.

5 Murphy, J.B., Nance, R.D., Cawood, P.A., 2009. Contrasting modes of  
6 supercontinent formation and the conundrum of Pangea. *Gondwana*  
7 *Research* 15, 408-420.

8 Ostera, H.A., Linares, E., Haller, M.J., Cagnoni, M.C., López de Luchi, M.,  
9 2001. A widespread Devonian metamorphic episode in Northern Patagonia,  
10 Argentina. III Simposio de Geología Isotópica, Pucón, Chile, Abstract  
11 Volume on CD-ROM, 600-603.

12 Pankhurst, R.J., Rapela, C.W., Loske, W.P., Márquez, M., Fanning, C.M., 2003.  
13 Chronological study of the pre-Permian basement rocks of southern  
14 Patagonia. *Journal of South American Earth Sciences* 16, 27-44.

15 Pankhurst, R.J., Rapela, C.W., Fanning, C.M., Márquez, M., 2006. Gondwanide  
16 continental collision and the origin of Patagonia. *Earth-Science Reviews* 76,  
17 235-257.

18 Ramos, V.A., 1984. Patagonia: ¿un continente paleozoico a la deriva? IX.  
19 Congreso Geológico Argentino. San Carlos de Bariloche, Actas 2, 311-325.

20 Ramos, V., 2008. Patagonia: a Paleozoic continent adrift? *Journal of South*  
21 *American Earth Sciences* 26, 235-251.

22 Ramos, V.A., Jordan, T.E, Allmendinger, R.W., Mpodozis, C., Kay, S.M., Cortés,  
23 J.M., Palma, M., 1986. Paleozoic terranes of the Central Argentine-Chilean  
24 Andes. *Tectonics* 5, 855-880.

1  
2  
3  
4  
5  
6  
7  
8  
9  
10  
11  
12  
13  
14  
15  
16  
17  
18  
19  
20  
21  
22  
23  
24  
25  
26  
27  
28  
29  
30  
31  
32  
33  
34  
35  
36  
37  
38  
39  
40  
41  
42  
43  
44  
45  
46  
47  
48  
49  
50  
51  
52  
53  
54  
55  
56  
57  
58  
59  
60  
61  
62  
63  
64  
65

1 Ramos, V., García Morabito, E., Hervé, F., Fanning, C.M., 2010. Grenville age  
2 sources in Cuesta de Rahue, Northern Patagonia: constraints from U-Pb  
3 SHRIMP ages from detrital zircons. Geosur 2010, Mar del Plata, Bolletino di  
4 Geofísica teórica ed applicata Vol. 51(supplement), 42

5 Ramos, V. , Mosquera, A., Folguera,A. and García Morabito,E., 2011.  
6 Evolución tectónica de los Andes y del engolfamiento neuquino adyacente.  
7 Relatorio del 18° Congreso Geologico Argentino, Neuquén, 335-348.

8 Rapalini, A., López de Luchi, M., Martínez Dopico, C., Lince Klinger, F.,  
9 Giménez, M., Martínez, P., 2010. Did Patagonia collide with Gondwana in  
10 the Late Paleozoic? Some insights from a multidisciplinary study on  
11 magmatic units of the North Patagonian Massif. Geologica Acta 8, 349-371.

12 Rapela, C.W., Pankhurst, R.J., Casquet, C., Fanning, C.M., Baldo, E.G.,  
13 González-Casado, J.M., Galindo, C., Dahquist, J., 2007. The Río de la Plata  
14 craton and the assembly of SW Gondwana. Earth-Science Reviews 83, 49-  
15 82.

16 Rapela, C.W., Baldo, E.G., Pankhurst, R.J., Fanning, C.M., 2008. The Devonian  
17 Achala batholith of the Sierras Pampeanas: F-rich, aluminous A-type  
18 granites. In: Linares, E., Cabaleri, N.G., Do Campo, M.G., Duós, E.I. &  
19 Panarello, H.O. (Eds), VI SSAGI Bariloche, Abstracts, INGEIS, University of  
20 Buenos Aires, 104-111.

21 Richter, P., Ring, U., Willner, A.P., Leiss, B., 2007. Structural contacts in  
22 subduction complexes and their tectonic significance: Journal of the  
23 Geological Society of London 164, 203-214.

24 Rocha-Campos, A.C., Basei, M.A., Nutman, A.P., Kleiman, Laura E, Varela, R.,  
25 Llambias, E., Canile, F.M., da Rosa, O.C.R., 2011. 30 million years of

1  
2  
3  
4  
5  
6  
7  
8  
9  
10  
11  
12  
13  
14  
15  
16  
17  
18  
19  
20  
21  
22  
23  
24  
25  
26  
27  
28  
29  
30  
31  
32  
33  
34  
35  
36  
37  
38  
39  
40  
41  
42  
43  
44  
45  
46  
47  
48  
49  
50  
51  
52  
53  
54  
55  
56  
57  
58  
59  
60  
61  
62  
63  
64  
65

1 Permian volcanism recorded in the Choiyoi igneous province (W Argentina)  
2 and their source for younger ash fall deposits in the Paraná Basin: SHRIMP  
3 U-Pb zircon geochronology evidence. *Gondwana Research* 19, 509-523.  
4 Sims, J. P., Ireland, T. R., Camacho, A., Lyons, P., Pieters, P. E., Skirrow, R.  
5 G., Stuart-Smith, P.G., 1998. U-Pb, Th-Pb and Ar-Ar geochronology from  
6 the southern Sierras Pampeanas, Argentina: implications for the Palaeozoic  
7 tectonic evolution of the western Gondwana margin. In: Pankhurst, R.J.,  
8 Rapela, C.W. (Eds), *The Proto-Andean Margin of Gondwana*, Geological  
9 Society of London, Special Publications 142, 259-281.  
10 Söllner, F., Alfaro, G., Miller, H., 2000. A Carboniferous-Permian meta-  
11 ignimbrite from Coastal Cordillera West of Puerto Montt, Los Lagos Region,  
12 Chile. 9 Congreso Geológico Chileno, Puerto Varas, Actas, Vol. 2, 764-769.  
13 Stuart-Smith, P.G., Camacho, A., Sims, J.P., Skirrow, R.G., Lyons, P., Pieters,  
14 P.E., Black, L.P., Miró, R., 1999. Uranium-lead dating of felsic magmatic  
15 cycles in the southern Sierras Pampeanas, Argentina: Implications for the  
16 tectonic development of the proto-Andean Gondwana margin. In Ramos,  
17 V.A., Keppie, J.D. (Eds.), *Laurentia-Gondwana Connections before Pangea*.  
18 Geological Society of America, Special Paper 336, Boulder, Colorado, 87-  
19 114.  
20 Suárez, M., De La Cruz, R., Fanning, M. & Etchart, H., 2008. Carboniferous,  
21 Permian and Toarcian Magmatism in Cordillera del Viento, Neuquén,  
22 Argentina: First U-Pb shrimp dates and tectonic implications. 17° Congreso  
23 Geológico Argentino, Actas 2, 906-907.

1  
2  
3  
4  
5  
6  
7  
8  
9  
10  
11  
12  
13  
14  
15  
16  
17  
18  
19  
20  
21  
22  
23  
24  
25  
26  
27  
28  
29  
30  
31  
32  
33  
34  
35  
36  
37  
38  
39  
40  
41  
42  
43  
44  
45  
46  
47  
48  
49  
50  
51  
52  
53  
54  
55  
56  
57  
58  
59  
60  
61  
62  
63  
64  
65

1 Varela, R., Basei, M., Cingolani, C., Siga, O., Passarelli, C., 2005. El  
2 basamento cristalino de los Andes Patagónicos en Argentina: geocronología  
3 e interpretación tectónica. *Revista Geológica de Chile* 32, 167-187.

4 Verdecchio, S.O., Casquet, C., Baldo, E.G., Pankhurst, R.J., Rapela, C.W.,  
5 Fanning, C.M., Galindo, C., 2011. Mid to Late Cambrian docking of the Río  
6 de la Plata craton to southwestern Gondwana: age constraints from U-Pb  
7 SHRIMP detrital zircon ages from Sierras de Ambato and Velasco (Sierras  
8 Pampeanas, Argentina). *Journal of the Geological Society, London* 168,  
9 1061-1071

10 Williams, I.S., 1998. U-Th-Pb geochronology by ion microprobe. In: McKibben,  
11 M.A., Shanks, W.C., Ridley, W.I.(Eds.), *Applications of Microanalytical  
12 Techniques to Understanding Mineralizing Processes. Reviews in Economic  
13 Geology* 7, 1-35.

14 Williams. I.S., Goodge, J., Myrow, P., Burke, K. & Kraus, J., 2002: Large scale  
15 sediment dispersal associated with the Late Neoproterozoic assembly of  
16 Gondwana. *Abstracts of the 16th Australian Geological Convention*, 67, 238

17 Willner, A.P., 2005. Pressure Temperature evolution of a Late Paleozoic paired  
18 metamorphic belt in North-Central Chile (34°–35°30'S). *Journal of Petrology*  
19 46 (9), 1805–1833.

20 Willner, A. P., Glodny, J., Gerya, T. V., Godoy, E., Massonne, H.-J., 2004. A  
21 counterclockwise PTt-path of high pressure-low temperature rocks from the  
22 Coastal Cordillera accretionary complex of South Central Chile: constraints  
23 for the earliest stage of subduction mass flow. *Lithos* 75, 283-310.

24 Willner, A.P., Thomson, S.N., Kröner, A., Wartho, J.A., Wijbrans, J., Hervé, F.,  
25 2005. Time markers for the evolution and exhumation history of an Upper

1  
2  
3  
4  
5  
6  
7  
8  
9  
10  
11  
12  
13  
14  
15  
16  
17  
18  
19  
20  
21  
22  
23  
24  
25  
26  
27  
28  
29  
30  
31  
32  
33  
34  
35  
36  
37  
38  
39  
40  
41  
42  
43  
44  
45  
46  
47  
48  
49  
50  
51  
52  
53  
54  
55  
56  
57  
58  
59  
60  
61  
62  
63  
64  
65

1 Paleozoic paired metamorphic belt in Central Chile (34°-35°30'S). Journal of  
2 Petrology 46, 1835-1858.

3 Willner, A., Gerdes, A., Massonne, H.J., 2008. History of crustal growth and  
4 recycling at the Pacific convergent margin of South America at latitudes 29°-  
5 36° S revealed by a U-Pb and Lu-Hf isotope study of detrital zircon from late  
6 Paleozoic accretionary systems. Chemical Geology 253, 114-129.

7 Willner, A., Gerdes, A., Massonne, H.J., Schmidt, A., Sudo, M., Thomson, S.,  
8 Vujovich, G., 2010. The geodynamics of collision of a microplate (Chilenia)  
9 in Devonian times deduced by the pressure-temperature-time evolution  
10 within part of a collisional belt (Guarguaraz complex), W Argentina.  
11 Contributions to Mineralogy and Petrology, DOI 10.1007/s00410-010-0598-  
12 8.

13 Woodhead, J. and Hergt, J., 2005. A preliminary appraisal of seven natural  
14 zircon reference materials for in situ Hf isotope determination. Geostandards  
15 and Geoanalytical Research, 29, 183-195.

1 **Figure captions**

2  
3  
4 **Figure 1.** Geological sketch map of the studied area (34–42°S) with location of  
5 the analysed samples. For each sample studied for provenance the minimum  
6 detrital zircon age and the percentage of Proterozoic zircons is shown. Ages of  
7 the Coastal Batholith are indicated in italics. Additional age data are U-Pb zircon  
8 crystallization ages (^: Duhart, 2008) and Lu-Hf mineral isochron ages (\*:  
9 Willner et al., 2010) and electron microprobe Th-U-total Pb monazite ages (\*\*:  
10 Martinez et al., 2011) for garnetiferous metamorphic rocks. Heavy line-work  
11 represents various generations of brittle and ductile faults.

12 **Figure 2.** Histogram and age vs. probability diagram for detrital zircons of the  
13 northern segments of the Western and Eastern Series from Willner et al. (2008).

14  
15 **Figure 3.** Histogram and probability vs. age diagrams for detrital zircons of the  
16 Western Series of the accretionary complex of the coast ranges of Central  
17 Chile.

18  
19 **Figure 4.** Histogram and probability vs. age diagram for detrital zircons of the  
20 Eastern Series of the accretionary complex of Central Chile.

21  
22 **Figure 5.** Histogram and probability vs. age diagram for detrital zircons of a  
23 metasedimentary succession previously mapped as part of the Eastern Series  
24 (Gana and Hervé, 1983) but in fact corresponding to Jurassic deposits.

1  
2  
3  
4  
5  
6  
7  
8  
9  
10  
11  
12  
13  
14  
15  
16  
17  
18  
19  
20  
21  
22  
23  
24  
25  
26  
27  
28  
29  
30  
31  
32  
33  
34  
35  
36  
37  
38  
39  
40  
41  
42  
43  
44  
45  
46  
47  
48  
49  
50  
51  
52  
53  
54  
55  
56  
57  
58  
59  
60  
61  
62  
63  
64  
65



1 **Figure 6.** Histogram and age vs. probability diagrams for detrital zircons of the  
2 Liquiñe (FO0605) and Parque Alerce Andino (FO0935) gneisses. CL images of  
3 selected grains in both samples with the location of analysed spots also shown.  
4 Banded mylonite (FO0606) and mylonitized hornblende-biotite tonalite  
5 (FO0609) spatially associated to the Liquiñe gneiss give Jurassic crystallisation  
6 ages.

7  
8 **Figure 7.** Age vs. probability diagrams of the San Martin de los Andes  
9 orthogneiss, Huingancó granite and Andacollo rhyolite on the eastern flank of  
10 the Andes, Argentina. These samples were analysed on the premise that they  
11 could be part of the source area for detrital zircons in the coastal range  
12 accretionary complex.

13  
14 **Figure 8.** (a) Age vs.  $\epsilon_{\text{Hf}}$  diagram for detrital zircons of the accretionary  
15 complex of Central Chile, (b) Age vs  $\delta^{18}\text{O}\%$  diagram for detrital zircons of the  
16 accretionary complex of Southern Chile.

17  
18 **Figure 9.** Hypothetical paleogeographic and paleotectonic development of the  
19 accretionary complex of Central Chile.

20  
21  
22 **Table captions**

23  
24 **Table 1.** Sample Localities and brief rock descriptions.

25

1  
2  
3  
4  
5  
6  
7  
8  
9  
10  
11  
12  
13  
14  
15  
16  
17  
18  
19  
20  
21  
22  
23  
24  
25  
26  
27  
28  
29  
30  
31  
32  
33  
34  
35  
36  
37  
38  
39  
40  
41  
42  
43  
44  
45  
46  
47  
48  
49  
50  
51  
52  
53  
54  
55  
56  
57  
58  
59  
60  
61  
62  
63  
64  
65

1 **Table 2.** Summary of the geochronological results on detrital zircons obtained in  
2 this study

3

4

5 **Electronic Supplementary Data**

6

7 Tables S1 to S18 U-Pb analytical data for the analysed samples.

8 Table S19 Lu-Hf and O analytical data for the analysed samples.

9

1  
2  
3  
4  
5  
6  
7  
8  
9  
10  
11  
12  
13  
14  
15  
16  
17  
18  
19  
20  
21  
22  
23  
24  
25  
26  
27  
28  
29  
30  
31  
32  
33  
34  
35  
36  
37  
38  
39  
40  
41  
42  
43  
44  
45  
46  
47  
48  
49  
50  
51  
52  
53  
54  
55  
56  
57  
58  
59  
60  
61  
62  
63  
64  
65

1           **Provenance variations in the Late Paleozoic accretionary complex of**  
2  
3  
4  
5           **central Chile as indicated by detrital zircons.**

6  
7  
8  
9  
10  
11   F. Hervé<sup>a\*,b</sup>, M.Calderón<sup>c</sup>, C.M. Fanning<sup>d</sup>, , R.J. Pankhurst<sup>e</sup>, E. Godoy<sup>a</sup>

12  
13  
14  
15   <sup>a</sup> Departamento de Geología, Universidad de Chile, Casilla 13518, Correo 21,  
16  
17   Santiago, Chile

18  
19   <sup>b</sup> Escuela de Ciencias de la Tierra, Universidad Andrés Bello, República 230,  
20  
21   Santiago, Chile.

22  
23   <sup>c</sup> Servicio Nacional de Geología y Minería, Av. Santa María 0104, Providencia  
24  
25   Santiago, Chile

26  
27   <sup>d</sup> Research School of Earth Sciences, Australian National University, Canberra,  
28  
29   ACT 0200, Australia

30  
31   <sup>e</sup> Visiting Research Associate, British Geological Survey, Keyworth, Nottingham  
32  
33   NG12 5GG, U.K.

34  
35  
36  
37  
38  
39   \*Corresponding author e-mail: [fherve@cec.uchile.cl](mailto:fherve@cec.uchile.cl), [fherve@unab.cl](mailto:fherve@unab.cl)

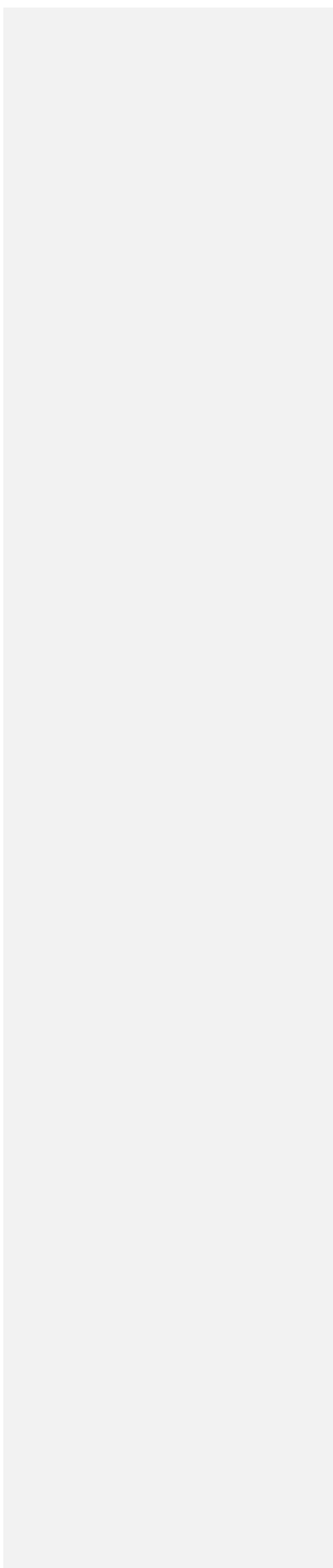
1  
2  
3 **Abstract**  
4  
5  
6

7 We present detrital zircon U–Pb SHRIMP age patterns for the central segment  
8 (34–42°S) of an extensive accretionary complex along coastal Chile and  
9 together with ages for some relevant igneous rocks ~~for the central segment (34–~~  
10 ~~42°S) of an extensive accretionary complex along coastal Chile.~~ The complex  
11 consists of a basally accreted high pressure/low temperature Western Series  
12 ~~that formed crops out~~ outboard of ~~the a~~ frontally accreted Eastern Series that  
13 was overprinted by high temperature/low pressure metamorphism. Eleven new  
14 SHRIMP detrital zircon age patterns have been obtained for metaturbidites from  
15 the central (34–~~42°S~~) segment of the accretionary complex, together with  
16 seven crystallization ages from the associated mid-Carboniferous Coastal  
17 Batholith, four four from previously undated metamorphic complexes and  
18 associated intrusive rocks from the main Andean cordillera, and three from  
19 igneous rocks in Argentina that were considered as possible sediment source  
20 areas. There are no Mesozoic detrital zircons in the accretionary rocks. Early  
21 Paleozoic zircons are an essential component of the provenance, and Grenville-  
22 age zircons and isolated grains as old as 3 Ga occur in most rocks, although  
23 much less commonly in the Western Series of the southern sector. In the  
24 northernmost sector (34–~~39°S~~38°–30′-S) Proterozoic zircon grains constitute  
25 more than 50% of the detrital spectra, in contrast with less than 10% in the  
southern sector (39–42°S). The youngest igneous detrital zircons in both the  
northern Western (~~330–307~~ 330–307 Ma) and Eastern Series (345 Ma) are considered to  
closely date sedimentation of the protoliths. Both oxygen and Lu-Hf isotopic  
analyses of a selection of Permian to Neoproterozoic detrital zircon grains

1  
2  
3  
4  
5  
6  
7  
8  
9  
10  
11  
12  
13  
14  
15  
16  
17  
18  
19  
20  
21  
22  
23  
24  
25  
26  
27  
28  
29  
30  
31  
32  
33  
34  
35  
36  
37  
38  
39  
40  
41  
42  
43  
44  
45  
46  
47  
48  
49  
50  
51  
52  
53  
54  
55  
56  
57  
58  
59  
60  
61  
62  
63  
64  
65

1 indicate that the respective igneous source rocks ~~are not juvenile, but~~ had  
2 significant crustal contributions. The results suggest that Early Paleozoic  
3 orogenic belts (Pampean and Famatinian) containing material recycled from  
4 cratonic areas of South America supplied detritus to this part of the paleo-  
5 Pacific coast. In contrast, in the southern exposures of the Western Series  
6 studied here, Permian detrital zircons (253–295 Ma) dominate, indicating much  
7 younger deposition. The northern sector has scarce Early to Middle Devonian  
8 detrital zircons, prominent south of ~~about~~ 39°S. The sedimentary protolith of  
9 the northern sector was probably deposited in a passive margin setting starved  
10 of Devonian (Achalian) detritus by a topographic barrier formed by the  
11 Precordillera, and possibly Chilenia, terranes. Devonian subduction-related  
12 metamorphic and plutonic rocks developed south of 39°S, beyond the possible  
13 southern limit of Chilenia, where sedimentation of accretionary rocks continued  
14 until Permian times.

17 **Keywords:** SHRIMP detrital zircon ages, Devonian, Carboniferous, Permian,  
18 accretionary complex, Central Chile

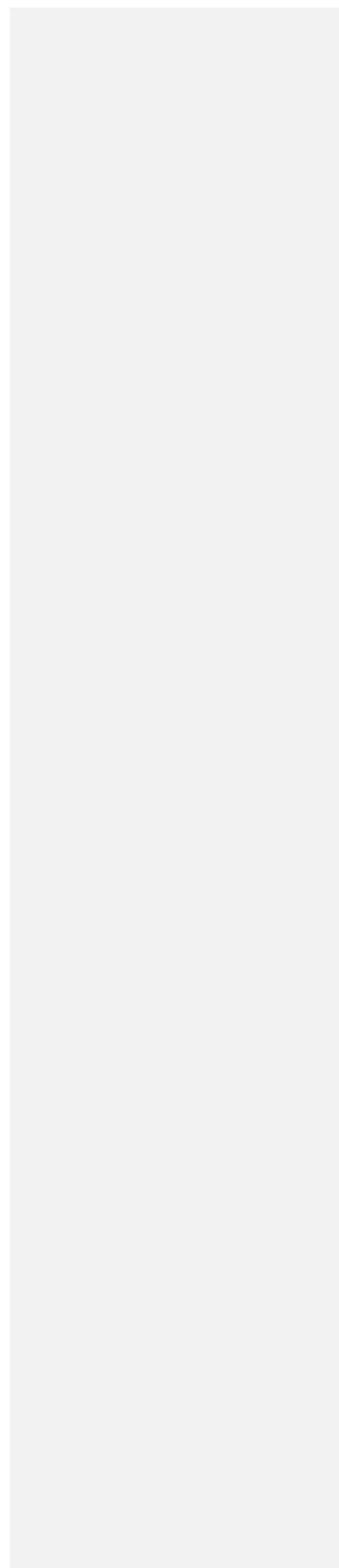


1  
2  
3  
4  
5  
6  
7  
8  
9  
10  
11  
12  
13  
14  
15  
16  
17  
18  
19  
20  
21  
22  
23  
24  
25  
26  
27  
28  
29  
30  
31  
32  
33  
34  
35  
36  
37  
38  
39  
40  
41  
42  
43  
44  
45  
46  
47  
48  
49  
50  
51  
52  
53  
54  
55  
56  
57  
58  
59  
60  
61  
62  
63  
64  
65

1  
2  
3  
4  
5  
6  
7  
8  
9  
10  
11  
12  
13  
14  
15  
16  
17  
18  
19  
20  
21  
22  
23  
24  
25  
26  
27  
28  
29  
30  
31  
32  
33  
34  
35  
36  
37  
38  
39  
40  
41  
42  
43  
44  
45  
46  
47  
48  
49  
50  
51  
52  
53  
54  
55  
56  
57  
58  
59  
60  
61  
62  
63  
64  
65

## 1. Introduction

A fossil Late Paleozoic subduction complex is exposed continuously along the Chilean margin south of 34°S. [Willner \(2005\)](#) quantified the metamorphic P-T conditions which affected the rocks near the northern end of the 34°--42°S sector considered here, and [Glodny et al. \(2005, 2008\)](#) suggested accretionary modes for different portions of the complex, mainly south of 36°S (see below). Dating of metamorphic processes has also been dealt with in a number of papers since [Munizaga et al. \(1974\)](#) with K-Ar, [Hervé et al. \(1982\)](#) with Rb-Sr whole rock methods and more recently by [Willner et al. \(2005\)](#) with Ar-Ar and [Glodny et al. \(2008\)](#) with Rb-Sr mineral whole rock isochrons. ~~This has resulted in a good definition of metamorphic episodes~~ . Detrital zircon age data, however, have remained ~~are~~ very scarce or nonexistent for large tracts of the accretionary complex between 34 and 42°S. [Willner et al \(2008\)](#) presented the results of two samples analysed by ICP-MS and [Duhart et al \(2001\)](#) presented data for individual detrital zircons for several samples of the southern (39°--42°S) sector, analysed by TIMMS. In this contribution, 13 new metasedimentary samples were analysed for their U-Pb detrital zircon age spectra with SHRIMP and age determinations are presented for three samples from possible source igneous rocks in Argentina and two foliated granitoids from Liquiñe, east of the accretionary complex. [The main purpose of this study is to examine the detrital](#)



1  
2  
3 1 zircon population present in the accretionary complex, detect their variations in  
4  
5 2 space if any, try to relate them to source areas and interpret the tectonic setting  
6  
7 3 of deposition. Additionally, isotopic studies of the detrital zircons were made to  
8  
9 4 improve the possibilities of identifying the source areas, and to characterize  
10  
11 5 some aspects of their geologic evolution. The results obtained indicate that  
12  
13 6 previously unknown large variations in the areal distribution of the detrital  
14  
15 7 populations of zircon are detectable in the accretionary prism. N-S variations in  
16  
17 8 these populations are described and interpreted in terms of their geological  
18  
19 9 significance for the Late Paleozoic development of the continental margin of  
20  
21 10 Pangea in this portion of Terra Australis orogen (~~Cawwood~~Cawood, 2005) which  
22  
23 11 represent the vestiges of tectonic activity within the paleo-Pacific Ocean  
24  
25 12 (Murphy et al., 2009).

## 14 2. Geological setting

15  
16 16 Two units with differing lithology and structure are recognized within the  
17  
18 17 complex - the Western and Eastern series (Godoy, 1970; Aguirre et al., 1972).  
19  
20 18 These have been recognised as paired metamorphic belts (sensu Miyashiro,  
21  
22 19 1961), now interpreted as representing the products of basal and frontal  
23  
24 20 accretion respectively in an active continental margin (Willner et al., 2005;  
25  
26 21 Richter et al., 2007; Glodny et al., 2008). The Eastern Series is intruded by the  
27  
28 22 N-S elongated Coastal -Batholith of Late Paleozoic age (see below).  
29  
30 23

31  
32  
33 24 In the study area (Fig. 1) the southern section is dominated by the Western  
34  
35 25 Series (WS) whereas in the northern section it is confined to relatively small  
36  
37  
38  
39  
40  
41  
42  
43  
44  
45  
46  
47  
48  
49  
50  
51  
52  
53  
54  
55  
56  
57  
58  
59  
60  
61  
62  
63  
64  
65

1 coastal outcrops. Although the limit between these sectors is not precisely  
2 determined, it must be close to the north-west trending Lanalhue lineament (Fig.  
3 1), which has been interpreted as a suture zone (Ernst, 1973), a sharp transition  
4 between the two series (Hervé, 1977) and more recently as the Lanalhue Fault  
5 Zone (~~LFZ~~, Glodny et al., 2008). ~~After the latter, The last authors state that “the~~  
6 Lanalhue Fault Zone juxtaposes Permo-Carboniferous magmatic arc granitoids  
7 and associated, frontally accreted metasediments (Eastern Series) in the  
8 northeast with a late –Carboniferous to Triassic basal-accretionary forearc  
9 wedge complex (Western Series) in the southwest”. ~~These authors-y further~~  
10 considered that an Early Permian period of subduction erosion to the north of  
11 the LFZ contrasted with ongoing accretion to the south, which resulted in so that  
12 the coastal batholith appears to be displaced 100 km to the west north of the  
13 LFZ fault zone, and that with contrasting lithologies and metamorphic signatures  
14 are now present north and south of the LFZ across it.

15  
16 The Eastern Series (ES) consists of alternating metasandstones and  
17 metapelites, with preserved bedding except in the easternmost, higher-grade  
18 areas; volumetrically small but ubiquitous calc-silicate pods are found  
19 throughout. The WS is composed of micaschists, greenschists, quartzites and  
20 scarce serpentinite bodies; rare primary sedimentary structures are observed,  
21 as well as occasional pillow structures in the greenschists.

22  
23 The rocks of the two series differ in fabric and small-scale deformational  
24 features. The ES is mainly deformed into upright folds with subvertical  $S_1$   
25 foliation or cleavage in the metapelites, in which a less steep  $S_2$  foliation is

Formatted: Subscript

Formatted: Subscript



1 occasionally observed. In contrast, the main foliation in the WS rocks is  
2 generally  $S_2$ , accompanied by the main recrystallization and with transposition  
3 of earlier primary and tectonic fabrics. Peak metamorphic conditions also differ  
4 in the two series. Following Hervé (1977) it is clear that the ES represents low  
5 P/T (pressure/temperature) metamorphic gradients and the WS higher ones,  
6 the thermal gradient for the latter estimated by Willner et al. (2005) as about 10  
7 to 12°C/km.

Formatted: Subscript

10 Paleotectonic models of the evolution of the south-western Gondwana margin  
11 include the hypothesis (Ramos et al., 1986) that between 28–39° S an exotic  
12 continental block called Chilenia collided with Gondwana during the Devonian,  
13 with the suture lying east of the present Andean Cordillera in Argentina. South  
14 of this latitude the Paleozoic development has also been interpreted as  
15 indicating collision of Patagonia with Gondwana (Ramos, 1984, 2008;  
16 Pankhurst et al., 2006). The coastal accretionary complex studied here should  
17 contain a record that might help to confirm the occurrence of such collisional  
18 events.

### 20 3. Methods

22 Samples were collected from localities that displayed the typical outcrop  
23 characteristics of either the WS or the ES. Zircons were recovered from heavy  
24 mineral concentrates obtained by the standard method of crushing, grinding,  
25 Wilfley table, magnetic and heavy liquid separation at Universidad de Chile. Not

1  
2  
3  
4  
5  
6  
7  
8  
9  
10  
11  
12  
13  
14  
15  
16  
17  
18  
19  
20  
21  
22  
23  
24  
25  
26  
27  
28  
29  
30  
31  
32  
33  
34  
35  
36  
37  
38  
39  
40  
41  
42  
43  
44  
45  
46  
47  
48  
49  
50  
51  
52  
53  
54  
55  
56  
57  
58  
59  
60  
61  
62  
63  
64  
65

1 all the samples yielded zircons, and from several only a few grains were  
2 obtained; the proportion of failed separates probably reflects a characteristic of  
3 the rocks, as this problem was unusual in previous work by the authors in the  
4 metasedimentary complexes in southern Chile. It is possible that the protolith of  
5 many of the WS schists was originally made up of distal fine-grained turbidites  
6 or mafic igneous rocks, relatively devoid of zircon crystals.

7  
8 Zircon analyses were undertaken at RSES (Research School of Earth  
9 Sciences, The Australian National University, Canberra). The grains were  
10 mounted in epoxy, polished to about half-way through the grains, and CL  
11 (~~cathode~~cathodo-luminescence) images were obtained for every zircon. U-Th-  
12 Pb analyses were then conducted using two sensitive high-resolution ion  
13 microprobes (SHRIMP II and SHRIMP RG) following the procedures described  
14 by Williams (1998). In some cases fewer than 70 individual zircon crystals were  
15 analysed (see Electronic Supplement), which may lead to enhanced  
16 uncertainties in the identification of detrital zircon age populations, although the  
17 general consistency of the resulting age distributions suggests that that this is  
18 not a significant problem.

19  
20 Oxygen ( $^{18}\text{O}/^{16}\text{O}$ ) and Lu-Hf ( $^{176}\text{Lu}/^{177}\text{Hf}$  and  $^{176}\text{Hf}/^{177}\text{Hf}$ ) isotope ratios were  
21 measured in a selection of detrital zircons from various samples with the aim of  
22 better defining possible source rocks. Following the U-Pb analyses, the  
23 SHRIMP 1-2 $\mu\text{m}$  deep U-Pb pits were lightly polished away and oxygen isotope  
24 analyses made in exactly the same location using SHRIMP II fitted with a Cs ion  
25 source and electron gun for charge compensation as described by Ickert et al.

1  
2  
3  
4  
5  
6  
7  
8  
9  
10  
11  
12  
13  
14  
15  
16  
17  
18  
19  
20  
21  
22  
23  
24  
25  
26  
27  
28  
29  
30  
31  
32  
33  
34  
35  
36  
37  
38  
39  
40  
41  
42  
43  
44  
45  
46  
47  
48  
49  
50  
51  
52  
53  
54  
55  
56  
57  
58  
59  
60  
61  
62  
63  
64  
65

(2008). Oxygen isotope ratios were determined in multiple collector mode using an axial continuous electron multiplier (CEM) triplet collector, and two floating heads with interchangeable CEM - Faraday Cups. The Temora 2, Temora 3 and FC1 reference zircons were analysed to monitor and correct for isotope fractionation. The measured  $^{18}\text{O}/^{16}\text{O}$  ratios and calculated  $\delta^{18}\text{O}_{\text{VSMOW}}$  values have been normalised relative to an FC1 weighted mean  $\delta^{18}\text{O}$  value of +5.4 ‰ (Ickert et al., 2008). Reproducibility in the Duluth Gabbro FC1 reference zircon  $\delta^{18}\text{O}$  value ranged from  $\pm 0.23$  ‰ to 0.47 ‰ ( $2\sigma$  uncertainty) for the analytical sessions, with most of the reference zircon analytical uncertainties in the range 0.21-0.42 ‰ ( $\pm 2\sigma$ ). As a secondary reference, zircons from the Temora 2 or Temora 3 zircons analysed in the same analytical sessions gave  $\delta^{18}\text{O}$  values of +8.2 ‰ and +7.59 ‰ respectively, in agreement with data reported by Ickert et al. (2008) and unpublished data for the Temora 3 reference zircon.

Lu-Hf isotopic measurements were conducted by laser ablation multi-collector inductively coupled plasma mass spectroscopy (LA-MC-ICPMS) using a Neptune MC-ICPMS coupled with a 193 nm ArF Excimer laser; similar to procedures described in Munizaga et al. (2008). Laser ablation analyses were centred on the same locations within single zircon grains used for both the U-Pb and oxygen isotope analyses described above. For all analyses of unknowns or secondary standards, the laser spot size was c. 47  $\mu\text{m}$  in diameter. The mass spectrometer was first tuned to optimal sensitivity using a large grain of zircon from the Mud Tank carbonatite (see Woodhead and Hergt, 2005). Isotopic masses were measured simultaneously in static-collection mode. A gas blank was acquired at regular intervals throughout the analytical session (every 12

1  
2  
3  
4  
5  
6  
7  
8  
9  
10  
11  
12  
13  
14  
15  
16  
17  
18  
19  
20  
21  
22  
23  
24  
25  
26  
27  
28  
29  
30  
31  
32  
33  
34  
35  
36  
37  
38  
39  
40  
41  
42  
43  
44  
45  
46  
47  
48  
49  
50  
51  
52  
53  
54  
55  
56  
57  
58  
59  
60  
61  
62  
63  
64  
65

1 analyses). The laser was fired with typically 5-8 Hz repetition rate and 50-60 mJ  
2 energy. Data were acquired for 100 seconds, but in many cases ~~we only a~~  
3 selected ~~an~~ interval ~~with a reasonably consistent signal was used in data~~  
4 ~~reduction over which the <sup>176</sup>Hf/<sup>177</sup>Hf ratios were consistent~~. Throughout the  
5 analytical session several widely used reference zircons (91500, FC-1, Mud  
6 Tank and Temora-2 or -3) were analysed to monitor data quality and  
7 reproducibility. Signal intensity was typically ca.5-6 V for total Hf at the  
8 beginning of ablation, and decreased over the acquisition time to 2 V or less.  
9 Isobaric interferences of <sup>176</sup>Lu and <sup>176</sup>Yb on the <sup>176</sup>Hf signal were corrected by  
10 monitoring signal intensities of <sup>175</sup>Lu and <sup>173</sup>Yb, <sup>172</sup>Yb and <sup>171</sup>Yb. The calculation  
11 of signal intensity for <sup>176</sup>Hf also involved independent mass bias corrections for  
12 Lu and Yb.

#### 4. Analysed samples

16 The age spectra of detrital zircons from six samples of micaschist from the WS  
17 and four metasediments from the ES were determined. ~~Analyses~~  
18 were also made on samples whose relationships with the coastal accretionary  
19 complex are not well established. These are a white mica-biotite paragneiss, a  
20 biotite-hornblende tonalite and a mylonite from a hitherto undated igneous and  
21 metamorphic complex at Liquiñe and a biotite-muscovite paragneiss from the  
22 Parque Alerce Andino area, whose relationships with the coastal accretionary  
23 complex are not well established, were also analysed. A felsic volcanic rock  
24 (FO0603), a biotite-perthite granodiorite (belonging to the ~~Huinganco-Huingancó~~  
25 complex at Huaraco) and a biotite-hornblende tonalitic gneiss (SMA) from

Formatted: English (U.K.), Superscript  
Formatted: English (U.K.), Superscript

1  
2  
3  
4  
5  
6  
7  
8  
9  
10  
11  
12  
13  
14  
15  
16  
17  
18  
19  
20  
21  
22  
23  
24  
25  
26  
27  
28  
29  
30  
31  
32  
33  
34  
35  
36  
37  
38  
39  
40  
41  
42  
43  
44  
45  
46  
47  
48  
49  
50  
51  
52  
53  
54  
55  
56  
57  
58  
59  
60  
61  
62  
63  
64  
65

1 neighbouring parts of Argentina were dated, as they were considered potential  
2 source rocks for the detrital zircons of the coastal accretionary complex. The  
3 geographical location of all samples is listed in Table 1 and shown in Fig. 1,  
4 together with U-Pb ages for the mid-Carboniferous Coastal Batholith samples.  
5 Brief sample-petrographic descriptions of analysed samples are given in Table  
6 1. The most important place names referred to in the text are partly shown in  
7 Fig. 1; for others please refer to the corresponding references.

8  
9 **5. Previous geochronological data**

10  
11 Existing detrital zircon age data from this great expanse of the Chilean  
12 metamorphic basement is very scarce. Two U-Pb LA-ICP-MS detrital zircon  
13 patterns reported by Willner et al. (2008) - one each from WS and ES rocks,  
14 near the northern end of the study area - are shown in Fig. 2. The ES sample is  
15 in reasonable agreement with the data obtained here, but the WS sample  
16 shows significant differences, lacking any prominent Carboniferous zircon  
17 grains as reported herein (see below).

18  
19 Duhart et al. (2001) report sparse detrital zircon TIMS U-Pb data for WS  
20 samples from the southern area. They obtained an upper intercept age of  $266 \pm$   
21  $14$  Ma based on analysis of 6 discordant zircon crystals from Hueyusca and  
22 suggested maximum depositional ages based on single concordant grains of  
23  $275$  Ma and  $305$  Ma (Pucatrihue),  $278$  Ma (Isla Mancera) and  $285$  Ma (Punta  
24 Huezhui), as well as older limits of  $369$  Ma (El Mirador) and  $388$  Ma (Guabún).  
25 In addition, they reported a U-Pb zircon crystallization age of  $396 \pm 1$  Ma for a

1  
2  
3  
4  
5  
6  
7  
8  
9  
10  
11  
12  
13  
14  
15  
16  
17  
18  
19  
20  
21  
22  
23  
24  
25  
26  
27  
28  
29  
30  
31  
32  
33  
34  
35  
36  
37  
38  
39  
40  
41  
42  
43  
44  
45  
46  
47  
48  
49  
50  
51  
52  
53  
54  
55  
56  
57  
58  
59  
60  
61  
62  
63  
64  
65

1 trachyte at Zarao emplaced in mafic schists. Söllner et al. (2000) report a  
2 discordia line with a lower intercept of  $293 \pm 23$  Ma interpreted as the  
3 crystallization age of a meta-ignimbrite, a rare constituent of the WS.  
4  
5 Metamorphic ages can also be used to place a limit on the time of deposition,  
6 but give no information with respect to provenance. Hervé et al. (1984) reported  
7 a Rb-Sr whole-rock isochron age of  $310 \pm 11$  Ma ( $2\sigma$ ) for  
8 blueschists/greenschists at Pichilemu (WS, northern area). Willner et al. (2005)  
9 used the Ar-Ar method on white mica to date the high P/T metamorphism of the  
10 WS to between 320 and 288 Ma and the high-temperature metamorphism of  
11 the ES to between 302 and 294 Ma, near the northern part of the study area. In  
12 the southern portion of the WS, Duhart et al. (2001) concluded, based on  
13 numerous Rb-Sr, K-Ar and Ar-Ar ages that the main metamorphism occurred at  
14 260-220 Ma, and the high P/T blueschist metamorphism at ~~320~~300 Ma. More  
15 recently, Glodny et al. (2008) obtained Rb-Sr mineral isochron ages (essentially  
16 white mica ages) between 307 and 272 Ma for the ES outcrops north of the  
17 Lanalhue Fault Zone and 295 to 255 Ma for the WS to the south. Kato and  
18 Godoy (1995) dated white micas ( $304 \pm 9$  Ma, K-Ar) in rare eclogite boulders in  
19 the ~~ES-WS~~ at Los Pabilos; these rocks subsequently yielded Ar-Ar ages of  $325$   
20  $\pm 1$  Ma for white mica (Kato et al., 1997) and  $361 \pm 2$  Ma for amphibole relict from  
21 the eclogite facies metamorphism (Kato et al., 2008). The overprinting event  
22 was dated at  $305 \pm 3$  Ma from a Rb-Sr mineral isochron by Willner et al. (2004),  
23 who dispute the older age of Kato et al. (1997).

24 ~~Conclusions based on these previous data are summarised in Table 2.~~

1 The Liquiñe gneisses have been poorly dated at  $242 \pm 42$  Ma by the Rb-Sr  
2 isochron whole-rock method (Hervé and Munizaga, 1979).

3 [Rocks dated as possible components of the source areas for the accretionary](#)  
4 [prism sediments as t](#)The deformed tonalitic intrusive body at San Martin de los  
5 Andes has been dated as Devonian by U-Pb methods on zircon by Varela et al.  
6 (2005) and Pankhurst et al. (2006), the latter authors reporting a result of  $401 \pm$   
7  $3$  Ma, with a further age of  $395 \pm 3$  Ma for a granite outcrop 10km to the north.

8 [Also the Huingancó granite and a rhyolite from the Arroyo del Torreón](#)  
9 [Formation of Cordillera del Viento had previous SHRIMP U-Pb zircon ages of](#)  
10 [327.9  \$\pm\$  2 Ma \(Suarez et al., 2008\) and 281.8  \$\pm\$  2.1 Ma respectively \(in](#)  
11 [Ramos et al, 2011\), in close coincidence with our results \(see below\)](#)

## 12

### 13 6. Results

#### 14

#### 15 6.1. U-Pb Zircon Data

16

17 Analytical data for the studied samples are presented in [Supplementary Data](#)  
18 [Tables S1 to S18. Supplementary Tables S1 to S18, available from journal](#)  
19 [website](#). Age versus probability density diagrams for all the samples are  
20 presented in Figs 3-7. The most striking difference in the age distributions  
21 recorded is between the southern segment of the WS and the other samples.

22

23 All samples of the ES (Fig. 3) and the northern area WS samples (Fig. 4) show  
24 major input from Ordovician (c. 470 Ma = Famatinian) sources. In addition  
25 peaks at 530-510 Ma (Pampean), and 950-1250 Ma ('Grenvillian') are present

1  
2  
3  
4  
5  
6  
7  
8  
9  
10  
11  
12  
13  
14  
15  
16  
17  
18  
19  
20  
21  
22  
23  
24  
25  
26  
27  
28  
29  
30  
31  
32  
33  
34  
35  
36  
37  
38  
39  
40  
41  
42  
43  
44  
45  
46  
47  
48  
49  
50  
51  
52  
53  
54  
55  
56  
57  
58  
59  
60  
61  
62  
63  
64  
65

1 | in many, albeit in variable proportions, and sparse 'Brasiliano' (640–590 Ma)  
2 | and Paleoproterozoic to Archaean ages are sometimes observed. These  
3 | constitute the main features of a typical [western](#) 'Gondwana' margin  
4 | provenance signature (Ireland et al.1998; Cawood et al.1999; Hervé et al. 2003;  
5 | Goodge et al. 2004). In the northern segment, ES and WS samples have  
6 | similar detrital zircon age spectra but the maximum possible sedimentation  
7 | ages determined by the youngest reliable detrital zircons are significantly  
8 | younger in the latter (mostly c. 330 Ma as opposed to mostly c. 345 Ma). This  
9 | difference is also apparent in the two samples analysed by Willner et al. (2008),  
10 | albeit with older limits of 335 Ma (WS) and 365 Ma (ES). All zircons are older  
11 | than the mid-Carboniferous Coastal Batholith, with the exception of some as  
12 | young as 305 Ma in the sample from Putu (FO1015). There is a high proportion  
13 | of Proterozoic zircon grains (Table 32), although this is significantly lower in the  
14 | younger Putu sample. With the exception of FO0966 and the two samples  
15 | analysed by Willner et al. (2008), there are few zircons in the age range 350–  
16 | 450 Ma, a robust peak at 465-470 Ma and a significant proportion in the range  
17 | 500–530 Ma.  
18 |  
19 | FO1018D (Fig. 5) is an exception, as it was previously mapped as part of the  
20 | ES, but the well cleaved metasandstone-metapelite alternation gives a Jurassic  
21 | sedimentation age and thus belong to the units deposited in the Hualañé-  
22 | Gualleco extensional basin (Belmar and Morata, 2005), lying unconformably  
23 | over the accretionary rocks. Its zircon age pattern indicates derivation from the  
24 | erosion of the accretionary prism together with zircons from the Coastal  
25 | Batholith (see below) and Jurassic igneous rocks.



1  
2  
3  
4  
5  
6  
7  
8  
9  
10  
11  
12  
13  
14  
15  
16  
17  
18  
19  
20  
21  
22  
23  
24  
25  
26  
27  
28  
29  
30  
31  
32  
33  
34  
35  
36  
37  
38  
39  
40  
41  
42  
43  
44  
45  
46  
47  
48  
49  
50  
51  
52  
53  
54  
55  
56  
57  
58  
59  
60  
61  
62  
63  
64  
65

1  
2 In the southern segment, the ES provenance patterns (Fig. 3) are similar to  
3 those in the north, but the WS samples (Fig. 4) have very different detrital zircon  
4 age spectra. All of the latter have a predominant population of zircons in the  
5 range 250–300 Ma (with a peak at c. 290 Ma). As in all the ES samples, the  
6 youngest Carboniferous zircons are around 345 Ma, but there is a significant  
7 Devonian input with ages between 350 and 420 Ma (peaking at around 380  
8 Ma). The Ordovician peak at 470 Ma is essentially absent from the southern  
9 WS spectra and the proportion of Neoproterozoic ages is much smaller (<  
10 20%); zircons older than 'Grenvillian' are completely absent.

11  
12 The Coastal Batholith yielded very consistent mid-Carboniferous U-Pb zircon  
13 ages of ~~310–305~~ to ~~319–320~~ Ma (late Mississippian to early Pennsylvanian)  
14 along its 700 km extent (see Fig. 1). ~~These ages are 5 to 15 Ma older than ages~~  
15 ~~obtained in previous U-Pb, Rb-Sr and K-Ar studies.~~ The significance of the  
16 results from the Coastal Batholith, including O and Lu-Hf isotope determinations  
17 on zircons, will be presented in a separate paper (Deckart et al., in prep).

18  
19 The Liquiñe gneisses are considered to form part of the Colohuincul complex,  
20 whose main outcrops are on the eastern slope of the Andes in Argentina (Hervé  
21 et al. 1974). Sample FO0605 (Fig. 6) has a relatively low yield of complex  
22 zircon grains and only 30 grains have been analysed. A number of the grains  
23 have a zoned core and homogeneous rim structure as seen under CL imaging  
24 (Fig. 6), or show a mottled texture consistent with alteration of mostly primary  
25 igneous zircon. The resultant age spectra is quite varied, suggesting a

1  
2  
3  
4  
5  
6  
7  
8  
9  
10  
11  
12  
13  
14  
15  
16  
17  
18  
19  
20  
21  
22  
23  
24  
25  
26  
27  
28  
29  
30  
31  
32  
33  
34  
35  
36  
37  
38  
39  
40  
41  
42  
43  
44  
45  
46  
47  
48  
49  
50  
51  
52  
53  
54  
55  
56  
57  
58  
59  
60  
61  
62  
63  
64  
65

1 polygenetic provenance. Three metamorphic rims, with low Th/U ratios ( $\leq 0.01$ )  
2 record Triassic ages; one of these grains has a Devonian core (grain 25 at c.  
3 400 Ma). Four other grains record ages  $\leq 380$  Ma and three of these have low  
4 Th/U ratios  $\leq 0.01$ ; namely, analyses of mottled areas in grains 4 and 9, and an  
5 interpreted metamorphic rim to grain 14. Note that grain 14 also has a Devonian  
6 core (c. 380 Ma). The zoned igneous core to grain 21 is c. 330 Ma and has a  
7 normal Th/U ratio for igneous zircon (c. 0.36). Whilst a single analysis does not  
8 constrain the maximum time of deposition for the protolith to this Liquiñe gneiss  
9 it is either at c. 330 Ma, or the grouping at c. 380 Ma [indicating a possible](#)  
10 [Devonian depositional age](#) (Fig. 6).

11  
12 In the Parque Alerce Andino sample (FO0935; Fig. 6), many of the zircon grains  
13 have thin, ragged homogeneous CL overgrowths that are less than 10  $\mu\text{m}$  in  
14 width. The main components of these grains range in CL structure from  
15 oscillatory (grain 55) and sector zoning (grain 67) to more homogeneous,  
16 interpreted metamorphic CL features (grain 61). Core and rim areas were  
17 analysed on 4 grains, mostly recording Devonian or older ages. Grain 8  
18 however has a Triassic rim with a Grenville-age core. Four other grains record  
19 relatively young ages  $\leq 230$  Ma (grains 1, 55, 61 and 67) demonstrating that this  
20 rock has a protolith as young as Late Triassic or Early Jurassic. The prominent,  
21 but thin metamorphic rims probably formed in response to the Jurassic 182 and  
22 162 Ma intrusive event indicated by the mylonite (FO0606) and mylonitic  
23 granodiorite (FO0609) of the Liquiñe area, which has not up to now been  
24 detected in the poorly studied Alerce Andino area.

1  
2  
3 1 The orthogneiss from San Martin de los Andes in Argentina records a well  
4  
5 2 defined magmatic zircon crystallization age of  $393 \pm 3$  Ma in good agreement  
6  
7 3 with the ~~published  $401 \pm 3$  Ma results listed above~~ of Pankhurst et al. (2006).  
8  
9 4 Crystallization ages of  $283 \pm 2$  Ma (~~Huinganco-Huingancó~~ granite) and  $326 \pm 3$   
10  
11 5 Ma for a rhyolite of the Arroyo del Torreón Formation (Llambías et al (2007)  
12  
13 6 (Andacollo rhyolite) were obtained from Cordillera del Viento in Argentina.  
14  
15 7 These results, mentioned by Godoy et al. (2008), are shown in Figure 7.  
16  
17 8

## 19 9 **6.2. Oxygen and Lu-Hf isotope data in zircons**

20  
21 10  
22  
23 11 In order to characterise, and trace potential source(s) of the detrital zircon  
24  
25 12 grains oxygen and Lu-Hf isotope ratios were determined on a selection of the  
26  
27 13 zoned igneous zircon components discussed above, mostly in the age range  
28  
29 14 250-580 Ma, with some random older grains (Supplementary Table S19). Whilst  
30  
31 15 some Hf data are available from both detrital zircons and source rocks of  
32  
33 16 geological units related to the ones studied here, there are few or no published  
34  
35 17 oxygen isotope data. Hf studies have thus far concentrated on detrital zircon  
36  
37 18 and in general the aim in such studies has been to cover the full gambit of the  
38  
39 19 age spectra recorded; see for example Willner et al. (2008), Bahlburg et al.  
40  
41 20 (2009), Rapela et al. (2010). More focussed studies on specific age ranges are  
42  
43 21 less common, but likely to be of greater value in unravelling specific detrital  
44  
45 22 zircon sources (see Fanning et al., 2011). Further, by combining Lu-Hf with  
46  
47 23 oxygen isotope analyses an extra dimension in characterisation and source  
48  
49 24 identification is likely.  
50  
51 25

1  
2  
3  
4  
5  
6  
7  
8  
9  
10  
11  
12  
13  
14  
15  
16  
17  
18  
19  
20  
21  
22  
23  
24  
25  
26  
27  
28  
29  
30  
31  
32  
33  
34  
35  
36  
37  
38  
39  
40  
41  
42  
43  
44  
45  
46  
47  
48  
49  
50  
51  
52  
53  
54  
55  
56  
57  
58  
59  
60  
61  
62  
63  
64  
65

1 The Lu-Hf data on detrital zircons are presented in Figure 8a. Most of the  
2 analysed grains are typical magmatic zircons, with well developed oscillatory or  
3 sector zoning. In the samples from the WS, all the Permian zircons have  
4 negative initial  $\epsilon_{\text{Hf}}$  values (-1 to -8) similar to those shown by detrital zircons of  
5 similar age on the basement units of southern Chile and Antarctic Peninsula  
6 (Fanning et al., 2011). This indicates that the magmatic sources are evolved  
7 and have resided in the continental lithosphere for some time; i.e., there is a  
8 strong crustal contribution. The Early Paleozoic zircons include some with  
9 slightly positive  $\epsilon_{\text{Hf}}$  values (up to +2), suggesting that the source of these  
10 zircons has been influenced by the addition of mantle-derived components  
11 within predominantly crustal magmas. The main exception, however, is for  
12 zircons that crystallized during the period c. 330 to 305 Ma, which have  
13 uniformly positive initial  $\epsilon_{\text{Hf}}$  values (+4 to +5) indicating a pulse of relatively  
14 juvenile magma overlapping emplacement of the Coastal Batholith. The  
15 Permian [Hualaceo-Huingancó granite pluton](#) in the Cordillera del Viento of  
16 Argentina is more juvenile than the rest of the predominant coeval [detrital](#)  
17 grains, with  $\epsilon_{\text{Hf}}$  values mostly in the range zero to -2.

18  
19 O isotope data on the same detrital zircons are presented in Figure 8b. The  
20  $\delta^{18}\text{O}$  values are mostly more positive than +6.5‰, well above the range  
21 recorded by zircons with a mantle oxygen isotope signature. This data confirms  
22 the strong crustal influence, especially in the pre-Carboniferous zircons, with a  
23 general trend to more primitive compositions, lower  $\delta^{18}\text{O}$ , from the older to the  
24 younger grains. Again, the only typical mantle values are shown by some of the

1  
2  
3 1 | grains in the age range of the Coastal Batholith and slightly older, i.e., 305–330  
4 2 | Ma.

## 3 4 7. Discussion

### 5 6 7.1. Provenance indications

7  
8 The older components in the provenance patterns of all samples show a range  
9 of Early Paleozoic, Neoproterozoic and scarce older detrital zircons typical of  
10 the Early Paleozoic ~~mobile-tectonomagmatic~~ belts of southern South America,  
11 notably the Pampean (Cambrian) and Famatinian (Ordovician) belts of western  
12 Argentina (e.g., Rapela et al., 2007; Verdecchio et al., 2011). These belts  
13 formed on the paleo-Pacific margin of the continent and are the most obvious  
14 sources for the older zircons in the basement complexes west of the Andes.  
15 The scarce Paleoproterozoic and Archaean content is similarly attributable,  
16 having been reworked from cratonic sources that are not specifically  
17 identifiable. The samples analysed in this study are more remarkable for the  
18 variations in their Late Paleozoic provenance, which are more diagnostic of  
19 tectonic influences in the sedimentary environment.

20  
21 The prominent Early Permian provenance in the southern sector WS, which is  
22 absent from the remaining basement areas studied here, is traceable to the  
23 voluminous Permian igneous rocks of the Choyoi province and/or the  
24 presumably related subvolcanic granites of the North Patagonian Massif, the  
25 latter occurring directly to the present east of the coastal basement outcrops at

1  
2  
3  
4  
5  
6  
7  
8  
9  
10  
11  
12  
13  
14  
15  
16  
17  
18  
19  
20  
21  
22  
23  
24  
25  
26  
27  
28  
29  
30  
31  
32  
33  
34  
35  
36  
37  
38  
39  
40  
41  
42  
43  
44  
45  
46  
47  
48  
49  
50  
51  
52  
53  
54  
55  
56  
57  
58  
59  
60  
61  
62  
63  
64  
65

1 40°-41°S. Although the major Choiyoi rhyolite volcanism occurred rather later  
2 (250-260 Ma), recently published U-Pb zircon ages confirm an early phase at c.  
3 280 Ma (Rocha-Campos et al., 2011) and many of the Patagonian granites  
4 were emplaced at this time (Pankhurst et al., 2006), as was the [Hualaceo](#)  
5 [Huingancó granite](#). ~~granodiorite~~. Such a correlation would be compatible with  
6 the broadly crustal Hf isotope signature noted above for the Permian zircons  
7 (Fanning et al., 2011). The Choyoi province exhibits its major development  
8 north of about 34°S, but the absence of similar detritus from the ES and the  
9 northern sector of the WS is explained by the fact that these rocks were  
10 deposited earlier, in Carboniferous times.

11  
12 The Carboniferous provenance of the basement samples studied here indicated  
13 by the major peaks in their detrital zircon patterns are c. 345 Ma in the ES and  
14 c. 330 Ma in the northern sector WS. These are maximum ages for deposition,  
15 which as discussed above was pre-Permian. The fact that the ES is intruded by  
16 the ~~305-300~~ [320-319-20](#) Ma Coastal Batholith and the absence of zircons  
17 derived therefrom means that these peak ages are probably very close  
18 estimates of sedimentation age, which is thus constrained to the Mississippian  
19 (Early Carboniferous). Early Carboniferous subduction-related granitoids of  
20 predominantly A-type geochemistry, many with U-Pb zircon ages of c. 340-350  
21 Ma, occur in the Eastern Sierras Pampeanas of Argentina at 27-30°S (see  
22 Alasino et al., in press, and references therein). It seems quite possible that  
23 similar magmatism extended farther south than the Sierras Pampeanas, which  
24 are only exposed as a result of uplift and exhumation above the 'flat-slab'  
25 portion of the Andean subduction system, and that this is the source of the

1  
2  
3 1 detrital zircons in the ES. Carboniferous subduction-related magmatism  
4  
5 2 migrated or jumped towards the Pacific during the mid-Carboniferous and arc-  
6  
7 3 derived I-type granitoids of 310-330 Ma are known in the Frontal Cordillera itself  
8  
9 4 (albeit so far without U-Pb zircon ages). This event is also registered in the  
10  
11 5 western border of the North Patagonian Massif (Pankhurst et al., 2006) and  
12  
13 6 there is no doubt that subduction was active at this time along the whole of the  
14  
15 7 Chilean proto-Pacific margin. This is the obvious source of the younger  
16  
17 8 Carboniferous detrital zircon peaks seen in the northern sector WS. The virtual  
18  
19 9 absence of zircons of Carboniferous age from the post-Early Permian southern  
20  
21 10 WS -probably indicates that the Coastal Batholith was not exhumed in this area  
22  
23 11 during the Permian. The remaining difference between the northern and  
24  
25 12 southern sectors is the significant proportion of Devonian detrital zircon in the  
26  
27 13 latter which is largely absent from the former (although a few grains are seen in  
28  
29 14 the northern WS samples). [Bahlburg et al \(2009\) also noted the scarcity or](#)  
30  
31 15 [absence of Devonian detrital zircons in late Paleozoic metasedimentary rocks in](#)  
32  
33 16 [northern Chile \(31°--22°-S\)](#). This is discussed further below.

## 18 **7.2. Provenance of Devonian magmatism and metamorphism detrital** 19 **zircons**

20  
21 [There is abundant evidence for Devonian magmatism and deformation in the](#)  
22 [eastern flank of the main Andean cordillera between 39° and 42°S that can be](#)  
23 [considered the most likely source of Devonian detrital zircons in the southern](#)  
24 [part of the Western Series. This is represented around San Martin de los Andes](#)  
25 [\(c. 40°S, 71°W; see Fig. 1\) by small outcrops of variably deformed igneous.](#)

1  
2  
3 1 orthogneissic and migmatitic rocks, consistently dated at c. 385–405 Ma by  
4  
5 2 Varela et al. (2005), Pankhurst et al. (2006), Godoy et al. (2008) and the  
6  
7 3 present paper (sample SMA, 393.5 ± 32.6 Ma). Such a belt could even extend  
8  
9 4 southeastwards to Colan Conhué at 43°S, 70°W (see figure 3 of Pankhurst et  
10  
11 5 al. 2006). Lucassen et al. (2004) published a Rb-Sr mineral isochron age of 368  
12  
13 6 ± 9 Ma for a migmatite from San Martín de Los Andes, and a <sup>206</sup>Pb-<sup>238</sup>U age of  
14  
15 7 380 ± 2 Ma for titanite from a gneiss–migmatite association 100 km further  
16  
17 8 southeast near Piedra del Aguila, interpreted as approximating the time of the  
18  
19 9 metamorphic peak. In the Alumine area at c. 39°S, approximately 150 km north  
20  
21 10 of San Martín, the oldest K-Ar age on fine fractions of metamorphic schists (c.  
22  
23 11 370 Ma; Franzese, 1995) indicates Late Devonian deformation or cooling of  
24  
25 12 these rocks, and the overall range (c. 300–370 Ma) is consistent with partial  
26  
27 13 resetting of the K-Ar system by contact metamorphism in the late Paleozoic.  
28  
29 14 Devonian Rb-Sr whole-rock isochron ages have been obtained from  
30  
31 15 metasedimentary rocks of the Cushamen Formation in the North Patagonian  
32  
33 16 Massif close to Colan Conhué (Ostera et al., 2001). Recently, Martínez et al.  
34  
35 17 (2012<sup>1</sup>) have published single electron microprobe Th-U-total Pb monazite  
36  
37 18 ages of 392 ± 4 Ma and 350 ± 6 Ma (interpreted as indicating collision  
38  
39 19 metamorphism and a later retrograde event, respectively) in schists belonging  
40  
41 20 to the Colohuincul complex on the eastern slope of the Andes near San Carlos  
42  
43 21 de Bariloche (41°S). Ramos et al. (2010) have shown that Colohuincul complex  
44  
45 22 rocks include Devonian detrital zircon grains. Even farther south at 42°–43°S in  
46  
47 23 the western flank of the Andes, albeit on the coast, Duhart (2008) reports the  
48  
49 24 existence of foliated granitoids of similar Devonian ages: the Chaitén  
50  
51 25 metatonalite (c. 400 Ma) and the Pichicolo microdiorite (c. 386 Ma).  
52  
53  
54  
55  
56  
57  
58  
59  
60  
61  
62  
63  
64  
65



1  
2  
3 1 Campos et al. (1998) report a 383 Ma granite clast in the Eastern Series at  
4  
5 2 Lago Ranco. Fortey et al. (1996) describe the presence of Lower to Middle  
6  
7 3 Devonian (Emsian-Eifolian; 410-390 Ma) trilobites in slates at Buill, in a basin  
8  
9 4 described by Fortey et al. (1992) as the western part of an extended platform  
10  
11 5 connected by seaways to the Falkland/Malvinas and South Africa. The  
12  
13 6 sedimentation in this basin shortly preceded and/or was synchronous with the  
14  
15 7 emplacement of the igneous protoliths of the Devonian orthogneisses, granite  
16  
17 8 and microdiorite mentioned above.  
18  
19 9 In one respect, the absence of Devonian detrital zircon in the northern region of  
20  
21 10 the Central Chile basement is notable. Devonian granite magmatism and  
22  
23 11 shearing in the sierras of Córdoba and San Luis of northwest Argentina have  
24  
25 12 been dated by U-Pb and Ar-Ar methods and interpreted as constituting the  
26  
27 13 Achalian orogeny (see Sims et al., 1998; Stuart-Smith et al., 1999). Dorais et al.  
28  
29 14 (1997) and Rapela et al. (2008) have dated the major intrusive representative,  
30  
31 15 the Achala granite batholith, with U-Pb zircon ages of  $368 \pm 2$  to  $379 \pm 4$  Ma.  
32  
33 16 From c. 200 km to the southwest, in the Frontal Cordillera, Willner et al. (2010)  
34  
35 17 published Lu-Hf mineral isochrons for garnetiferous pelitic schists and  
36  
37 18 amphibolites of the Guarguaraz complex, obtaining consistent ages of  $390 \pm 2$   
38  
39 19 Ma. Additionally, Heredia et al. (2012) report the presence of clasts of plutonic  
40  
41 20 rocks of western provenance in the Devonian Vallecito Formation on the  
42  
43 21 eastern slope of the Andes at 34°S, which they relate to magmatism in Chileña  
44  
45 22 during pre-collisional west-directed subduction of the intervening ocean  
46  
47 23 between Chileña and Gondwana. Thus, although genetically different from the  
48  
49 24 Devonian belt 600 km away in the southern region, there is clear expression of  
50  
51  
52  
53  
54  
55  
56  
57  
58  
59  
60  
61  
62  
63  
64  
65

1  
2  
3 1 a contemporaneous mid-Devonian igneous and metamorphic belt to the east of  
4  
5 2 the northern part of our study area, at latitudes 31–33° S.

6  
7 3 ~~Devonian granite magmatism and shearing events in the sierras of Córdoba~~  
8  
9 4 ~~and San Luis of northwest Argentina have been dated by U-Pb and Ar-Ar~~  
10  
11 5 ~~methods and interpreted as constituting the Achaian orogeny (see Sims et al.,~~  
12  
13 6 ~~1998; Stuart-Smith et al., 1999). Dorais et al. (1997) and Rapela et al. (2008)~~  
14  
15 7 ~~have dated the major intrusive representative, the Acahala granite batholith,~~  
16  
17 8 ~~with U-Pb zircon ages of  $368 \pm 2$  to  $379 \pm 4$  Ma. From a little farther south, in~~  
18  
19 9 ~~the Frontal Cordillera, Willner et al. (2010) published Lu-Hf mineral isochrons for~~  
20  
21 10 ~~garnetiferous pelitic schists and amphibolites of the Guarguaraz complex,~~  
22  
23 11 ~~obtaining consistent ages of  $390 \pm 2$  Ma. This mid-Devonian igneous and~~  
24  
25 12 ~~metamorphic belt lies to the east of the northern part of our study area, at~~  
26  
27 13 ~~latitudes 31–33° S.~~

28  
29 14  
30  
31 15 ~~In the eastern flank of the main Andean cordillera between 39° and 42° S a~~  
32  
33 16 ~~'block' or 'belt' of Devonian rocks occurs widely, including the SMA orthogneiss.~~  
34  
35 17 ~~Part of this block, around San Martín de los Andes (c. 40°S–71°W; see Fig. 1) is~~  
36  
37 18 ~~characterized by scarce and small outcrops of variably deformed igneous,~~  
38  
39 19 ~~orthogneissic and migmatitic rocks, consistently dated at c. 385–405 Ma by~~  
40  
41 20 ~~Varela et al. (2005), Pankhurst et al. (2006) and Godoy et al. (2008), which~~  
42  
43 21 ~~could even extend southeastwards to Colán Conhué at 43°S, 70°W. Lucassen~~  
44  
45 22 ~~et al. (2004) published an internal Rb-Sr isochron age of  $368 \pm 9$  Ma for a~~  
46  
47 23 ~~migmatite from San Martín de los Andes, and a  $^{206}\text{Pb}$ - $^{238}\text{U}$  age of  $380 \pm 2$  Ma~~  
48  
49 24 ~~for titanite in a calcsilicate rock from a gneiss/migmatite association near Piedra~~  
50  
51 25 ~~del Águila, interpreted as close to the metamorphic peak. Devonian Rb-Sr~~

1 whole-rock isochron ages have been obtained from metasedimentary rocks of  
2 the Cushamen Formation in the North Patagonian Massif close to Colan  
3 Conhué (Ostera et al. 2001). Farther north, the oldest K-Ar age on fine fractions  
4 of metamorphic schists from the Alumine area (c. 370 Ma; Franzese, 1995)  
5 indicates Late Devonian deformation or cooling of these rocks, and the overall  
6 range (c. 370–300 Ma) is consistent with partial resetting of the K-Ar system by  
7 contact metamorphism in the late Paleozoic. Recently, Cruz et al. (2012) have  
8 published single electron microprobe Th-U-total Pb monazite ages of  $392 \pm 4$   
9 Ma and  $350 \pm 6$  Ma, interpreted as indicating collision metamorphism, and a  
10 later retrograde event in schists belonging to the Colohuincul complex on the  
11 eastern slope of the Andes near San Carlos de Bariloche (41°S); Ramos et al.  
12 (2010) have shown that Colohuincul complex rocks at Cuesta de Rahue include  
13 Devonian zircon grains.

14  
15 In the western flank of the Andes Duhart (2008) reports the existence of foliated  
16 granitoids of similar Devonian ages at 42°–43°S: the Chaitén metatonalite (c.  
17 400 Ma) and the Pichicolo microdiorite (c. 386 Ma). Campos et al. (1998) report  
18 a 383 Ma granite clast in the Eastern Series at Lago Ranco. Fortey et al. (1996)  
19 describe the presence of Lower to Middle Devonian (Emsian–Eifelian; 410–390  
20 Ma) trilobites in slates at Buill, in a basin described by Fortey et al. (1992) as  
21 the western part of an extended platform connected by seaways to the  
22 Falkland/Malvinas and South Africa. The sedimentation in this basin shortly  
23 preceded and/or was synchronous with the emplacement of the igneous  
24 protoliths of the Devonian orthogneisses, granite and microdiorite mentioned  
25 above.

### 7.3. Tectonic considerations

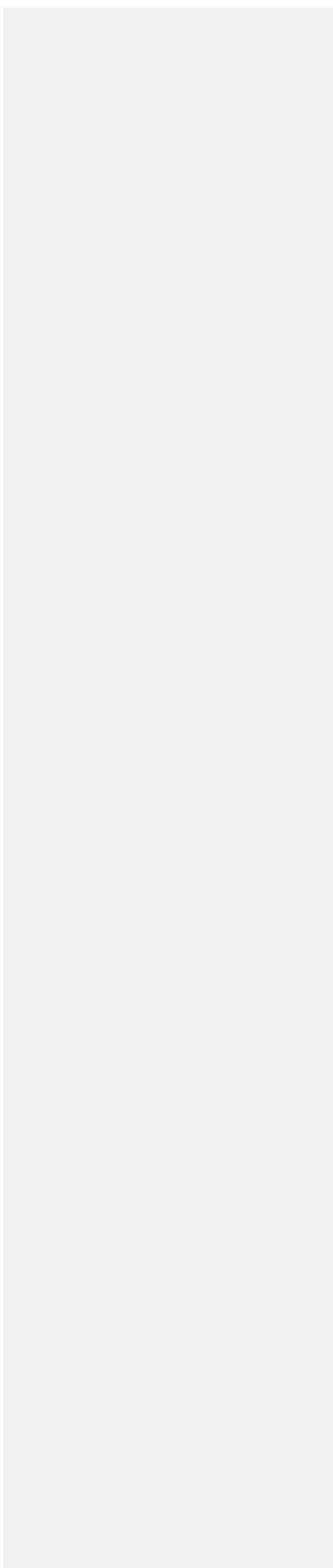
~~Thus contemporaneous Mid-to-Late Devonian~~ We suggest that a possibly continuous belt of Devonian ~~plutons-granitoids~~ and ~~metasediments~~metasedimentary rocks, variously affected by tectonism, and metamorphic/thermal events, developed ~~along-within~~ the western margin of this segment of Gondwana from c. 28° to 42° or even 43°S (Fig. 9). ~~These~~ Regardless of their varied petrogeneses, these Devonian rocks constituted an eroding area while sediments of the southern portion of the WS were being deposited during the Permian, as Devonian zircon ~~ages~~ are found therein. The fact that few detrital zircons of this age reached the Early Carboniferous proto-Pacific margin deposits in the north may mean that they were still unexhumed at that time, but is almost certainly due to more probably indicate the presence of a topographical barrier. The Precordillera terrane could have formed such a barrier, having been accreted to the margin during the Ordovician Famatinian orogeny. Additionally, Stuart-Smith et al. (1999) ascribed the Achalian magmatic and tectonic cycle to the Devonian collision of a further terrane to the west, i.e., Chilenia (Ramos et al., 1986). Massonne and ~~Galderon~~Calderón (2008) and Willner et al. (2010) also argued that the P-T path determined for the metasedimentary rocks indicated crustal thickening, consistent with a Devonian terrane collision. A similar explanation for the metamorphism of the Colohuincul complex at 41°S was given by ~~Cruz~~ Martinez et al. (20122011). A problem with the latter interpretation is that, according to current models, the southern limit of the Chilenia terrane is the E-W Huincul lineament, located near the latitude of the Lanalhue ~~lineament~~Fault

1  
2  
3  
4  
5  
6  
7  
8  
9  
10  
11  
12  
13  
14  
15  
16  
17  
18  
19  
20  
21  
22  
23  
24  
25  
26  
27  
28  
29  
30  
31  
32  
33  
34  
35  
36  
37  
38  
39  
40  
41  
42  
43  
44  
45  
46  
47  
48  
49  
50  
51  
52  
53  
54  
55  
56  
57  
58  
59  
60  
61  
62  
63  
64  
65

1 | [Zone \(39°-37°—38°30'-S\)](#). Extension of Chilenia to 41°S to explain the  
2 | Devonian metamorphism is problematic since at that latitude the coastal  
3 | accretionary complex extends eastwards as far as the western flank of the  
4 | present-day Andes, leaving little space for an intervening continental sliver. As  
5 | suggested by Kato et al. (2008), subduction was already active here in the  
6 | Devonian, a view that is supported by data presented here and ~~in~~[by](#)  
7 | McDonough et al. (~~as cited by~~[in](#) Duhart et al., 2001). Thus the proposed  
8 | Devonian metamorphism of the Colohuincul complex could be related to the  
9 | subduction episode that gave rise to the Devonian arc plutons, probably in a  
10 | back-arc position. Another possible alternative is that the [Lake Nahuelhuapi](#)  
11 | ~~rocks~~[rocks studied by Martinez et al \(2011\)](#) were tectonically “extruded” to the  
12 | south of the Chilenia terrane limit during and or after the Chilenia- Gondwana  
13 | collision. Also, as already pointed out by Duhart et al. (2001), sedimentation of  
14 | the southern portion of the WS took place during the Permian, well after the  
15 | peak metamorphism of the eclogites and blueschists.

16  
17 | Further difficulties for the Chilenia hypothesis are that no Devonian I-type  
18 | plutons are known from the northern area and Rapela et al. (2008) showed the  
19 | Achala granites to be geochemically peraluminous A-type rather than collision-  
20 | related S-type. Alasino et al. (in press) have argued that the Devonian and Early  
21 | Carboniferous A-type granites were generated above a zone of flat-slab  
22 | subduction followed by rapid roll-back and renewed subduction with  
23 | increasingly I-type magmatism at the Late Carboniferous margin outboard of an  
24 | extensive retro-arc.

25



1  
2  
3  
4  
5  
6  
7  
8  
9  
10  
11  
12  
13  
14  
15  
16  
17  
18  
19  
20  
21  
22  
23  
24  
25  
26  
27  
28  
29  
30  
31  
32  
33  
34  
35  
36  
37  
38  
39  
40  
41  
42  
43  
44  
45  
46  
47  
48  
49  
50  
51  
52  
53  
54  
55  
56  
57  
58  
59  
60  
61  
62  
63  
64  
65

1 Thus the mid-Carboniferous metasedimentary basement of the northern sector  
2 should have involved a wide Late Paleozoic depositional basin prior to the  
3 establishment of the Coastal Batholith. This basin developed either on the  
4 trailing edge of an exotic terrane accreted in the Devonian (Chilenia) or a long-  
5 lived accretionary platform west of the Precordillera terrane accreted in the  
6 Ordovician. Sedimentary detritus could have been received from  
7 contemporaneous Early Carboniferous I-type and A-type igneous activity far to  
8 the east but apparently did not include material from the Devonian complexes,  
9 which may have been buried at the time. It is also notable that there is a  
10 scarcity of zircons of c. 570 Ma, which Alvarez et al. (2011) suggested as  
11 possibly indicating the basement of Chilenia.

13 In northern Patagonia, Carboniferous I-type magmatism represents east-to-  
14 northeastward subduction at 330 Ma (Pankhurst et al., 2006). The northernmost  
15 proven outcrop of these rocks near Bariloche is less than 100 km south of the  
16 Devonian magmatic and metamorphic rocks around San Martin de los Andes  
17 (ibid., their figure 2) and thus appear to be slightly inboard of the Devonian  
18 margin. It is often considered that northern Patagonia collided with the rest of  
19 South America in the Carboniferous as in the model of Ramos (2008 for the  
20 latest version), and the paleomagnetic data would allow a separation of up to  
21 about 1500 km across the intervening 'Colorado Ocean' (Rapalini et al., 2010).  
22 If this were so we should expect a major discontinuity in the Devonian and Early  
23 Carboniferous record at the latitude of the Huincul Ridge at 39°S, which is not  
24 apparent. The collision suture suggested by Pankhurst et al. (2006) was south  
25 of the North Patagonian Massif and the Carboniferous outcrops, and so might

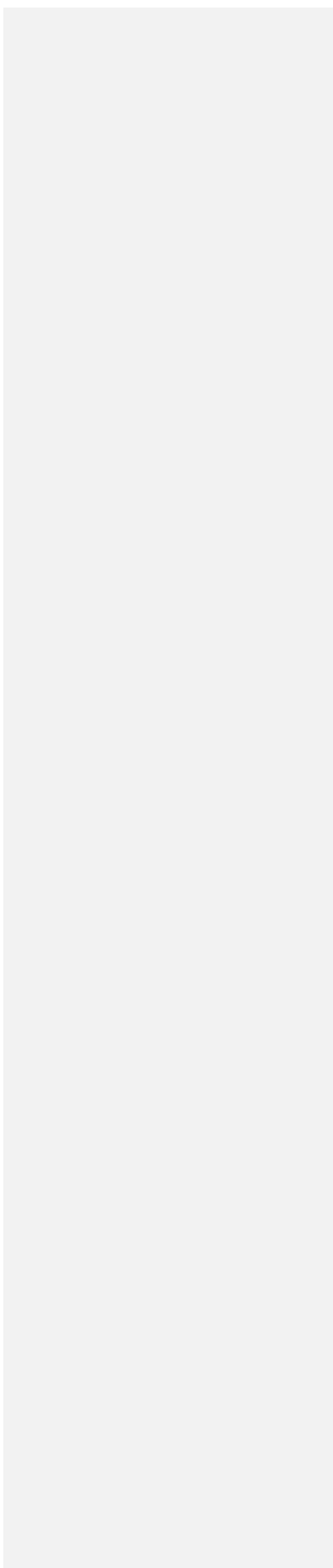
1  
2  
3  
4  
5  
6  
7  
8  
9  
10  
11  
12  
13  
14  
15  
16  
17  
18  
19  
20  
21  
22  
23  
24  
25  
26  
27  
28  
29  
30  
31  
32  
33  
34  
35  
36  
37  
38  
39  
40  
41  
42  
43  
44  
45  
46  
47  
48  
49  
50  
51  
52  
53  
54  
55  
56  
57  
58  
59  
60  
61  
62  
63  
64  
65

1 still be viable, but if the Devonian granite at Colan Conhue is considered to be a  
2 continuation of the Devonian belt at San Martin de los Andes, this model also  
3 would be doubtful.

## 4 5 **8. Conclusions**

6  
7 The metasedimentary basement rocks of Central Chile north of the Lanalhue  
8 lineament (c. [37°](#)–[38°30'S](#)) form a penecontemporaneous paired metamorphic  
9 belt. Our data show that the Eastern Series was deposited in Early  
10 Carboniferous times, shortly before the Western Series but both prior to  
11 emplacement of the 305-320 Ma subduction-related Coastal Batholith, which  
12 intrudes the former. The provenance for both series was older Gondwana  
13 margin basement of the Pampean and Famatinian belts, including reworked  
14 cratonic material, and Carboniferous magmatism east of the present-day  
15 Andes. Metamorphism of the accretionary wedge seems to have overlapped  
16 with the late plutonic phase, but may have continued later in the [HP](#) high P/T  
17 Western Series.

18  
19 The Eastern Series is of limited extent south of about 39°S, but is similar to the  
20 [LP](#) low P/T metasedimentary series in the north. However the predominant  
21 Western Series in the southern sector is much younger, with abundant Permian  
22 detritus derived from the Choiyoi province or subvolcanic plutonic rocks in the  
23 North Patagonian Massif. There is also a secondary provenance of Devonian  
24 age which is absent from its northern counterpart and the entire Eastern Series.



1  
2  
3  
4  
5  
6  
7  
8  
9  
10  
11  
12  
13  
14  
15  
16  
17  
18  
19  
20  
21  
22  
23  
24  
25  
26  
27  
28  
29  
30  
31  
32  
33  
34  
35  
36  
37  
38  
39  
40  
41  
42  
43  
44  
45  
46  
47  
48  
49  
50  
51  
52  
53  
54  
55  
56  
57  
58  
59  
60  
61  
62  
63  
64  
65

1 O and Lu-Hf data indicate a mature crustal source for all zircons except those  
2 that crystallized during Carboniferous subduction.  
3  
4 Analysis of igneous and metamorphic rocks from farther east show that inboard  
5 of the southern sector there is a Devonian igneous and metamorphic block or  
6 belt of more significant extent than has been previously noted, which is the  
7 presumed source of the detritus of this age in the southern Western Series. The  
8 relative paucity of Devonian provenance in the north is explained by a wide  
9 crustal zone separating the Devonian igneous rocks of the Sierras Pampeanas  
10 in Argentina from the site of the Carboniferous accretionary deposits, including  
11 the Precordillera terrane and possibly Chilenia, when subduction jumped to the  
12 west in the Early Carboniferous.

13  
14 The apparent continuity of the Devonian-Early Carboniferous magmatic and  
15 metamorphic rocks as far as 42°43'S or more does not support the idea that the  
16 North Patagonian Massif was separated from the rest of southern South  
17 America by a significant ocean at this time.

18  
19 **Acknowledgements**

20  
21 This research is a main part of the FONDECYT project 1095099 and the  
22 International Collaboration project 7095099 of Comisión Nacional de  
23 Investigación Científica y Tecnológica (CONICYT). Thorough reviews that  
24 helped to improve the original version were provided by Referees Dave Barbeau  
25 , Victor Ramos and an a-Anonymous provided with referee thorough revisions



1  
2  
3 | ~~which helped to improve the original version.~~ Dr. Vreni Hausserman of  
4  
5 | 2 Fundación Huinay provided logistic support to work on the extreme end of the  
6  
7 | 3 studied area. M. Solari, C. Maureira, P. Hervé and B. Keller accompanied some  
8  
9 | 4 of the field trips.

10  
11 | 5  
12  
13 | 6  
14  
15 | 7 [Supplementary item: Tables S1 to S189 available from the online version of the](#)  
16  
17 | 8 [journal at: yyyyyyy](#)  
18  
19 | 9

## 20 21 | 10 **References**

22  
23 | 11  
24  
25 | 12 Aguirre, L, Hervé, F, Godoy, E., 1972. Distribution of metamorphic facies in  
26  
27 | 13 Chile, an outline. Kristalinikum, Prague 9, 7-19.

28  
29 | 14 Alasino, P.H., Dahlquist, J.A., Pankhurst, R.J., Galindo, C., Casquet, C.,  
30  
31 | 15 Rapela, C.W., Larrovere, M., Fanning, C.M., in press. Early Carboniferous  
32  
33 | 16 sub- to mid-alkaline magmatism in the Eastern Sierras Pampeanas, NW  
34  
35 | 17 Argentina: a record of crustal growth by the incorporation of mantle-derived  
36  
37 | 18 material in an extensional setting. [Gondwana Research](#).

38  
39 | 19 Álvarez, J., Mpodozis, C., Arriagada, C., Astini., R., Morata, D., Salazar, E.,  
40  
41 | 20 Valencia, V.A., Vervoort, J.D., 2011. Detrital zircons from late Paleozoic  
42  
43 | 21 accretionary complexes in northcentral Chile (28°-32° S): Possible  
44  
45 | 22 fingerprints of the Chilenia Terrane. *Journal of South American Earth*  
46  
47 | 23 *Sciences*, doi: 10.1016/j.jsames.2011.06.002

48  
49 | 24 Augustsson, C., Munker, M., Bahlburg, H., Fanning, M., 2006. Provenance of  
50  
51 | 25 Late Palaeozoic metasediments of the SW South American Gondwana  
52  
53  
54  
55  
56  
57  
58  
59  
60  
61  
62  
63  
64  
65

Formatted: English (U.K.)

1  
2  
3  
4  
5  
6  
7  
8  
9  
10  
11  
12  
13  
14  
15  
16  
17  
18  
19  
20  
21  
22  
23  
24  
25  
26  
27  
28  
29  
30  
31  
32  
33  
34  
35  
36  
37  
38  
39  
40  
41  
42  
43  
44  
45  
46  
47  
48  
49  
50  
51  
52  
53  
54  
55  
56  
57  
58  
59  
60  
61  
62  
63  
64  
65

1 margin from combined U-Pb ages and Hf isotope compositions of single  
2 detrital zircons. Journal of the Geological Society, London 163, 983-995.  
3 Bahlburg, H., Vervoort, J.D., DuFrane, S.A., Bock, B., Augustsson, C., 2009.  
4 Timing of accretion and crustal recycling at accretionary orogens: insights  
5 learned from the western margin of South America. Earth-Science Reviews  
6 97, 227-253.  
7 Belmar, M., Morata, D., 2005. Nature and P-T-t constraints of very low-grade  
8 metamorphism in the Triassic-Jurassic basins, Coastal Range, central Chile.  
9 Revista Geológica de Chile 32 (2), 189-205.  
10 Campos, A., Moreno, H., Muñoz, J., Antinao, J., Clayton, J., Martin, M., 1998.  
11 Area de Futrono - Lago Ranco, Region de los Lagos. Mapas Geológicos,  
12 1:100.000, No. 8, SERNAGEOMIN, Santiago.  
13 Cawood, P.A., Nemchin, A.A., Leverenz, A., Saeed, A., Ballance, P.F., 1999.  
14 U/Pb dating of detrital zircons: implications for the provenance record of  
15 Gondwana margin terranes. Geological Society of America Bulletin 111,  
16 1107-1119.  
17 Cawood, P.A., 2005. Terra Australis orogen: Rodinia breakup and development  
18 of the Pacific and Iapetus margins of Gondwana during the Neoproterozoic  
19 and Paleozoic. Earth-Science Reviews 69, 249-279.  
20 ~~Cruz, J., Dristas, J., Massonne, H.-J., 2012. Paleozoic accretion of the~~  
21 ~~microcontinent Chilenia, North Patagonian Andes: high pressure~~  
22 ~~metamorphism and subsequent thermal relaxation. International Geology~~  
23 ~~Review 54 (4), 472-490.~~

Formatted: English (U.K.)

Formatted: Spanish (International Sort)

1  
2  
3  
4  
5  
6  
7  
8  
9  
10  
11  
12  
13  
14  
15  
16  
17  
18  
19  
20  
21  
22  
23  
24  
25  
26  
27  
28  
29  
30  
31  
32  
33  
34  
35  
36  
37  
38  
39  
40  
41  
42  
43  
44  
45  
46  
47  
48  
49  
50  
51  
52  
53  
54  
55  
56  
57  
58  
59  
60  
61  
62  
63  
64  
65

1 Deckart et al. (in prep). The central Chile coastal batholith : zircon SHRIMP  
2 ages and Lu-Hf and O isotopic evidence of a short emplacement on a  
3 recycling continental margin.

4 Dorais, M., Lira, R., Chen, Y., Tingey, D., 1997. Origin of biotite-apatite-rich  
5 enclaves, Achala Batholith, Argentina. Contributions to Mineralogy and  
6 Petrology 130, 31-46.

7 Duhart, P., Mc Donough, M., Muñoz, J., Martin, M., Villeneuve, M., 2001. El  
8 Complejo Metamórfico Bahía Mansa en la Cordillera de la Costa del centro-  
9 sur de Chile (39°30'-42°S): geocronología K-Ar, 40Ar/39Ar y U-Pb,  
10 implicancias en la evolución del margen sur-occidental de Gondwana.  
11 Revista Geológica de Chile 28, 179-208.

12 Duhart, P.L., 2008. Processos metalogeneticos em ambientes de arco  
13 magmático tipo andino, caso de estudio: mineralizacoes da regio dos  
14 Andes Patagónicos setentrionais do Chile. Ph. D Dissertation, Sao Paulo  
15 University, 215 p.-, Sao Paulo.

16 Ernst, G., 1973. Blueschist metamorphism and P-T regimes in active  
17 subduction zones. Tectonophysics 17, 255-272.

18 Fanning, C. M., Hervé, F., Pankhurst, R.J., Rapela, C.W., Kleiman, L.E.,  
19 Yaxley, G.M., Castillo, P., 2011. Lu-Hf isotope evidence for the provenance  
20 of Permian detritus in accretionary complexes of western Patagonia and the  
21 northern Antarctic Peninsula region. Journal of South American Earth  
22 Sciences 32, 485 - 496.

23 Flowerdew, M.J., Millar, I.L., Curtis, M.L., Vaughan, A.P.M., Horstwood, M.S.A.,

Formatted: French (France)

Formatted: Spanish (International Sort)

Formatted: Spanish (International Sort)

1  
2  
3  
4  
5  
6  
7  
8  
9  
10  
11  
12  
13  
14  
15  
16  
17  
18  
19  
20  
21  
22  
23  
24  
25  
26  
27  
28  
29  
30  
31  
32  
33  
34  
35  
36  
37  
38  
39  
40  
41  
42  
43  
44  
45  
46  
47  
48  
49  
50  
51  
52  
53  
54  
55  
56  
57  
58  
59  
60  
61  
62  
63  
64  
65

1 Whitehouse, M.J., Fanning, C.M., 2007. Combined U-Pb geochronology and Hf  
2 isotope geochemistry of detrital zircons Early Paleozoic Ellsworth Mountains  
3 Antarctica. Geological Society of America Bulletin 199, 275-288.

4 Fortey ,R., Pankhurst, R.J., Hervé, F., 1992. Devonian Trilobites at Buill, Chile  
5 (42°S). Revista Geológica de Chile 19, 133-144.

6 Franzese, J.R., 1995. El Complejo Piedra Santa (Neuquén, Argentina): parte de  
7 un cinturón metamórfico neopaleozoico del Gondwana suroccidental.  
8 Revista Geológica de Chile 22, 193-202.

9 Gana, P., Hervé, F., 1983. Geología del basamento cristalino de la Cordillera  
10 de la Costa entre los ríos Mataquito y Maule, VII Región. Revista Geológica  
11 de Chile 19, 37-56.

Formatted: Spanish (International Sort)

Formatted: English (U.K.)

12 Glodny, J., Lohrmann, J., Echtler, H., Gräfe, K., Seifert, W., Collao, S.,  
13 Figueroa, O., 2005. Internal dynamics of a paleoaccretionary wedge:  
14 insights from combined isotope tectonochronology and sandbox modelling of  
15 the south-central Chilean fore-arc. Earth and Planetary Science Letters 231,  
16 23-39.

17 Glodny, J., Echtler, H., Figueroa, O., Franz, G., Gräfe, K., Kernitz, H., Kramer,  
18 W., Krawczyk, C., Lohrmann, J., Lucassen, F., Melnick, D., Rosenau, M.,  
19 Seifert, W., 2006. Long-term geological evolution and mass flow balance of  
20 the South-Central Andes. In: Oncken, O., Chong, G., Franz, G., Giese, P.,  
21 Götze, H.-J., Ramos,V., Strecker, M., Wigger, P. (Eds.), The Andes - Active  
22 Subduction Orogeny. Frontiers in Earth Sciences, vol. 1. Springer Verlag,  
23 Berlin, pp. 401-442.

24 Glodny, J., Echtler, H., Collao, S., Ardiles, M., Burón, P., Figueroa, O., 2008.  
25 Differential Late Paleozoic active margin evolution in South-Central Chile

Formatted: Spanish (International Sort)

1  
2  
3  
4  
5  
6  
7  
8  
9  
10  
11  
12  
13  
14  
15  
16  
17  
18  
19  
20  
21  
22  
23  
24  
25  
26  
27  
28  
29  
30  
31  
32  
33  
34  
35  
36  
37  
38  
39  
40  
41  
42  
43  
44  
45  
46  
47  
48  
49  
50  
51  
52  
53  
54  
55  
56  
57  
58  
59  
60  
61  
62  
63  
64  
65

(37°S - 40°S) - the Lanalhue Fault Zone. *Journal of South American Earth Sciences* 26, 397-411.

Formatted: Spanish (International Sort)

Godoy, E., 1970. El granito de Constitución y su aureola de metamorfismo de contacto. Graduation Thesis, Geology Department, Universidad de Chile, Santiago, 140 p.

Godoy, E., Hervé, F., Fanning, M., 2008. Edades U-Pb SHRIMP en granitoides del macizo norpatagónico: implicancias geotectónicas. XVII Congreso Geológico Argentino Vol. 3, 1288-1289.

Formatted: Spanish (International Sort)

Goodge, J.W., Williams, I.S., Myrow, P., 2004. Provenance of Neoproterozoic and lower Paleozoic siliciclastic rocks of the central Ross orogen, Antarctica: Detrital record of rift-, passive-, and active-margin sedimentation. *Geological Society of America Bulletin* 116, 1253-1279.

~~[Heredia, N., Farias, P., García-Sanseguno, J and , Giambiagi, L., \(2012\).](#)~~

~~[The Basement of the Andean Frontal Cordillera in the Cordón del Plata](#)~~

~~[\(Mendoza, Argentina\): Geodynamic Evolution. \*Andean Geology\* 39 \(2\), 242-257.](#)~~

Formatted: English (U.K.)

Formatted: Indent: Hanging: 0.63

Hervé, F., 1977. Petrology of the Crystalline Basement of the Nahuelbuta Mountains, Southcentral Chile. In Ishikawa, T. and Aguirre L. (Eds.), *Comparative Studies on the Geology of the Circum Pacific Orogenic Belt in Japan and Chile*. Japan Society for the Promotion of Science, 1-51, Tokyo.

Hervé, M., Munizaga, F., 1979. Antecedentes geocronológicos del área al este de Liqueñe, Cordillera de los Andes, latitud 39°45' S, Chile. Resúmenes, II Congreso Geológico Chileno, Arica, 45-46.

Formatted: Spanish (International Sort)

1  
2  
3  
4  
5  
6  
7  
8  
9  
10  
11  
12  
13  
14  
15  
16  
17  
18  
19  
20  
21  
22  
23  
24  
25  
26  
27  
28  
29  
30  
31  
32  
33  
34  
35  
36  
37  
38  
39  
40  
41  
42  
43  
44  
45  
46  
47  
48  
49  
50  
51  
52  
53  
54  
55  
56  
57  
58  
59  
60  
61  
62  
63  
64  
65

1 | Hervé, F., Moreno, H., Parada, M.A., 1974. Granitoids of the Andean Range,  
2 | Valdivia Province, Chile. Pacific Geology 8, 39-45.

Formatted: English (U.K.)

3 | Hervé, F., Kawashita, K., Munizaga, F., Basei, M., 1984. Rb-Sr isotopic ages  
4 | from late Paleozoic metamorphic rocks of Central Chile. Journal of the  
5 | Geological Society, London 141, 877-884.

6 | Hervé, F., Fanning, C.M., Pankhurst, R.J., 2003. Detrital zircon age patterns  
7 | and provenance in the metamorphic complexes of Southern Chile. Journal  
8 | of South American Earth Sciences 16, 107-123.

9 | Ickert, R.B., Hiess, J., Williams, I.S., Holden, P., Ireland, T.R., Lanc, P.,  
10 | Schram, N., Foster, J.J., Clement, S.W., 2008. Determining high precision,  
11 | in situ, oxygen isotope ratios with a SHRIMP II: Analyses of MPI-DING  
12 | silicate-glass reference materials and zircon from contrasting granites.  
13 | Chemical Geology 257, 114-128.

14 | Ireland, T.R., Flötmann, T., Fanning, C.M., Gibson, G.M., Preiss, W.V., 1998.  
15 | Development of the early Paleozoic Pacific margin of Gondwana from  
16 | detrital-zircon ages across the Delamerian orogen. Geology 26, 243-246.

17 | Kato, T.T., Godoy, E., 1995. Petrogenesis and tectonic significance of Late  
18 | Paleozoic coarse-crystalline blueschist and amphibolite boulders in the  
19 | coastal range of Chile. International Geology Review 37, 992- 1006.

20 | Kato, T.T., Godoy, E., McDonough, M., Duhart, P., Martin, M., Sharp, W., 1997.

21 | Un modelo preliminar de deformación transpresional mesozoica y gran  
22 | desplazamiento hacia el norte de parte de la serie occidental, complejo  
23 | acrecionario (38°S a 43°S), Cordillera de la Costa. Actas 8. Congreso  
24 | Geológico Chileno, Antofagasta,1, 98-102.

Formatted: Spanish (International Sort)

Formatted: English (U.K.)

1  
2  
3  
4  
5  
6  
7  
8  
9  
10  
11  
12  
13  
14  
15  
16  
17  
18  
19  
20  
21  
22  
23  
24  
25  
26  
27  
28  
29  
30  
31  
32  
33  
34  
35  
36  
37  
38  
39  
40  
41  
42  
43  
44  
45  
46  
47  
48  
49  
50  
51  
52  
53  
54  
55  
56  
57  
58  
59  
60  
61  
62  
63  
64  
65

1 Kato, T.T., Sharp, W., Godoy, E., 2008. Inception of a Devonian subduction  
2 zone along the southwestern Gondwana margin: 40Ar/39Ar dating of  
3 eclogite - amphibolite assemblage in blueschist boulders from the Coastal  
4 Range of Chile (41°S). Canadian Journal of Earth Sciences 45, 337-351.

5 Llambías, E., Leanza, H., Carbone, O., 2007. Evolución tectono-magmática  
6 durante el Pérmico al Jurásico temprano en la Cordillera del Viento  
7 (37°05'/37°15'S): nuevas evidencias geológicas y geoquímicas del inicio de  
8 la cuenca neuquina. Revista de la Asociación Geológica Argentina 62, 217-  
9 235.

10 Lucassen, F., Trumbull, R., Franz, G., Creixell, C., Vásquez, P., Romer, R.L.,  
11 Figueroa, O., 2004. Distinguishing crustal recycling and juvenile additions at  
12 active continental margins: the Paleozoic to recent compositional evolution  
13 of the Chilean Pacific margin (36°-41°S). Journal of South American Earth  
14 Sciences 17, 103-119.

15 Martinez, J.C., Dristas, J., Massonne, H.-J., 2012. Paleozoic accretion of the  
16 microcontinent Chilenia, North Patagonian Andes: high pressure  
17 metamorphism and subsequent thermal relaxation. International Geology  
18 Review 54 (4), 472-490.

19 Massonne, H.-J., Calderón, M. 2008., P-T evolution of metapelites from the  
20 Guarguaraz Complex, Argentina: evidence for Devonian) crustal thickening  
21 close to the western Gondwana margin. Revista Geológica de Chile 35, 215-  
22 231.

23 Miyashiro, A., 1961. Evolution of metamorphic belts. Journal of Petrology 2,  
24 277-311.

Formatted: Spanish (International Sort)

1  
2  
3  
4  
5  
6  
7  
8  
9  
10  
11  
12  
13  
14  
15  
16  
17  
18  
19  
20  
21  
22  
23  
24  
25  
26  
27  
28  
29  
30  
31  
32  
33  
34  
35  
36  
37  
38  
39  
40  
41  
42  
43  
44  
45  
46  
47  
48  
49  
50  
51  
52  
53  
54  
55  
56  
57  
58  
59  
60  
61  
62  
63  
64  
65

1 Munizaga, F., Maksaev, V., Fanning, C.M., Giglio, S., Yaxley, G., Tassinari,  
2 C.C.G., 2008. Late Paleozoic-Early Triassic magmatism on the western  
3 margin of Gondwana: Collahuasi area, Northern Chile. *Gondwana Research*  
4 13, 407-427.

5 Murphy, J.B., Nance, R.D., Cawood, P.A., 2009. Contrasting modes of  
6 supercontinent formation and the conundrum of Pangea. *Gondwana*  
7 *Research* 15, 408-420.

8 Osters, H.A., Linares, E., Haller, M.J., Cagnoni, M.C., López de Luchi, M.,  
9 2001. A widespread Devonian metamorphic episode in Northern Patagonia,  
10 *Argentina. III Simposio de Geología Isotópica, Pucón, Chile, Abstract*  
11 *Volume on CD-ROM, 600-603.*

Formatted: English (U.K.)

12 Pankhurst, R.J., Rapela, C.W., Loske, W.P., Márquez, M., Fanning, C.M., 2003.  
13 *Chronological study of the pre-Permian basement rocks of southern*  
14 *Patagonia. Journal of South American Earth Sciences* 16, 27-44.

15 Pankhurst, R.J., Rapela, C.W., Fanning, C.M., Márquez, M., 2006. Gondwanide  
16 continental collision and the origin of Patagonia. *Earth-Science Reviews* 76,  
17 235-257.

18 Ramos, V.A., 1984. Patagonia: ¿un continente paleozoico a la deriva? IX.  
19 *Congreso Geológico Argentino. San Carlos de Bariloche, Actas* 2, 311-325.

Formatted: English (U.K.)

20 Ramos, V., 2008. Patagonia: a Paleozoic continent adrift? *Journal of South*  
21 *American Earth Sciences* 26, 235-251.

22 Ramos, V.A., Jordan, T.E., Allmendinger, R.W., Mpodozis, C., Kay, S.M., Cortés,  
23 J.M., Palma, M., 1986. Paleozoic terranes of the Central Argentine-Chilean  
24 *Andes. Tectonics* 5, 855-880.



1  
2  
3  
4  
5  
6  
7  
8  
9  
10  
11  
12  
13  
14  
15  
16  
17  
18  
19  
20  
21  
22  
23  
24  
25  
26  
27  
28  
29  
30  
31  
32  
33  
34  
35  
36  
37  
38  
39  
40  
41  
42  
43  
44  
45  
46  
47  
48  
49  
50  
51  
52  
53  
54  
55  
56  
57  
58  
59  
60  
61  
62  
63  
64  
65

1 Ramos, V., García Morabito, E., Hervé, F., Fanning, C.M., 2010. Grenville age  
2 sources in Cuesta de Rahue, Northern Patagonia: constraints from U-Pb  
3 SHRIMP ages from detrital zircons. Geosur 2010, Mar del Plata, Bolletino di  
4 Geofísica teórica ed applicata Vol. 51(supplement), 42-45.

Formatted: Italian (Italy)

5 Ramos, V. , Mosquera, A., Folguera,A. and García Morabito,E., 2011.  
6 Evolución tectónica de los Andes y del engolfamiento neuquino adyacente.  
7 Relatorio del 18° Congreso Geologico Argentino, Neuquén, 335-348.

8 Rapalini, A., López de Luchi, M., Martínez Dopico, C., Lince Klinger, F.,  
9 Giménez, M., Martínez, P., 2010. Did Patagonia collide with Gondwana in  
10 the Late Paleozoic? Some insights from a multidisciplinary study on  
11 magmatic units of the North Patagonian Massif. Geologica Acta 8, 349-371.

Formatted: Spanish (International Sort)

12 Rapela, C.W., Pankhurst, R.J., Casquet, C., Fanning, C.M., Baldo, E.G.,  
13 González-Casado, J.M., Galindo, C., Dahquist, J., 2007. The Río de la Plata  
14 craton and the assembly of SW Gondwana. Earth-Science Reviews 83, 49-  
15 82.

16 Rapela, C.W., Baldo, E.G., Pankhurst, R.J., Fanning, C.M., 2008. The Devonian  
17 Achala batholith of the Sierras Pampeanas: F-rich, aluminous A-type  
18 granites. In: Linares, E., Cabaleri, N.G., Do Campo, M.G., Duós, E.I. &  
19 Panarello, H.O. (Eds), VI SSAGI Bariloche, Abstracts, INGEIS, University of  
20 Buenos Aires, 104-111.

21 Richter, P., Ring, U., Willner, A.P., Leiss, B., 2007. Structural contacts in  
22 subduction complexes and their tectonic significance: Journal of the  
23 Geological Society of London 164, 203-214.

Formatted: English (U.K.)

24 Rocha-Campos, A.C., Basei, M.A., Nutman, A.P., Kleiman, Laura E, Varela, R.,  
25 Llambias, E., Canile, F.M., da Rosa, O.C.R., 2011. 30 million years of

Formatted: Italian (Italy)

1  
2  
3  
4  
5  
6  
7  
8  
9  
10  
11  
12  
13  
14  
15  
16  
17  
18  
19  
20  
21  
22  
23  
24  
25  
26  
27  
28  
29  
30  
31  
32  
33  
34  
35  
36  
37  
38  
39  
40  
41  
42  
43  
44  
45  
46  
47  
48  
49  
50  
51  
52  
53  
54  
55  
56  
57  
58  
59  
60  
61  
62  
63  
64  
65

1 Permian volcanism recorded in the Choiyoi igneous province (W Argentina)  
2 and their source for younger ash fall deposits in the Paraná Basin: SHRIMP  
3 U-Pb zircon geochronology evidence. *Gondwana Research* 19, 509-523.  
4 Sims, J. P., Ireland, T. R., Camacho, A., Lyons, P., Pieters, P. E., Skirrow, R.  
5 G., Stuart-Smith, P.G., 1998. U-Pb, Th-Pb and Ar-Ar geochronology from  
6 the southern Sierras Pampeanas, Argentina: implications for the Palaeozoic  
7 tectonic evolution of the western Gondwana margin. In: Pankhurst, R.J.,  
8 Rapela, C.W. (Eds), *The Proto-Andean Margin of Gondwana*, Geological  
9 Society of London, Special Publications 142, 259-281.  
10 Söllner, F., Alfaro, G., Miller, H., 2000. A Carboniferous-Permian meta-  
11 ignimbrite from Coastal Cordillera West of Puerto Montt, Los Lagos Region,  
12 Chile. 9 Congreso Geológico Chileno, Puerto Varas, Actas, Vol. 2, 764-769.  
13 Stuart-Smith, P.G., Camacho, A., Sims, J.P., Skirrow, R.G., Lyons, P., Pieters,  
14 P.E., Black, L.P., Miró, R., 1999. Uranium-lead dating of felsic magmatic  
15 cycles in the southern Sierras Pampeanas, Argentina: Implications for the  
16 tectonic development of the proto-Andean Gondwana margin. In Ramos,  
17 V.A., Keppie, J.D. (Eds.), *Laurentia-Gondwana Connections before Pangea*.  
18 Geological Society of America, Special Paper 336, Boulder, Colorado, 87-  
19 114.  
20 [Suárez, M., De La Cruz, R., Fanning, M. & Etchart, H., 2008. Carboniferous,](#)  
21 [Permian and Toarcian Magmatism in Cordillera del Viento, Neuquén,](#)  
22 [Argentina: First U-Pb shrimp dates and tectonic implications. 17° Congreso](#)  
23 [Geológico Argentino, Actas 2, 906-907.](#)

Formatted: Italian (Italy)

1  
2  
3  
4  
5  
6  
7  
8  
9  
10  
11  
12  
13  
14  
15  
16  
17  
18  
19  
20  
21  
22  
23  
24  
25  
26  
27  
28  
29  
30  
31  
32  
33  
34  
35  
36  
37  
38  
39  
40  
41  
42  
43  
44  
45  
46  
47  
48  
49  
50  
51  
52  
53  
54  
55  
56  
57  
58  
59  
60  
61  
62  
63  
64  
65

Varela, R., Basei, M., Cingolani, C., Siga, O., Passarelli, C., 2005. El basamento cristalino de los Andes Patagónicos en Argentina: geocronología e interpretación tectónica. *Revista Geológica de Chile* 32, 167-187.

Verdecchio, S.O., Casquet, C., Baldo, E.G., Pankhurst, R.J., Rapela, C.W., Fanning, C.M., Galindo, C., 2011. Mid to Late Cambrian docking of the Río de la Plata craton to southwestern Gondwana: age constraints from U-Pb SHRIMP detrital zircon ages from Sierras de Ambato and Velasco (Sierras Pampeanas, Argentina). *Journal of the Geological Society, London* 168, 1061-1071

Williams, I.S., 1998. U-Th-Pb geochronology by ion microprobe. In: McKibben, M.A., Shanks, W.C., Ridley, W.I.(Eds.), *Applications of Microanalytical Techniques to Understanding Mineralizing Processes. Reviews in Economic Geology* 7, 1-35.

Williams, I.S., Goodge, J., Myrow, P., Burke, K. & Kraus, J., 2002: Large scale sediment dispersal associated with the Late Neoproterozoic assembly of Gondwana. *Abstracts of the 16th Australian Geological Convention*, 67, 238

Willner, A.P., 2005. Pressure Temperature evolution of a Late Paleozoic paired metamorphic belt in North-Central Chile (34°–35°30'S). *Journal of Petrology* 46 (9), 1805–1833.

Willner, A. P., Glodny, J., Gerya, T. V., Godoy, E., Massonne, H.-J., 2004. A counterclockwise PTt-path of high pressure-low temperature rocks from the Coastal Cordillera accretionary complex of South Central Chile: constraints for the earliest stage of subduction mass flow. *Lithos* 75, 283-310.

Willner, A.P., Thomson, S.N., Kröner, A., Wartho, J.A., Wijbrans, J., Hervé, F., 2005. Time markers for the evolution and exhumation history of an Upper

Formatted: Italian (Italy)

Formatted: Spanish (International Sort)

Formatted: English (U.K.)

Formatted: Indent: First line: 0 cm

1  
2  
3 1 Paleozoic paired metamorphic belt in Central Chile (34°-35°30'S). Journal of  
4  
5 2 Petrology 46, 1835-1858.

6  
7 3 Willner, A., Gerdes, A., Massonne, H.J., 2008. History of crustal growth and  
8  
9 4 recycling at the Pacific convergent margin of South America at latitudes 29°-  
10  
11 5 36° S revealed by a U-Pb and Lu-Hf isotope study of detrital zircon from late  
12  
13 6 Paleozoic accretionary systems. Chemical Geology 253, 114-129.

14  
15 7 Willner, A., Gerdes, A., Massonne, H.J., Schmidt, A., Sudo, M., Thomson, S.,  
16  
17 8 Vujovich, G., 2010. The geodynamics of collision of a microplate (Chilenia)  
18  
19 9 in Devonian times deduced by the pressure-temperature-time evolution  
20  
21 10 within part of a collisional belt (Guarguaraz complex), W Argentina.  
22  
23 11 Contributions to Mineralogy and Petrology, DOI 10.1007/s00410-010-0598-  
24  
25 12 8.

26  
27 13 [Woodhead, J. and Hergt, J., 2005. A preliminary appraisal of seven natural](#)  
28  
29 14 [zircon reference materials for in situ Hf isotope determination. Geostandards](#)  
30  
31 15 [and Geoanalytical Research, 29, 183-195.](#)  
32

33 16  
34  
35 17  
36  
37 18  
38  
39 19  
40  
41 20  
42  
43 21 **Figure captions**

44  
45 22  
46  
47 23 **Figure 1.** Geological sketch map of the studied area (34–42°S) with location of  
48  
49 24 the analysed samples. For each sample studied for provenance the minimum  
50  
51 25 detrital zircon age and the percentage of Proterozoic zircons is shown. Ages of  
52  
53  
54  
55  
56  
57  
58  
59  
60  
61  
62  
63  
64  
65

1  
2  
3 1 the Coastal Batholith are indicated in italics. Additional age data are U-Pb zircon  
4 crystallization ages (^: Duhart, 2008) and Lu-Hf mineral isochron ages (\*:  
5 Willner et al., 2010) and electron microprobe Th-U-total Pb monazite ages (\*\*:  
6 Martinez et al., 2011) for garnetiferous metamorphic rocks. Heavy line-work  
7 represents various generations of brittle and ductile faults.  
8  
9  
10  
11  
12  
13  
14  
15  
16  
17  
18  
19  
20  
21  
22  
23  
24  
25  
26  
27  
28  
29  
30  
31  
32  
33  
34  
35  
36  
37  
38  
39  
40  
41  
42  
43  
44  
45  
46  
47  
48  
49  
50  
51  
52  
53  
54  
55  
56  
57  
58  
59  
60  
61  
62  
63  
64  
65

8 **Figure 2.** Histogram and age vs. probability diagram for detrital zircons of the  
9 northern segments of the Western and Eastern Series from Willner et al. (2008).

11 **Figure 3.** Histogram and probability vs. age diagrams for detrital zircons of the  
12 Western Series of the accretionary complex of the coast ranges of Central  
13 Chile.

15 **Figure 4.** Histogram and probability vs. age diagram for detrital zircons of the  
16 Eastern Series of the accretionary complex of Central Chile.

18 **Figure 5.** Histogram and probability vs. age diagram for detrital zircons of a  
19 metasedimentary succession previously mapped as part of the Eastern Series  
20 (Gana and Hervé, 1983) but in fact corresponding to Jurassic deposits.

22 **Figure 6.** Histogram and age vs. probability diagrams for detrital zircons of the  
23 Liquiñe (FO0605) and Parque Alerce Andino (FO0935) gneisses. CL images of  
24 selected grains in both samples with the location of analysed spots also shown.  
25 Banded mylonite (FO0606) and mylonitized hornblende-biotite tonalite

(FO0609) spatially associated to the Liquiñe gneiss give Jurassic crystallisation ages.

**Figure 7.** Age vs. probability diagrams of the San Martin de los Andes

orthogneiss, ~~Hualaeo~~ **Huingancó** granite and Andacollo rhyolite on the eastern flank of the Andes, Argentina. These samples were analysed on the premise that they could be part of the source area for detrital zircons in the coastal range accretionary complex.

**Figure 8.** (a) Age vs.  $\epsilon_{\text{Hft}}$  diagram for detrital zircons of the accretionary complex of Central Chile, (b) Age vs  $\delta^{18}\text{O}_{\text{‰}}$  diagram for detrital zircons of the accretionary complex of Southern Chile.

**Figure 9.** Hypothetical paleogeographic and paleotectonic development of the accretionary complex of Central Chile.

## Table captions

**Table 1.** Sample Localities and brief rock descriptions.

~~Table 2.~~ **Table 2.** Summary of significant previous geochronological data

**Table 32.** Summary of the geochronological results on detrital zircons obtained in this study

1  
2  
3  
4  
5  
6  
7  
8  
9  
10  
11  
12  
13  
14  
15  
16  
17  
18  
19  
20  
21  
22  
23  
24  
25  
26  
27  
28  
29  
30  
31  
32  
33  
34  
35  
36  
37  
38  
39  
40  
41  
42  
43  
44  
45  
46  
47  
48  
49  
50  
51  
52  
53  
54  
55  
56  
57  
58  
59  
60  
61  
62  
63  
64  
65

1  
2  
3  
4  
5  
6  
7  
8  
9  
10  
11  
12  
13  
14  
15  
16  
17  
18  
19  
20  
21  
22  
23  
24  
25  
26  
27  
28  
29  
30  
31  
32  
33  
34  
35  
36  
37  
38  
39  
40  
41  
42  
43  
44  
45  
46  
47  
48  
49  
50  
51  
52  
53  
54  
55  
56  
57  
58  
59  
60  
61  
62  
63  
64  
65

**Electronic Supplementary Data**

- 5 | [Tables S1 to S18 U-Pb analytical data for the analysed samples.](#)
- 6 | [Table S19 Lu-Hf and O analytical data for the analysed samples.](#)
- 7 | ~~[Tables 1 to 18 Analytical data for the analysed samples.](#)~~

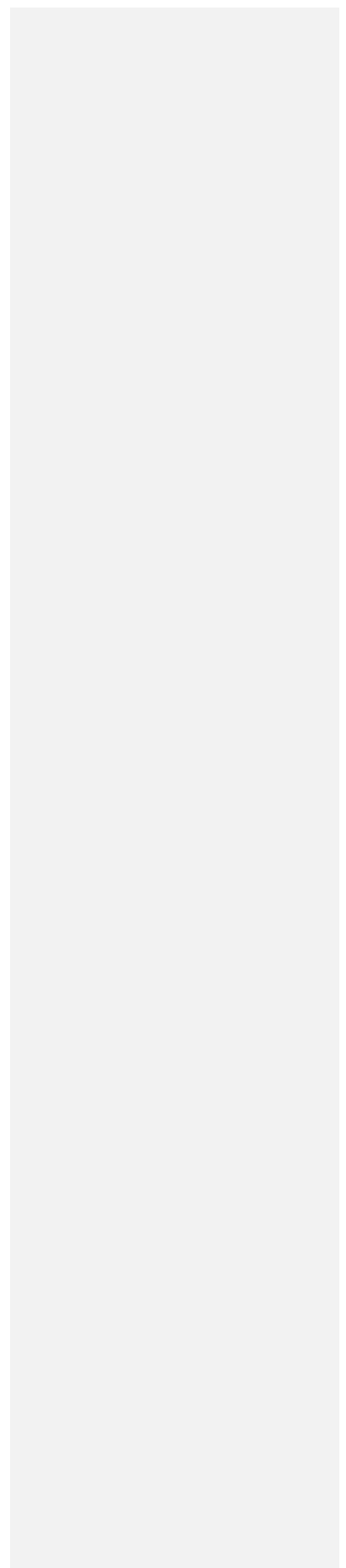


Figure  
[Click here to download high resolution image](#)

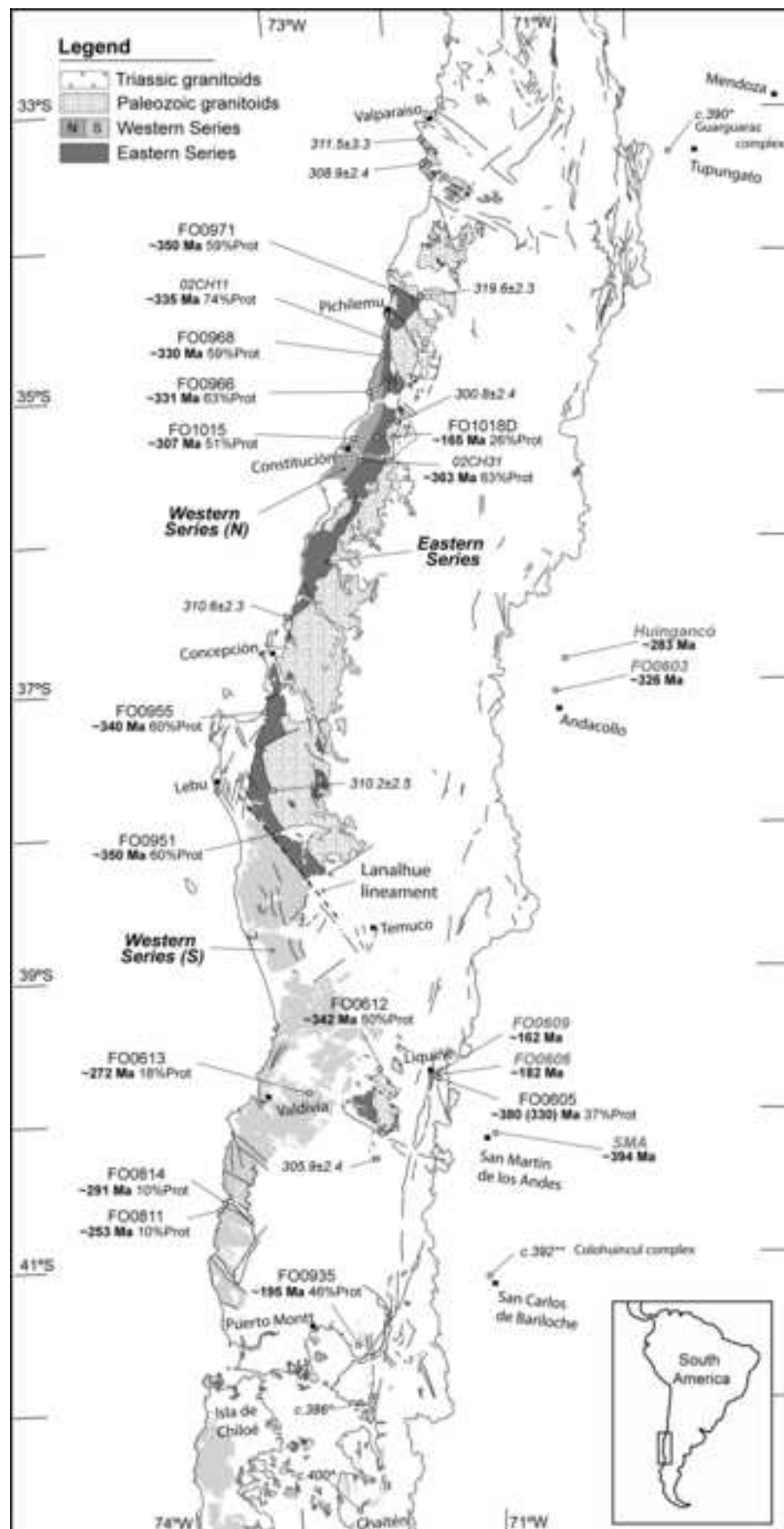


Figure 1. Hervé et al



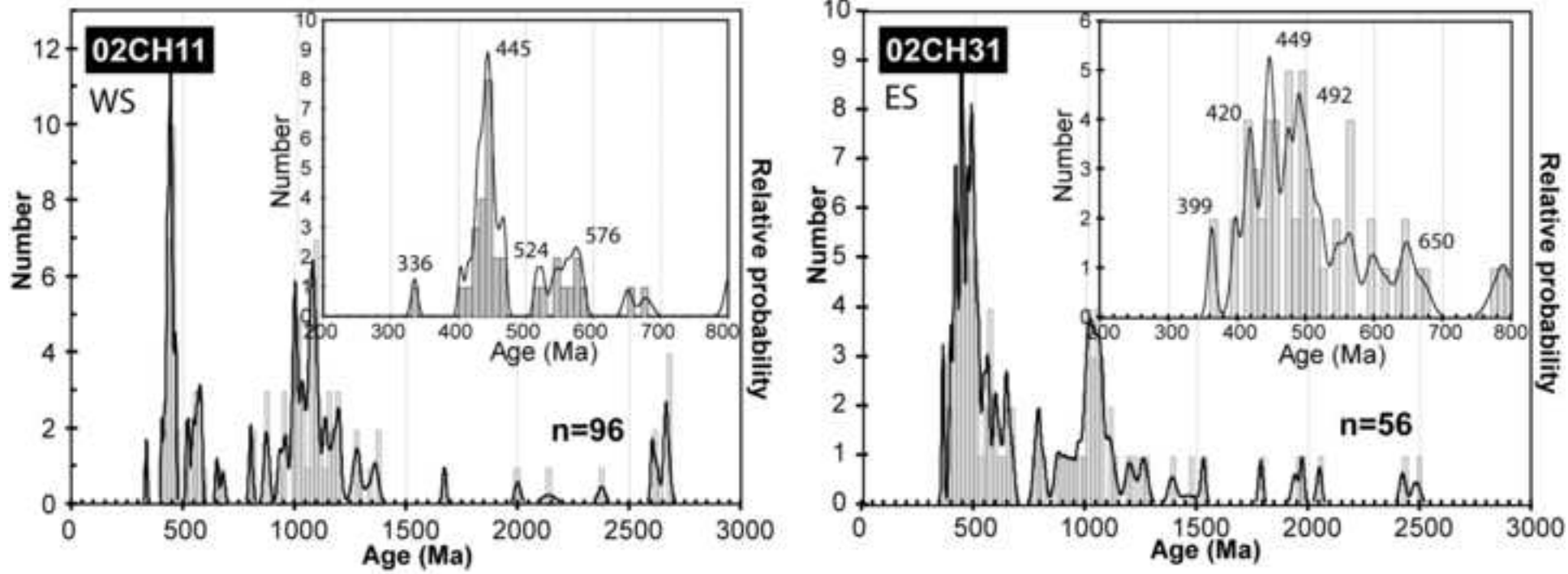


Figure 2. Hervé et al

Figure  
[Click here to download high resolution image](#)

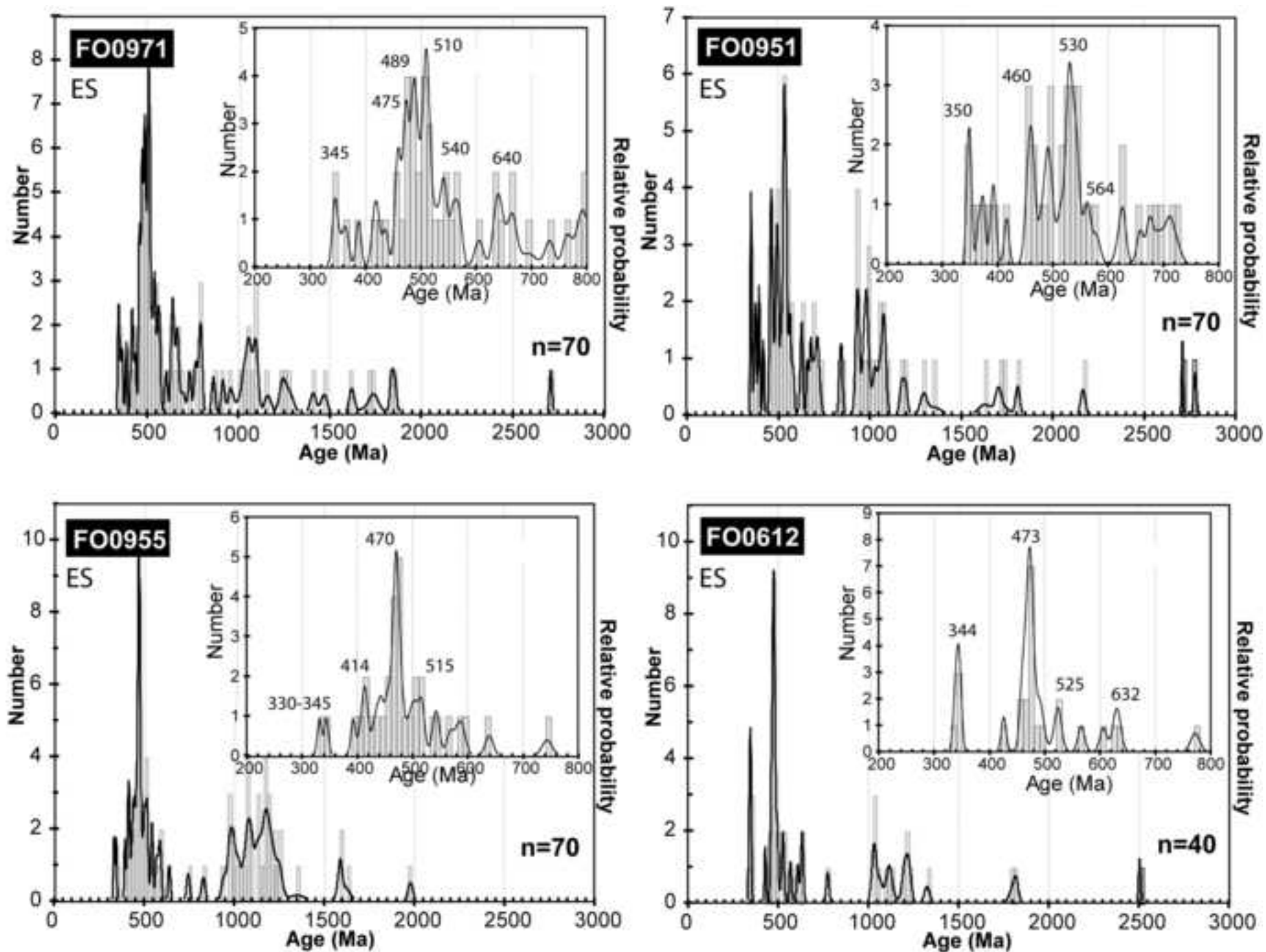


Figure 3. Hervé et al

Figure  
[Click here to download high resolution image](#)

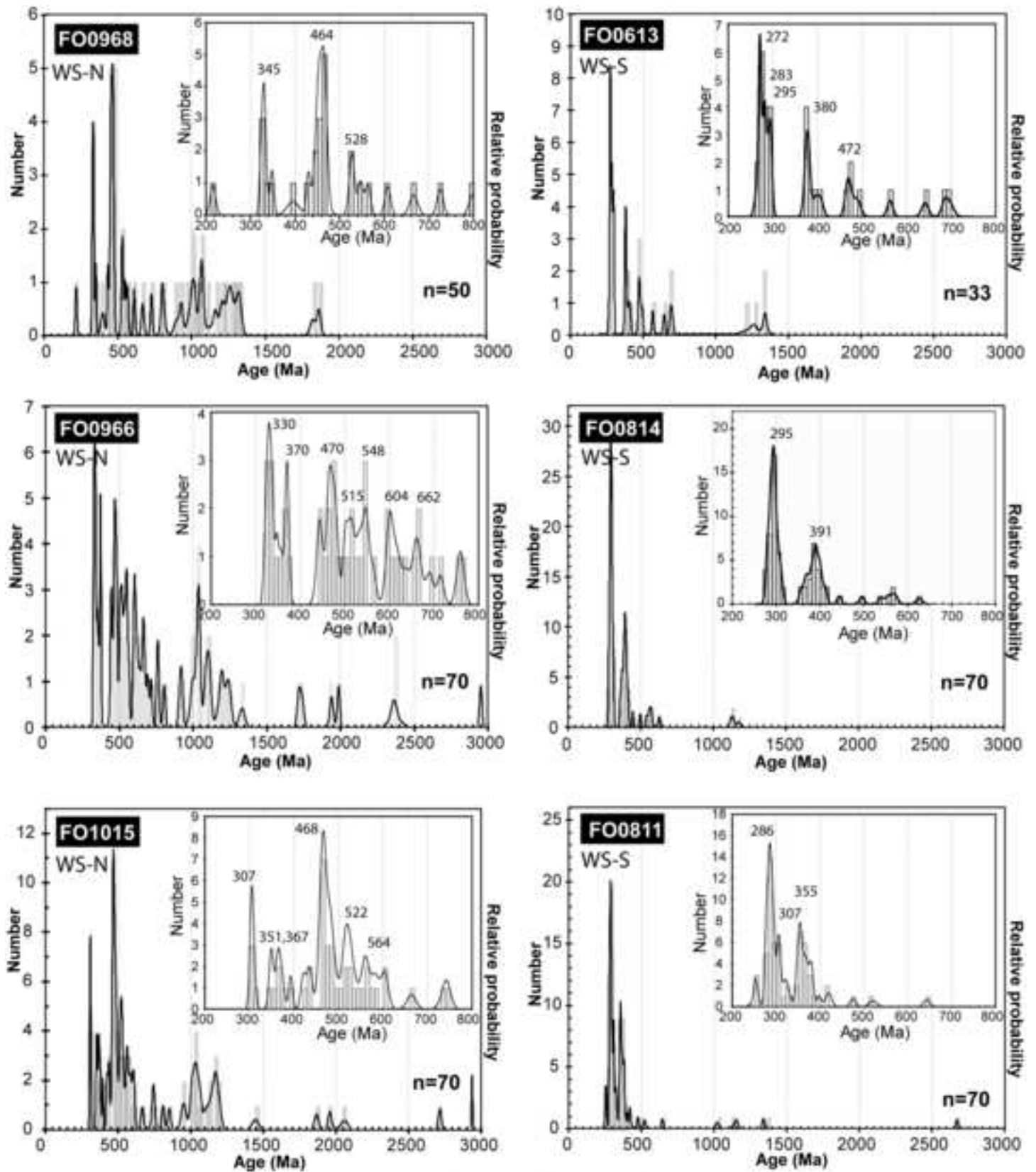


Figure 4- Hervé et al

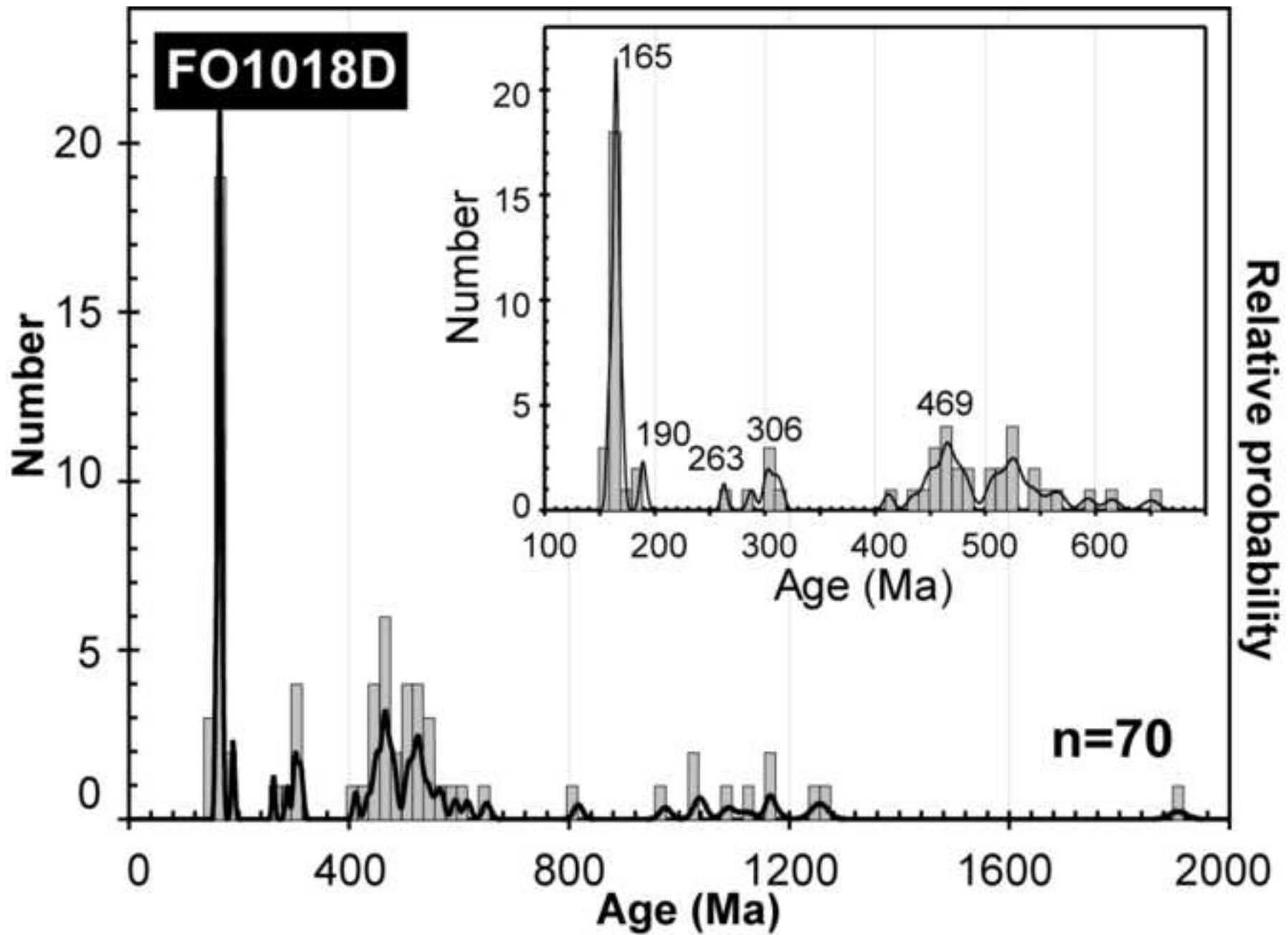


Figure 5. Hervé et al



Figure  
[Click here to download high resolution image](#)

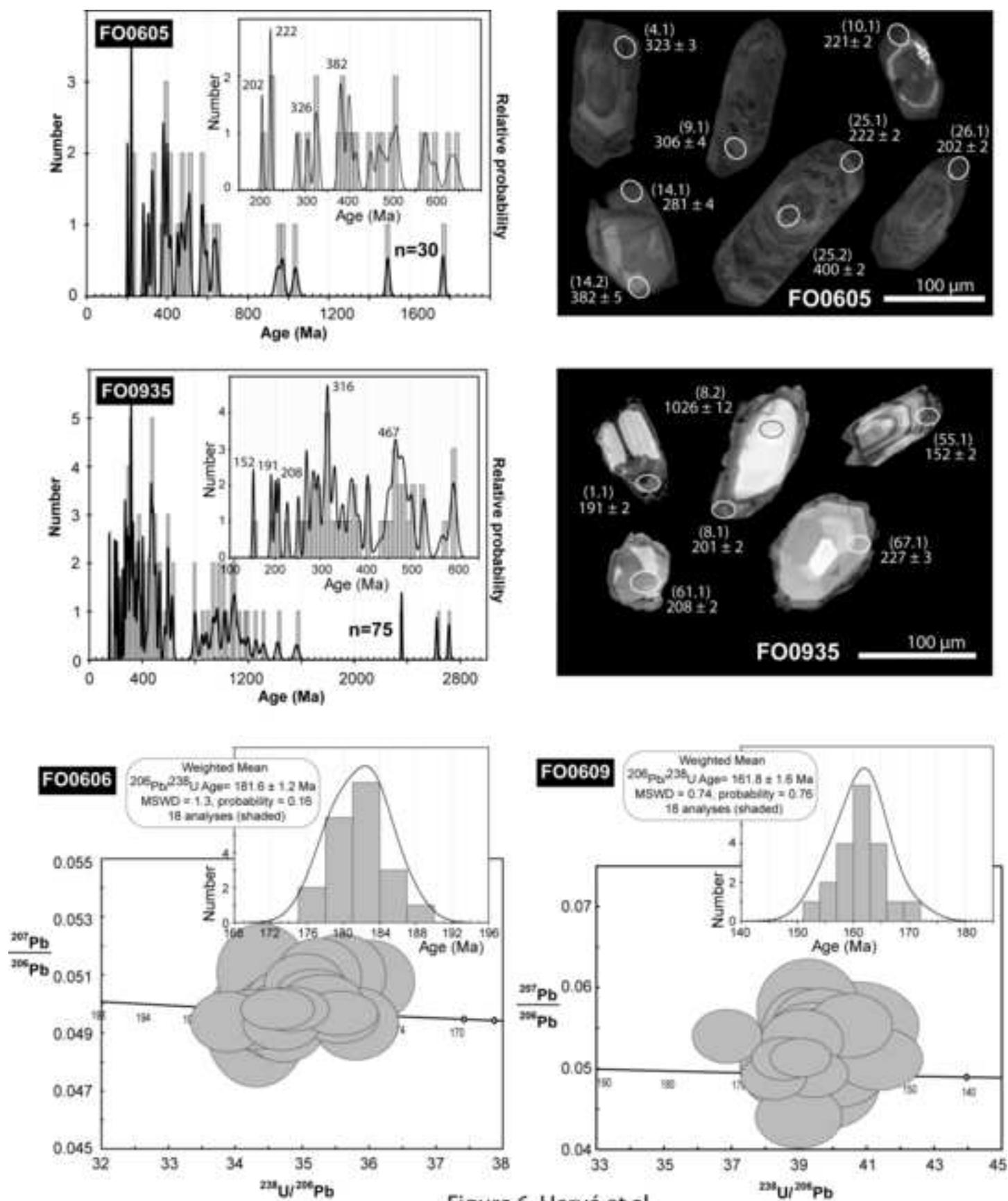


Figure 6. Hervé et al

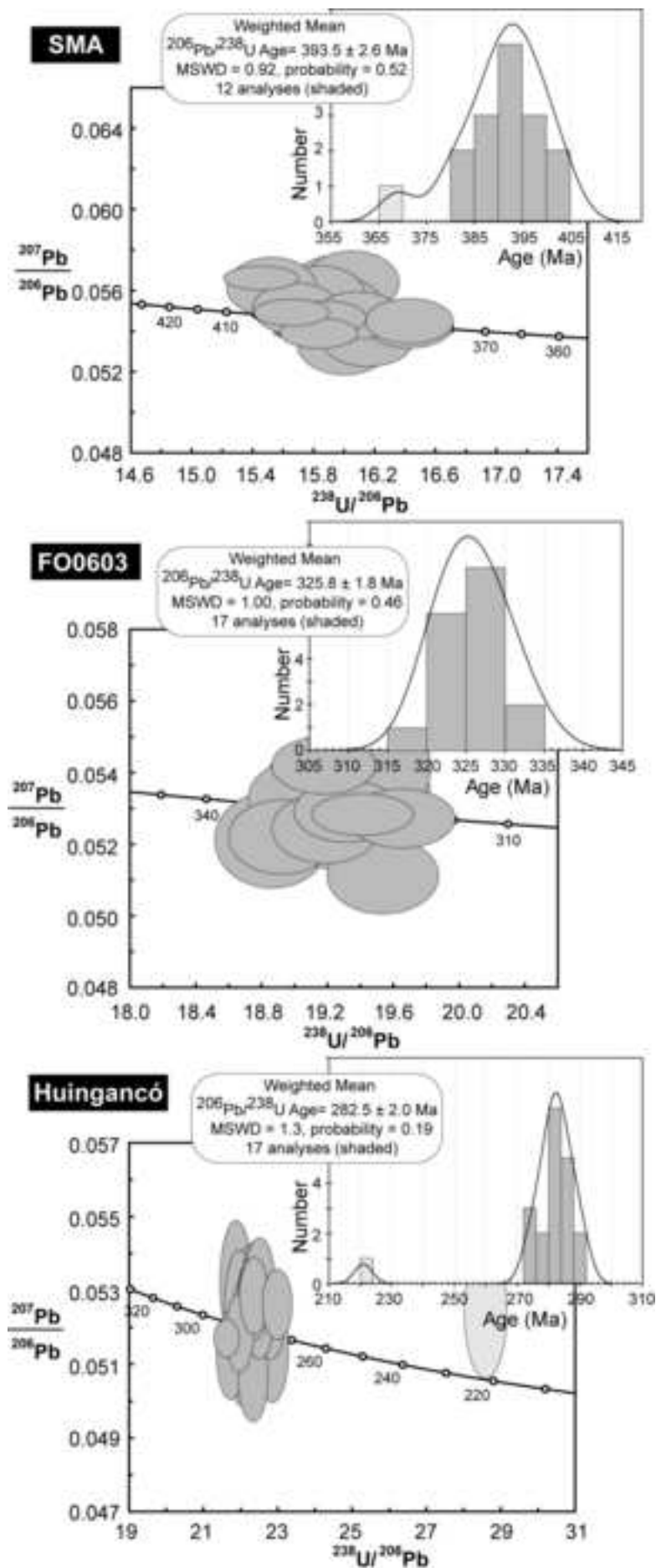


Figure 7. Hervé et al

Figure

[Click here to download high resolution image](#)

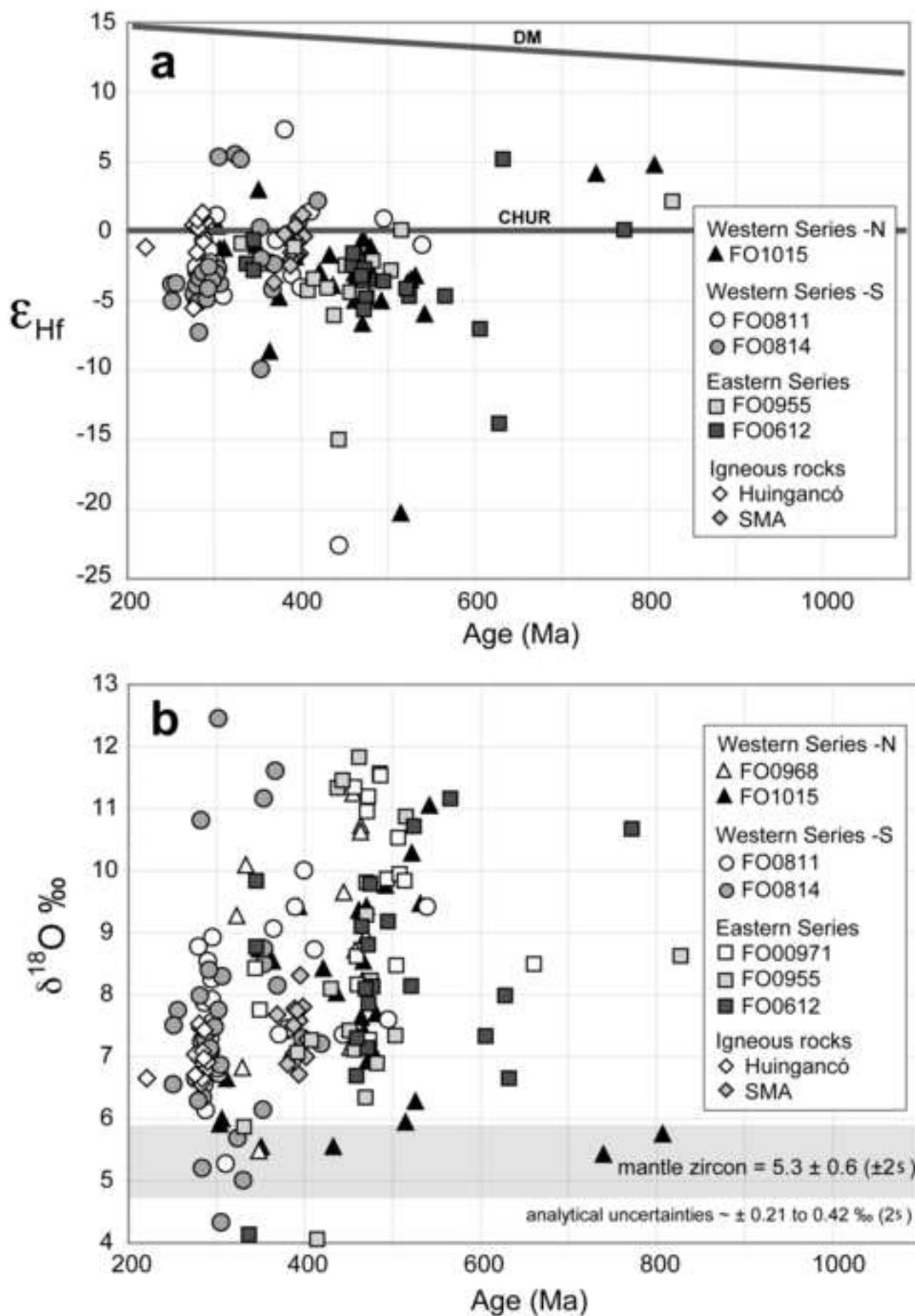


Figure 8. Hervé et al

Figure  
[Click here to download high resolution image](#)

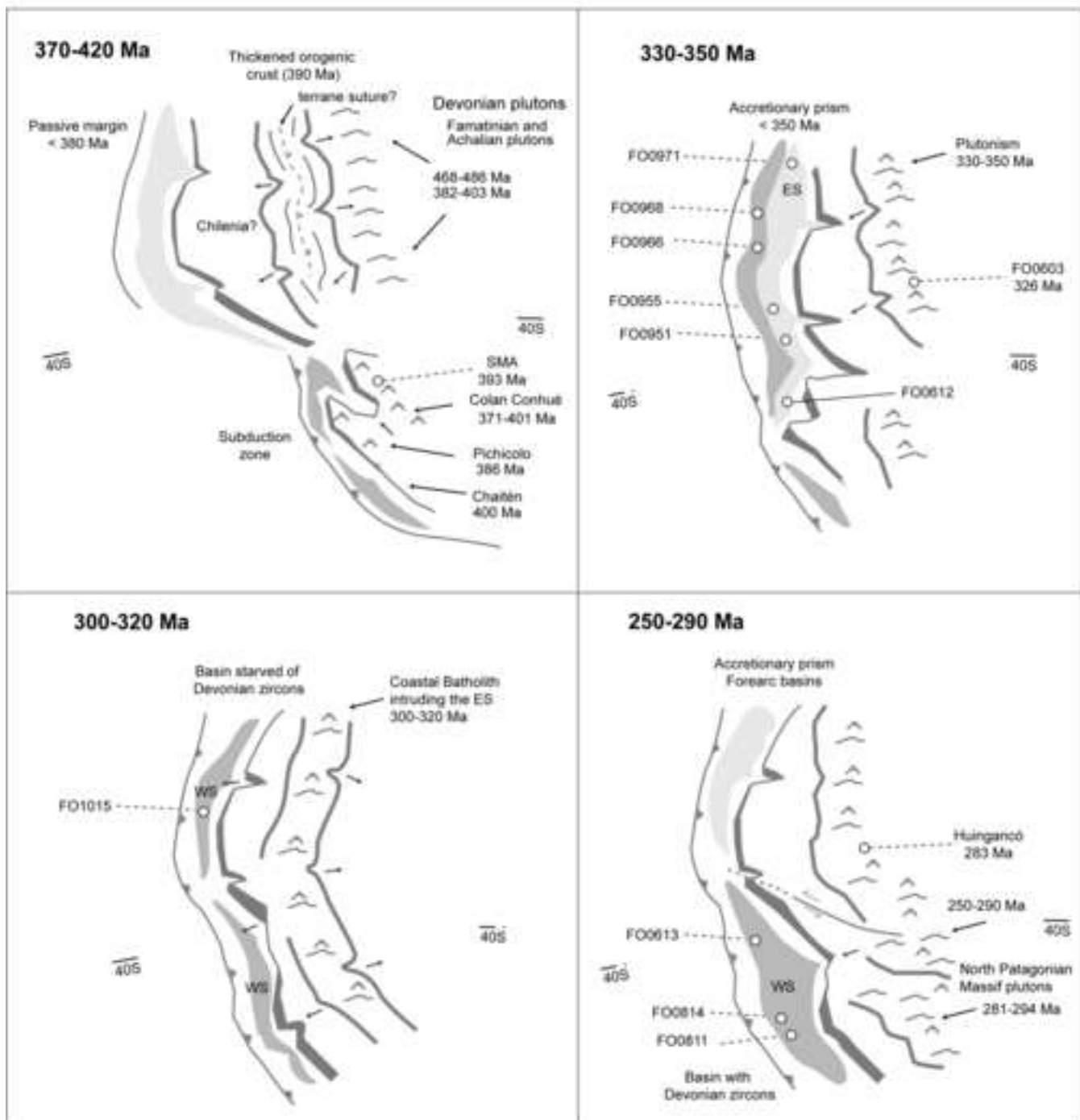


Figure 9. Hervé et al



Table 1 Sample Localities and Descriptions

	Lat °S	Long °W	Area	Lithology	Comments
<b>Western Series</b>					
FO0968	34.6890	72.0598	Boyeruca	Banded micaschist	well developed S <sub>2</sub> ; S <sub>1</sub> preserved in microlithons, Qtz veins and symmetrical lenses parallel to S <sub>2</sub>
FO0613	39.8110	72.3039	Antilhue	Micaschist	Qtz-albite composition, banded
FO0814			Pucatrihue	Metapsammite	m-thick layer in micaschist with bands parallel to predominant subhorizontal planar S <sub>2</sub>
FO0811			Maicolpue	Qtz micaschist	predominant planar S <sub>2</sub> foliation, parallel to lithological banding and quartz veins
FO0966	34.9393	72.1846	Iloca	Quartzite	micaceous, interleaved with albite-bearing quartz micaschists
FO1015	35.2622	72.3313	Putu	Psammopelitic schist	with quartz lenses parallel to the main flat-lying S <sub>2</sub> foliation
02CH11	34.5700	72.0680		Metagreywacke	Qtz, ab, white mica and Chl, recrystallized, with metamorphic banding formed by transposition foliation subparallel to former bedding. Willner et al. (2008)
<b>Eastern Series</b>					
FO0971	34.2280	71.9820	Tanume	St metasandstone	alternates with And-bearing metapelites with Qtz veins parallel to the axial planes of folds
FO0955	37.1520	73.1830	Chivilingo	Bt-Ms metasandstone	m-thick beds interleaved with And-bearing metapelites that contain calc-silicate lenses
FO0951	38.0270	73.1230	Puren	Bt-Ms metasandstone	mildly foliated, alternating with metapelites
FO0612	39.6759	72.3039	Playa Chauquen	Metasandstone	alternating with pelite in beds 5-10 cm thick, subvertical stratification
FO1018D	35.2630	72.1280	near Coipue	Metasandstone	alternates with metapelites, well developed axial planar cleavage and parallel lamination. Mapped as ES (Gana and Hervé, 1983) but has Jurassic detrital zircons
02CH31	35.4180	72.3250		Metagreywacke	Cf. 02CH11 except for Bt grown at the expense of Chl and Kfs due to high-T overprint. Willner et al. (2008)
<b>Liquiñe and Parque Alerce Andino paragneisses, mylonites and plutonic rocks</b>					
FO0605	39.7640	71.7810	east of Liquiñe	Bt-Ms banded paragneiss	tightly folded cm-scale Qtz-rich veins
FO0606	39.7580	71.8310	Furihuicul 4 bridge	Banded mylonite	intruded by mafic dykes parallel to the mylonitic foliation, and cut by low-angle faults with a 5 cm-thick gouge. N5E/73W foliation, with lineations plunging 23°N
FO0609	39.7560	71.8310	Furihuicul 2 bridge	Bt-Hbl tonalite	mylonitized, discrete anastomosing foliation planes separating m-long lenses of less deformed rock, cut by undeformed mafic dykes
FO0935	41.5937	72.5943	Parque Alerce Andino	Bt-Ms paragneiss	coarse-grained, well foliated with planar elongated Qtz lenses
<b>Argentina</b>					
FO0603	37.0663	70.6489	Cordillera del Viento	White rhyolite	ore mineralization on fractures. Grupo Andacollo unit of Llambías et al. (2007)
Huingancó			Cordillera del Viento	Bt-perthite granodiorite	coarse-grained, slightly altered. Huingancó volcano-plutonic complex of Llambías et al. (2007)
SMA			Lago Lacar, SE shore	Bt-Hbl tonalitic gneiss	coarse-grained, faintly foliated

Mineral abbreviations are: And, andalusite; Bt, biotite; Chl, chlorite; Hbl, hornblende; Kfs, K-feldspar; Ms, muscovite; Qtz, quartz; St, staurolite.

Table 2. Summary of the geochronological results on detrital zircons obtained in this

<b>Sample number / points analysed</b>	<b>Locality</b>	<b>Geological Unit</b>	<b>Youngest significant detrital age</b>
FO0966 / 70	Iloca	WS - N	330
FO0968 / 50	Boyeruca	WS - N	330
FO1015 / 70	Putu	WS - N	307
02CH11* / 96		WS - N	335
FO0613 / 33	Antilhue	WS - S	272
FO0814 / 70	Maicolpue	WS - S	291
FO0811 / 69	Pucatrihue	WS - S	253
FO0971 / 70	Tanume	ES - N	350
02CH31* / 94		ES - N	363
FO0955 / 70	Chivilingo	ES - N	340
FO0951 / 70	Puren	ES - S	350
FO0612 / 40	Playa Chauquen	ES - S	342
FO1018D / 70	Coipue	Hualañé-Gualleco basin	165
FO0605 / 30	Liquiñe		330 or 380
FO0935 / 54	Parque Alerce Andino		195 or 206

Western and Eastern Series rocks are differentiated into northern segment (N) and southern segment relative to the Lanalhue fault zone. \* indicates samples from Willner et al. (2008). Ages in Ma.

**e-component**

**[Click here to download e-component: Herve et al - Supplementary Data Tables S1 to S18- Shrimp data 18 samples.xls](#)**

**e-component**

**[Click here to download e-component: Herve et al - Supplementary Data Tables S19- Lu-Hf and O data 9 samples.xls](#)**